IN VITRO AND *IN CELLULO* INTERACTIONS OF PLATINUM AND RUTHENIUM ANTICANCER METALLODRUGS WITH RNA

by

ALETHIA A. HOSTETTER

A DISSERTATION

Presented to the Department of Chemistry
and the Graduate School of the University of Oregon
in partial fulfillment of the requirements
for the degree of
Doctor of Philosophy

March 2011

DISSERTATION APPROVAL PAGE

Student: Alethia A. Hostetter

Title: *In Vitro* and *In Cellulo* Interactions of Platinum and Ruthenium Anticancer Metallodrugs with RNA

This dissertation has been accepted and approved in partial fulfillment of the requirements for the Doctor of Philosophy degree in the Department of Chemistry by:

David Tyler	Chairperson
Victoria DeRose	Advisor
Darren Johnson	Member
Andy Berglund	Member
Alice Barkan	Outside Member

and

Richard Linton	Vice President for Research and Graduate Studies/Dean of the Graduate School

Original approval signatures are on file with the University of Oregon Graduate School.

Degree awarded March 2011

© 2011 Alethia A. Hostetter

DISSERTATION ABSTRACT

Alethia A. Hostetter

Doctor of Philosophy

Department of Chemistry

March 2011

Title: *In Vitro* and *In Cellulo* Interactions of Platinum and Ruthenium Anticancer Metallodrugs with RNA

Approved: _____
Dr. Victoria J. DeRose

Since its approval by the FDA in 1978 cisplatin (*cis*-diamminedichloroplatinum(II)) has revolutionized the treatment of several cancer types, particularly testicular cancer which now has a cure rate greater than 90%. Following the example set by its success, a broad range of antitumor metallodrugs is being developed. One of the most promising of these drugs, currently in Phase Two of clinical trials, is the Ru-based NAMI-A (imadozolium *trans*-[tetrachloro(dimethylsulfoxide)(imidazole)ruthenate(III)]) which displays low systemic toxicity and strong antimetastatic activity. The majority of anticancer metallodrugs (including NAMI-A and cisplatin) can bind to DNA, which, in many cases, is an important therapeutic target. Much effort has gone into characterizing the DNA binding properties of anticancer metallodrugs. Less study has gone into characterizing the interaction of anticancer mellodrugs with RNA even though RNA is chemically similar to DNA and plays important roles in gene expression and regulation. Focusing on the

extensively studied cisplatin, Chapter I covers both what is known about anticancer metallodrug-RNA binding and the information that can be gleaned from DNA binding and drug localization studies. Chapter II provides the details of a kinetic investigation of the *in vitro* binding of aquated cisplatin to an RNA sequence containing an internal loop derived from the core of the spliceosome, a related RNA hairpin, and the slower reacting DNA hairpin analog. Chapter III follows *in cellulo* studies with cisplatin-treated *S. cerevisiae* that demonstrate, using ICP-MS, differences in Pt accumulation in mRNA and rRNA. The effects of cisplatin treatment on *S. cerevisiae* cell growth and viability were investigated using clonogenic and morphologic assays. In Chapter IV the same protocols were applied in order to investigate Ru accumulation on RNA following *S. cerevisiae* treatment with NAMI-A. These *in cellulo* experiments were followed by *in vitro* binding studies that utilized MALDI-MS to compare Ru interactions with RNA and DNA oligonucleotides following treatment with NAMI-A under different solution conditions, finding enhanced binding in an acidic, reducing environment like that found in tumor tissue. Chapter V pulls together the knowledge gained so far and discusses questions for future investigation.

This dissertation includes both previously published and unpublished coauthored material.

CURRICULUM VITAE

NAME OF AUTHOR: Alethia A. Hostetter

GRADUATE AND UNDERGRADUATE SCHOOLS ATTENDED:

University of Oregon, Eugene, Oregon
Mills College, Oakland, California
Lane Community College, Eugene, Oregon

DEGREES AWARDED:

Doctor of Philosophy, Chemistry, 2011, University of Oregon
Bachelor of Arts, Chemistry, 2003, Mills College

AREAS OF SPECIAL INTEREST:

RNA biochemistry
Platinum anticancer drugs
Ruthenium anticancer drugs

PROFESSIONAL EXPERIENCE:

Graduate Teaching Fellow, University of Oregon, Eugene, Oregon, July 2005 – March 2011

Teaching Assistant Mills College, Oakland, California, January – May 2003

GRANTS, AWARDS, AND HONORS:

The Alie Ogburn Jackson Barry Prize for Excellence in Chemistry, Mills College, 2003

The Bruce McCullum Prize for Hightest Attainment in Scholarship, Mills College, 2003

Phi Beta Kappa, Mills College, 2002

Full tuition and Dean's Scholarships, Mills College, 2000-2003

PUBLICATIONS:

Hostetter, A. A.; Miranda, M. L.; DeRose, V. J.; Holman, K. L. M., "Ru Binding to RNA Following Treatment with the Anti-Metastatic Drug NAMI-A in *S. cerevisiae* and *In Vitro*" *Manuscript submitted.*

Chapman, E. G.; Hostetter, A. H.; Osborn, M. F.; Miller, A. L.; DeRose, V. J. "Binding of Kinetically Inert Metal Ions to RNA: The Case of Pt(II)" In *Metal Ions in Life Sciences: Structural and Catalytic Roles of Metal Ions in RNA*; Royal Society of Chemistry: Cambridge, UK, 2011; in press.

Hostetter, A. A.; Chapman, E. C.; DeRose, V. J. "Rapid Cross-linking of an RNA Internal Loop by the Anticancer Drug Cisplatin" *J. Am. Chem. Soc.* **2009**, *131*, 9250-9257.

ACKNOWLEDGMENTS

This has been a long process full of challenges, frustrations, surprises, confusion, insight, and problem-solving that has allowed me to grow more than I ever expected to. Along the way I have been helped by a great many people in more ways than I can count. I would like to thank my advisor Prof. Victoria J. DeRose for her guidance through this amazing process of learning and discovery. One of the greatest things I have learned from her is how to communicate science well and put ideas into pictures. My other committee members, Dave Tyler, Darren Johnson, Andy Berglund, and Alice Barkan have also been generous with their guidance and advice. I would like to thank them all for making themselves available and always having their doors open to me whenever I had a question or an experiment to discuss.

I am also deeply grateful to all the members of the DeRose lab, particularly Erich Chapman and Maire Osborn who have both given me invaluable feedback, assistance, and ideas and who have worked with me on several papers. This dissertation includes work that they have both coauthored. I am deeply grateful for the hard work and enthusiasm that Michelle Miranda, an exceptionally dedicated undergraduate, put into to the NAMI-A *in cellulo* experiments. Her careful work made that project come together. Thank you. In addition, I want to thank Christen Welsh who started the *in cellulo* research in *S. cerevisiae* and taught me all of the basics that I needed to know. I am also grateful to Amanda Miller for advice on MALDI and cell staining procedures and to Kate and Brandon Green who were in the DeRose Lab when Erich and I first joined. They both provided guidance, information, and perspective. Kate, in particular, patiently taught me many of the procedures that became the foundation of my later research.

Beyond the DeRose lab, my thanks go out to our collaborator Karen Holman for helping make the NAMI-A project possible, Andy Ungerer of the W. M. Keck Collaboratory for Plasma Spectrometry (Oregon State University) for assistance with the ICP-MS experiments, to the Steven's lab, particularly Dr. Laurie Graham, for assistance with protocols and imaging, the kind gift of several yeast strains, and for access to their Carl Zeiss Axioplan 2 fluorescence microscope, and to the whole community of researchers, professors, teachers, and staff and the University of Oregon for making a collaborative environment that is based on cooperation and sharing.

Finally, I cannot conclude this section without thanking my family, friends, and community. Words cannot express the ways in which you all have helped and supported me through this process, and before this, throughout my life so that I could get to a place where I was ready to enter graduate school. Now that this piece of my journey is coming to a close I particularly want to thank my partner, Tobi, for her love, patience, and support. Every time I got overwhelmed by a challenge facing me she was the one who was right there telling me that I could do it. Ronan, also, has really been there for me, encouraging and supporting me the whole way.

Thank you all. I could not have done this without you.

I dedicate this dissertation to Tobi and Ronan, whose support, caring, and encouragement have made everything possible

TABLE OF CONTENTS

Chapter Page

Chapter Page

LIST OF FIGURES

Figure Page

LIST OF TABLES

LIST OF SCHEMES

CHAPTER I

INTRODUCTION

This dissertation focuses on the effects of cisplatin and NAMI-A treatment on RNA both *in vitro* and *in cellulo* in order to gain insight into the binding of anticancer metallodrugs to RNA. The ultimate aims of this project are to gain information towards the elucidation of the roles that RNA plays in the mechanisms of anticancer metallodrugs and the development of a fundamental understanding of the ways that RNA can be targeted and impacted by metal based drugs. Chapter I gives an overview on what is known about the interaction of anticancer metallodrugs with RNA, focusing on cisplatin as it is the best studied anticancer metallodrug. It includes material adapted from: Chapman, E. G.; Hostetter, A. H.; Osborn, M. F.; Miller, A. L.; DeRose, V. J. "Binding of Kinetically Inert Metal Ions to RNA: The Case of Pt(II)" In *Metal Ions in Life Sciences: Structural and Catalytic Roles of Metal Ions in RNA*; Royal Society of Chemistry: Cambridge, UK, 2011; in press – Reproduced by permission of The Royal Society of Chemistry. This material was co-written and co-edited by me, Dr. Erich G. Chapman, Maire F. Osborn, and Amanda L. Miller with guidance and editing by Prof. Victoria J. DeRose. The material included in Chapter I from the above publication is taken from sections in which I had significant input.

Chapter II covers kinetic studies comparing the platination rate of cisplatin-treated RNA and DNA oligonucleotides, mapping experiments that localized the platinum binding sites, and MALDI-MS data that demonstrate the stoichiometry of the platinated products. It includes previously published coauthored material with contributions from

Dr. Erich G. Chapman and Prof. Victoria J. DeRose. Chapter III follows *in cellulo* studies of cisplatin-treated *S. cerevisiae* in which Pt accumulation in yeast RNA was quantified by ICP-MS, the effects of cisplatin treatment on *S. cerevisiae* were examined using growth and clonogenic assays combined with DAPI and TUNEL staining. Specific platinum binding sites in ribosomes were located with mapping experiments. It includes coauthored material intended for publication with contributions from Maire F. Osborn and Prof. Victoria J. DeRose. Chapter IV covers *in cellulo* studies of NAMI-A treated yeast and *in vitro* MALDI-MS experiments comparing binding to RNA and DNA oligonucleotides under different solution conditions. It includes material submitted for publication with contributions from Michelle L. Miranda, Prof. Victoria J. DeRose, and Prof. Karen L. McFarlane Holman. Chapter V pulls together the knowledge gained so far and discusses questions for future investigation.

Anticancer Metallodrugs

Cisplatin (*cis*-diamminedichloroplatinum(II), Figure 1.1) was the first clinically used metal-based anticancer drug. Particularly effective in the treatment of testicular, ovarian, oropharyngeal, broncogenic, cervical, and bladder carcinomas, and lymphoma, osteosarcoma, melanoma, and neuroblastoma, cisplatin has had a profound effect in making many types of cancer more treatable. Currently cisplatin and two structurally related Pt(II) drugs (carboplatin and oxaliplatin, Figure 1.1) are used in the treatment regimes of 50-70% of cancer patients.[1] However, both innate and acquired resistance limit the usefulness of these three drugs in other types of cancer, and cisplatin in particular has a high general toxicity that causes dose-limiting side effects. In addition,

while platinum anticancer drugs are highly active against primary tumors, they have limited activity against metastasis.[2]

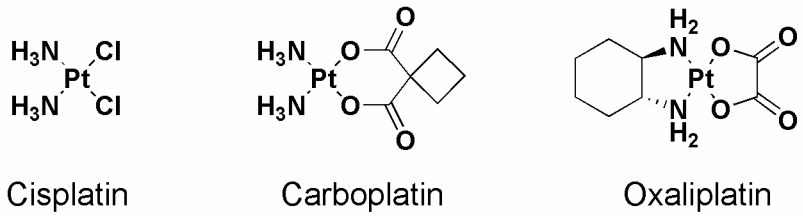

Figure 1.1. The structures of the three FDA-approved Pt antitumor drugs.

Both the success and limitations of cisplatin have spurred a great deal of effort to develop other platinum-based anticancer drugs. Thousands of platinum drugs have been synthesized and evaluated, but only two (carboplatin and oxaliplatin) have made it to worldwide clinical acceptance.[3] Carboplatin (*cis*-diammine(cyclobutanedicarboxylato)platinum(II)) contains the same active $Pt(NH_3)_2$ fragment as cisplatin and thus has the same mechanisms of action and resistance as cisplatin. However, carboplatin is less toxic than cisplatin, especially to the nervous system and kidneys.[4] Oxaliplatin (*cis*-oxalato-(*trans*-1)-1,2-(diaminocyclohexane)platinum(II)) also demonstrates lower toxicity than cisplatin and shows a lack of cross-resistance with cisplatin and carboplatin.[3,4] Despite the advances made, these three platinum antitumor drugs all have major drawbacks relating side-effects, intrinsic and acquired resistance,[5] and low effectiveness against metastasis.[6]

As a result of these limitations, studies have branched out and the anticancer properties of other transition metal drugs are being examined, including drugs based on ruthenium, arsenic, gallium, titanium, copper, iron, rhodium, and tin.[5,7] Of the transition

metals tested, the ruthenium-based pharmaceuticals are one of the most promising groups and have attracted a great deal of attention due to their multiple accessible oxidation states, ability to mimic iron, and favorable ligand exchange kinetics (similar to those of platinum). These properties have the potential to provide lower general toxicity, selective accumulation in tumor cells, selective activation by reduction within the tumor microenvironment, a different mechanism of action, and antimetastatic activity.[8] A prominent example of the Ru-based anticancer drugs is NAMI-A (imadozolium *trans*-[tetrachloro(dimethylsulfoxide)(imidazole)ruthenate(III)], Figure 1.2), a drug which is currently in Phase Two of clinical trials. NAMI-A exhibits low general toxicity, strong antimetastatic activity, and an alternate mechanism of action. It is one of the best studied Ru-based anticancer metallodrugs.[8]

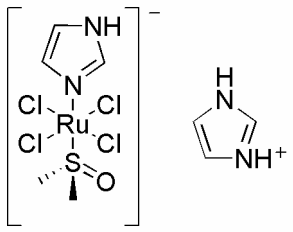

Figure 1.2. The structure of NAMI-A.

A feature common to the majority of transition metal-based anticancer drugs, including the platinum and ruthenium-based drugs, is an ability to bind to DNA. In many cases DNA is considered to be an important therapeutic target for drug activity.[7,3] This is certainly the case for cisplatin, which is the most thoroughly studied metal anticancer drug.[2] Although chemically similar to DNA, the RNA-binding of metal based anticancer

drugs is rarely tested, despite the importance of RNA in gene expression and regulation.[9,10] This is a gap that the work presented in this dissertation aims to address. Two broad, overarching goals guide this work. The first goal is to elucidate the role that RNA plays in the mechanisms of anticancer metallodrugs. The second is to gain insight into binding of metallodrugs to RNA in order to build a fundamental understanding of the ways that RNA can be targeted and impacted by drugs, whether they are metal-based or not. Since little is currently known, the studies presented here use cisplatin and NAMI-A to answer some basic questions about metallodrug-RNA binding in order to lay a foundation for future studies. This chapter will provide background on what is currently known, focusing on Pt(II) drugs, and cisplatin in particular, because they are the best studied anticancer metallodrugs and their nucleic acid binding properties have been elucidated in detail for DNA. First, an overview of cisplatin's mechanism of therapeutic action is given. In order to gain insight into what might be expected for RNA, both the solution chemistry of cisplatin and the DNA binding modes of its aquated species are examined. This is followed by a discussion about RNA as drug target. Next, the studies that have been done so far on the effect of cisplatin treatment on RNA and RNA-dependent processes are investigated. In order to gain an understanding of how Pt drugs may interact with RNA in a cellular context, studies on the types of biomolecules targeted by Pt(II) drugs *in cellulo* will be examined, followed by a discussion of *in cellulo* Pt(II) drug localization studies which may give an indication of the RNA species and processes that are likely targets of platinum drugs. Finally, both the solution chemistry of NAMI-A and the effects of NAMI-A treatment on DNA will be examined in order to

provide context for *in vitro* and *in cellulo* studies on the effects of NAMI-A treatment on RNA.

Cisplatin

Cisplatin is the best-studied anticancer metallodrug and, although there still are features of its mechanism of action that are not understood, many aspects of its solution chemistry, DNA binding, and biochemistry have been worked out. It is administered to patients intravenously. The two NH_3 ligands are kinetically inert. In the bloodstream the high concentration of chloride (100 mM) prevents the two labile chloride ligands from aquating. Upon entering a cell, through either passive diffusion or active transport, the lower chloride concentration present (4-12 mM) induces aquation to either the monoaqua or the diaqua form.[2] These cationic aqua derivatives are the biologically active forms which bind to 'soft' nucleophilic targets including the cysteine, methionine, and histidine residues on proteins, and the N7 site on guanine and adenine bases. Since cisplatin has two open coordination sites, the majority of the final platinated products formed are bifunctional cross-links.

On DNA the major products are intrastrand cross-links which distort the DNA backbone, resulting in pinching of the major groove and a widening of the minor grove. Multiple classes of proteins recognize this altered DNA structure, and it is believed that this recognition causes a series of cellular events which ultimately lead to cell cycle arrest at the G2 phase and the induction of apoptosis; many pieces of this mechanism, however, are not yet fully understood.[11] In addition, while intrastrand DNA adducts are known to inhibit transcription and replication, cisplatin treatment can also inhibit splicing and

translation in extracts.[12,13] As discussed below the nucleolus is a particular is target for platinum accumulation, and rRNA biogenesis, splicing, and mRNA maturation all take place there, making it likely that some of these processes will be disrupted.

Cisplatin Solution Chemistry and DNA Coordination

Since cisplatin is activated by aquation, a large number of studies have been done on cisplatin aquation in at wide range of different pH values, temperatures, and buffer conditions.[14] One of the studies that used solution conditions that were more biologically relevant than other studies was a NMR study by Daves *et al.* of 1.51 mM cisplatin at 25 ºC, pH 5.9, in 9 mM $NaClO_4$.[15] Scheme 1.1 shows the aquation of cisplatin. The rate obtained for the first step of cisplatin aquation is 2.38 (4) × 10^{-5} s^{-1}, while the anation rate (the rate of replacement of the water ligand with the chloride anion) is 4.6(3) × 10^{-3} M^{-1} s^{-1}. The rate constant for the aquation of the monoaqua species is 1.4(3) × 10^{-5} s^{-1}, and the anation rate is 81(22) × 10^{-3} $M^{-1}s^{-1}$. In both cases the chloride-dependant anation rate is at least two orders of magnitude larger than the aquation rate. Based on this, it is clear why the concentration of chloride ion is critical to activation of cisplatin inside the cell.[16] It is worth noting that the measured half-life of cisplatin aquation ranges from 2-8 h depending on the solution conditions used, with 2 h being a generally accepted number.[2,14,15] The pKa's of each of these species is shown in Scheme 1.1.[17] At neutral biological pH 7.4 (healthy tissue) we would expect to get a mixture of these species, with significant amounts of the less reactive hydroxo species, but at pH 6.0 (tumor tissue)[18] the majority of the species will be in the more reactive aqua forms.[19]

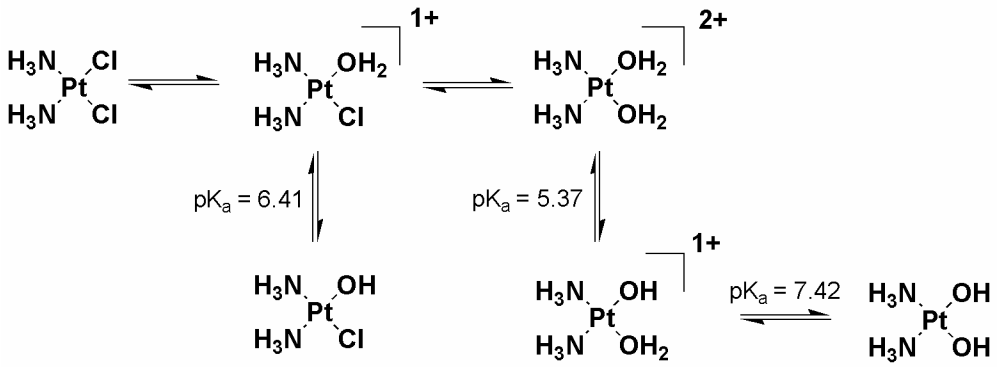

Scheme 1.1. The aquation of cisplatin with the pKas of the various aqua species shown. The pKa values were taken from 17.

Once formed, the cationic Pt(II) aqua species enter the condensed cationic atmosphere surrounding the polyanionic nucleic acid.[20-23] Here they may form transient associations with the negatively charged phosphodiester backbone before forming kinetically inert bonds to guanine and adenine N7 sites, forming first a monoadduct which then closes to form the diadduct. Because the bonds formed to the nucleobases are kinetically inert, binding with them by Pt(II) is under kinetic, rather than thermodynamic, control.[2] In addition, because the initial aquation of cisplatin is so slow, aquation is the rate-limiting step for reaction with DNA *in vivo*.[17] For this reason kinetic studies comparing the reaction rates with different targets, such as RNA or different DNA structures, use either $[Pt(NH_3)_2Cl(OH_2)]^{1+}$ or $[Pt(NH_3)_2(OH_2)_2]^{2+}$ in their reactions rather than freshly dissolved cisplatin.

The most common DNA adducts are 1,2 intrastrand cross-links, with 1,2-d(GpG) intrastrand cross-links accounting for 60-65% of adducts, and 1,2-d(ApG) intrastrand cross-links accounting for 20-25%, 1,3-d(GpNpG) intrastrand cross-links accounting for 5-10%, and interstrand cross-links, DNA-protein cross-links, and monofunctional adducts being rare, but observed (Figure 1.3).[24] The preference of guanine over adenine bases has

been proposed to be due to both the more favorable orbital overlap between the cisplatin LUMO and the guanine HOMO (due to the lower energy of the guanine HOMO) and the ability of the NH_3 ligand to form a hydrogen bond to the O6 keto oxygen of guanine.[25] Based on this, for RNA the same favoring of guanine over adenine would be expected.

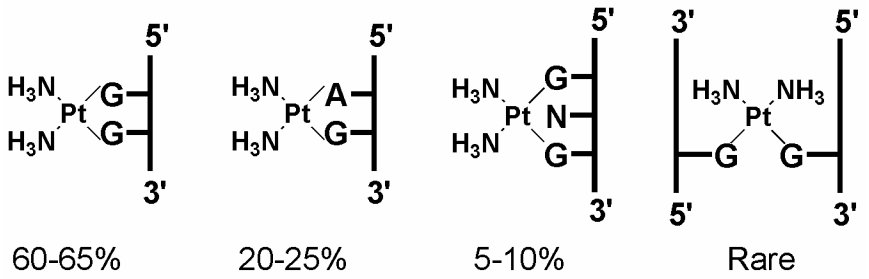

Figure 1.3. The main adducts formed upon treatment of DNA with cisplatin, from left to right: 1,2-d(GpG) intrastrand cross-link, 1,2-d(ApG) intrastrand cross-link, 1,3-d(GpNpG) intrastrand cross-link, and interstrand cross-link.

Many studies have been done on the influence of DNA structure on the rate of Pt(II) coordination. One study, of a DNA telomere quadruplex (a highly repetitive DNA sequence from the end of a chromosome capable of forming a four-stranded structure) with $[Pt(NH_3)_2(OH_2)_2]^{2+}$ demonstrated that platination of the telomere proceeded at twice the rate of the double stranded DNA which in turn proceeded at three times the rate of the single stranded DNA.[26] Several studies using the $[Pt(NH_3)_2(OH_2)_2]^{2+}$ species have looked at the closure of the monoadduct (an adduct in which platinum is bound to the DNA at a single coordination site) to either a bifunctional intrastrand or interstrand adduct (adducts in which two coordination sites of the same Pt are bound to the DNA at different bases). The rate of this chelation from the monoadduct to the bifunctional adduct is quite variable based on sequence and structure. For single-stranded DNA a significantly faster rate of chelation to the 1,2-intrastrand adduct is observed than for double-stranded

DNA.[27] In addition, the rate of closure to an interstrand cross-linked adduct is faster than 1,2-intrastrand chelation.[28] The effects of structure on closure rate shown here may mean that in RNA, where there is a much wider variety of structural motifs, a different set of adducts will be formed and that the structure of each RNA species will result in certain cross-links being kinetically favored.

RNA as a Drug Target

The field of RNA biology has grown considerably and there is increasing recognition of the importance of RNA-dependent cellular processes. In addition to well-known functional roles in translation (mRNA, tRNA, and ribosomes) a great deal is now being learned about the regulatory roles carried out by RNAs such as siRNA, microRNA, piwi-interacting RNA, and long noncoding RNA in both transcription and translation.[29] This importance of RNA-based processes is reflected by the complexity, careful regulation of, and considerable resources invested in processes such as ribosome biogenesis.[30] There is also a plethora of pathways that recognize and degrade damaged and non-functional RNA species, a number of which are only beginning to be elucidated. These degradation pathways include noncoding RNA decay,[31] no-go decay,[32] nonsense-mediated decay,[32] non-stop decay,[32] nonfunctional ribosomal decay,[33] and rapid tRNA decay.[34] There have also been reports of enzymes that can repair RNA, including two human AlkB homologues that repair methylated purine lesions in both DNA and RNA *in vitro* and when expressed in *E. coli*.[35] In addition, an activity has been reported in mitochondrial extract that can repair the 3'-ends of truncated tRNAs.[36] When damaged RNA is not degraded or repaired there can be serious consequences. For example, RNA

oxidation is an early event involved in the pathogenesis of many neurodegenerative disorders including Alzheimer's disease, Parkinson's disease, Epilepsy, spinal cord injury, and amyotrophic lateral sclerosis.[37]

At the same time that an understanding of the complexity and importance of RNA biology has been growing so has an understanding of the links between RNA and apoptosis, a type of programmed cell death typically exploited by anticancer drugs. The toxic proteins sarcin[38] and ricin[39] invoke apoptosis through their interaction with the sarcin/ricin loop of the large subunit of the eukaryotic ribosome. Proteins that play roles in both DNA repair and the decay of defective ribosomes have been discovered, coupling DNA and RNA surveillance mechanisms.[40] Connections between ribosome biogenesis, control of the cell cycle, and the tumor suppressor protein p53 (which is thought to play a pivotal role in cisplatin-induced apoptosis) have also been found in which the ribosomal proteins can activate p53 in response to ribosomal stress such as the inhibition of rRNA transcription or the induction of the unfolded protein response in the endoplasmic reticulum.[41-43] Disruption of rRNA processing and imbalances of the ribosomal protein pool can also activate p53.[44]

In addition, RNA has been postulated to play specific roles within apoptosis. Stress in known to induce tRNA cleavage[45] and rRNA is specifically degraded in response to apoptotic stimuli.[46,47] It is possible that these specific degradation fragments may play a role in cell signaling. In addition, tRNA has been shown to inhibit apoptosis. It does this through binding to cytochrome c, a key mediator of the intrinsic apoptotic pathway that is released from the mitochondria and subsequently binds to and activates the caspase activator Apaf-1 (caspases are the effectors of apoptosis). The binding of

tRNA to cytochrome c inhibits cytochrome c binding to Apaf-1 and subsequent caspase activation both *in vitro* and in living cells.[48]

Taken together, it is clear that RNA processes have many important functions in the cell, that disruption of these processes can have serious consequences, and that there are links between RNA pathways and programmed cell death. Therefore RNA could be an important target of anticancer metallodrugs.

Cisplatin and RNA

Effect on RNA Processes

A few studies have been done on both the effects of cisplatin treatment on RNA processes and the formation of specific Pt adducts on RNA. *In cellulo* studies have measured the effect of cisplatin treatment on replication, transcription, and translation through the incorporation of isotopically labeled nucleotides or amino acids in both *S. cerevisiae* and a human placental cell line.[49,50] Inhibition of replication occurred at a slightly lower concentration than transcription or translation, but all processes are capable of being significantly inhibited by cisplatin.

In vitro studies have examined the effects of cisplatin treatment on transcription, splicing, translation, and enzymatic RNA degradation (Figure 1.4). With the exception of certain RNA polymerase studies in which single platinum adducts were placed on DNA templates,[49,51] these studies were all carried out in complex systems with both protein and RNA components. This means that in these complex systems the cisplatin treatment could interfere with any of the RNA structures, RNA protein interactions, or protein-protein interactions. Ribosomal RNA transcription by RNA polymerase I has been shown

to be preferentially blocked in HeLa cells.[52] Arrest of RNA polymerase II at platinum-DNA lesions has been demonstrated *in vitro*,[53] in extracts,[51] and *in cellulo*[54] in mammalian cells. This arrest is caused by the inability of the platinum-DNA lesion to enter the active site of the polymerase. In HeLa cell nuclear extract cisplatin treatment was shown to cause dose-dependent inhibition of splicing. This inhibition was judged to occur during the initial stages of spliceosome assembly on pre-mRNA.[12] In addition, cisplatin treatment has also been shown to inhibit splicing in the protein-independent self-splicing Tetrahymena rRNA, possibly through the formation of an interstrand cross-link.[55]

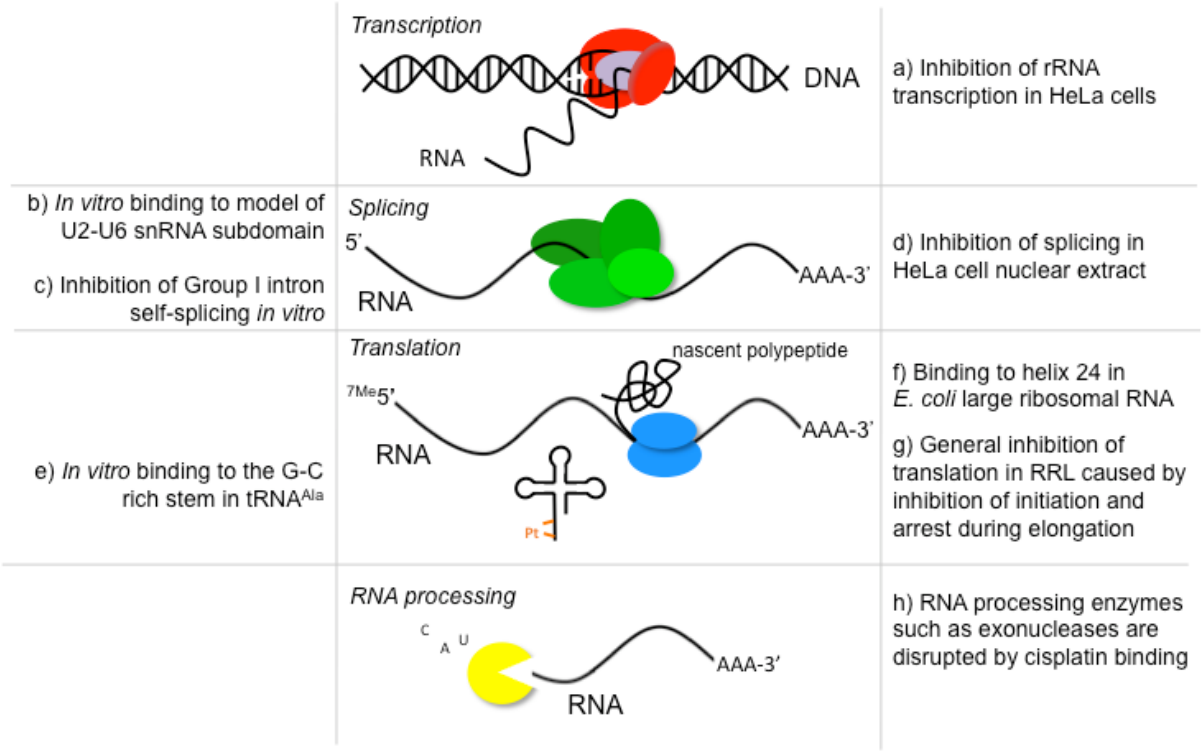

Figure 1.4. RNA processes inhibited by cisplatin treatment as determined by *in cellulo* and *in vitro* studies. References: a) 53, 54 b) 62 c) 55 d) 12 e) 66, 67 f) 61 g) 13, 56, 57 h) 60.

Rabbit reticulocyte lysate has been used to study the effect of cisplatin on mRNA, the translation machinery, and the resulting protein synthesis. In work done by Rosenburg and Sato incubation of mRNA with cisplatin inhibited translation with an IC_{50} of 39 M. Analysis of the peptide products showed greater inhibition of longer peptide sequences, indicating an obstruction of the elongation process.[13,56] When the extracts themselves were incubated with cisplatin, inhibition of protein synthesis was observed, but to a lesser extent. There was also a decrease of polysome intensity. This decrease, combined with the biphasic kinetics of inhibition, matched the effects of NaF, an inhibitor of translation initiation. This was interpreted to mean that cisplatin treatment of the lysates caused inhibition of the translational machinery at initiation.[13] A later study by Heminger and coworkers found a slightly different result. They observed a steady accumulation of higher order polysomes following cisplatin treatment, leading them to conclude that the translation machinery was inhibited at elongation, not initiation. However, the intensity of the polysome fractions appears to decrease following cisplatin treatment. Therefore it is likely that both effects are taking place.[57]

RNA nucleases are important in the RNA processing machinery, as well as the RNA surveillance and degradation machinery.[58,59] Platinum-RNA adducts have been shown to inhibit the activities of 5'-to-3' and 3'-to-5' exonucleases and purine-specific endoribonucleases *in vitro*.[60] Primer extension by reverse transcriptase has also been shown to be inhibited by platinum adducts.[60,61]

Specific Pt Adducts Formed on RNA

The formation of platinum adducts on RNA following cisplatin treatment has been studied kinetically on hairpin oligonucleotides, and mapped on hairpins, tRNA, and rRNA. The kinetics of the reaction of *cis*-$[PtCl(NH_3)_2(OH_2)]^+$ and two other platinum drugs with RNA and DNA hairpins was studied at pH 6.0 by Elmroth *et al.* using HPLC methodology.[63] The RNA hairpin reacted ~ 2 fold faster than DNA and the rate of reaction between the Pt compounds and both RNA and DNA showed a significant dependence on the monovalent ion concentration, with decreased reaction rate at higher monovalent ion concentrations. This dependence was more pronounced for RNA than DNA.

Early studies sought to identify platinum binding sites in $tRNA^{Phe}$ using pre-formed crystals. Sundarlingham and coworkers identified two adducts in the D arm of the tRNA at relatively low 5.5Å resolution.[64] Later, Dewan reported a 6Å structure with four platinated sites.[65] Elmroth and coworkers have mapped platination sites in cisplatin treated $tRNA^{Phe}$ as well as models of the anticodon loop and acceptor stem.[66,67] They found platinum binding at a G-C rich wobble basepair region in the acceptor stem that is critical for tRNA function. This binding is structurally sensitive and the binding pattern is altered by the introduction of a 5'-terminal phosphate and is inhibited by the replacement of the G•U wobble pair with a G-C base pair. Binding was also observed in the anticodon stem, where the substitution of a natural UG in the terminal loop with a GG increases the rate of platination alters the binding pattern in a manner similar to that observed for DNA.

An *in cellulo* study has been done on cisplatin-treated *E. coli*, locating specific platinum adducts on helix 24 of the 16S subunit of the ribosome by primer extension of extracted RNA.[61] Platinum adducts were located in several non-Watson-Crick base paired regions that were platinated in the presence of competing GG sequences. Taken together the adducts formed in this and the above studies show common features. Binding at purine bases, especially guanine, is strongly favored. Just like DNA, 1,2-d(GpG) intrastrand cross-link are common, especially in duplexed regions, but are also observed in non-duplexed regions. The structural diversity of RNA poses a wider range of possible binding sites and platination can occur in non-Watson-Crick paired regions. Local structure has tremendous influence on the adduct profile.

Measurements of *In Cellulo* Pt Binding Targets

In the context of a cell cisplatin and other Pt(II) drugs have the potential to bind a wide range of molecular targets. These targets may include small molecules like glutathione, membrane phospholipids, RNA, DNA and proteins.[11] An early study by Pascoe and Roberts sought to address which classes of biomolecules are targeted by Pt complexes in living cells by employing atomic absorption spectroscopy (AAS) to assay the amount of cisplatin and its non-pharmacologically active counterpart, transplatin (*trans*-diamminedichloro Pt(II)), bound to the RNA, DNA and protein components of HeLa cells. When considered on a Pt(II) per gram of biomolecule basis, the results of this study show that significantly more Pt is bound to RNA than to either DNA or protein for both Pt complexes. Interestingly, a noticeable difference in cellular uptake between the *cis*- and *trans*- isomers was also observed. At low micromolar concentrations, where only

cisplatin was observed to be cytotoxic, close to twice as much transplatin was found bound to RNA, DNA, and protein fractions, although at higher concentrations this difference was less pronounced. In addition to differential uptake, the isomeric complexes also displayed different extents of DNA interstrand cross-linking; when analyzed by density gradient cisplatin was shown to form 10-fold more interstrand cross-links than transplatin.[68]

A similar and more recent study by Miyahara and coworkers also assayed cisplatin binding to biomolecules in HeLa cells. By measuring the incorporation of ^{195m}Pt radiolabeled cisplatin into the protein, RNA, and DNA fractions of HeLa cell components researchers determined that the majority of ^{195m}Pt was bound to trichloroacetic acid insoluble protein components. Both nucleic acids displayed a similar, however lower, extent of drug binding.[69] When the experiment was repeated using transplatin it was again observed that higher amounts of ^{195m}Pt(II) were bound to all three classes of macromolecules, with the largest increase seen for RNA.[70] In addition to these studies, significant differences in tissue accumulation,[71] cellular accumulation[72,73] and DNA binding[74-78] for different Pt complexes have been observed by AAS and inductively coupled plasma mass spectrometry (ICP-MS). The differences observed in these studies indicate that, as is observed for cisplatin and transplatin, there could be important and pronounced variance in the way different Pt(II) drugs bind to cellular biomolecules, however in all cases RNA was a significant target for Pt(II) drugs.

Platinum Localization in the Cell

Characterizing the spatial distribution of Pt(II) binding within a cell provides additional information regarding which types of the cellular machines and architectures Pt(II) complexes may target. Major cellular targets, with regions important for RNA processes, are highlighted in Figure 1.5 and the accompanying studies are portrayed in Table 1.1. AAS and ICP-MS have been used as tools to measure Pt drug accumulation in several different types of organelles. Cisplatin accumulation in intact mitochondria,[79] and drug binding to mitochondrial DNA have been quantified using AAS and by immunodetection techniques.[80,81,82] Similarly, the accumulation of cisplatin and several other Pt(II) complexes in the nuclei of drug-treated cells has also been measured.[83] More recently, Pt accumulation has been detected in vesicles by ICP-MS following the treatment of cells with cisplatin, carboplatin and oxaliplatin.[84,85] The importance of Pt(II) accumulation in these types of cellular compartments is currently unknown. However, understanding where in the cell Pt(II) drugs bind may provide further information regarding which types of RNA may be targeted by Pt(II) complexes as well as insight into biological processing of drug damaged biomolecules.

Direct imaging techniques have also provided a powerful means to study platinum distribution in treated cells. These techniques divide into two main categories: elemental imaging, which directly measures the location of the Pt atoms in the cell, and fluorescent tagging, which identifies drug binding locations using the fluorescent properties of a covalent Pt(II) conjugated fluorophore.

Elemental Imaging Techniques

Elemental imaging techniques are capable of directly detecting the Pt(II) nuclei while the drug is in a cell and are therefore broadly applicable in the study of Pt(II) localization.[86] The majority of these techniques use characteristic X-ray fluorescence bands to specifically identify Pt(II) in the presence of other physiological metals. Excitation is typically achieved using either an electron beam, as in electron microprobe analysis and X-ray microanalysis, or by using an X-ray beam, as in X-ray fluorescence and synchrotron radiation-induced X-ray emission (SRIXE) studies. A similar technique, electron microscopy, locates Pt via its electron-dense nature.

This range of techniques has been applied to a variety of cancerous and non-cancerous cell lines and tissue samples. The results of these studies are in many cases conflicting; however, it is important to note that the significant variations observed are most likely due to the different cell lines, drug concentrations, and sample preparation techniques used in these studies. In addition, the resolution of elemental imaging is often limited, making identification of Pt accumulation in smaller organelles difficult to observe. It is important to note that in the following summarized elemental imaging studies, the cell lines were continuously treated with Pt(II) complexes for the duration of the experiment, and thus incubation time can be used as a basis for comparison.

Perego and coworkers used electron microscopy to study the early localization of cisplatin in an ovarian carcinoma cell line over times ranging from 5-30 minutes. Platinum deposits were observed at the plasma membrane, nuclear envelope, and in deposits scattered throughout the cytoplasm and nuclear matrices. Interestingly the authors also observed Pt deposits spanning through the membranes themselves.[87]

After 4-5 hr of drug treatment Pt is typically observed to accumulate in cell nuclei where in addition to DNA replication, transcription and critical RNA-processing events also take place. Following 4 hour treatment with cisplatin, Khan and Sadler have observed Pt binding in the nucleolus and on the inner edge of nuclear membrane of HeLa cells using a combination of electron microscopy and X-ray probe microanalysis.[88] Similarly, after 4 hours of drug treatment Kiyozuka et al. also identified Pt binding to the nucleolus and at the periphery of the nucleus in two ovarian carcinoma cell lines. In this study the authors noted Pt(II) accumulation in mitochondria[89] which is supported by similar findings by Meijer et al.[90] who observed Pt-DNA binding in mitochondrial DNA and in dense heterochromatin and granules surrounding the nucleoli. Interestingly, Pt-DNA binding was observed to take place in a cell-cycle dependent manner.[90] In a contrasting study, Ortega et al. reported uniform Pt distribution throughout human ovarian cancer cells following treatment for 5 hr with cisplatin.[91] At longer timepoints, Hambley and coworkers observe that cisplatin, several Pt(IV) prodrugs, and a Br-tagged cisplatin analogue accumulate exclusively in the nucleus of ovarian carcinoma cells.[92,93]

Platinum accumulation in non-cancerous tissues has been studied in order to understand the dose-limiting side-effects of Pt(II) complexes. In these tissues, different platinum accumulation patterns have been observed, which may be relevant in assessing which RNA-dependent processes are likely affected in different tissues. In human fibroblasts treated with cisplatin for 2 hr, Pt preferentially localized to the nucleolus,[94] as is observed in many cancerous cell lines. However, rabbit bone marrow treated with cisplatin for 10 and 20 hr showed Pt accumulation in the cytoplasm, but not the nucleus.[95] In animal models, Pt distribution has been shown to be tissue specific. In a rat model, Pt

accumulation has been observed in the vesicles and microbodies of liver cells and within the microbodies, lysosomes, and nuclear matrix of kidney cells.[96,97]

Fluorescently Labeled Pt Compounds

Fluorescently tagged platinum compounds have been used for visualizing the cellular localization of platinum drugs in real time. These drug conjugates typically utilize the chelating ligand ethylenediamine (en) as an anchor for attaching the labels such as fluorescein.[86] The effects of attaching a large, non-polar fluorophore on the biological distribution and processing of platinum drugs must be taken into account in interpreting these studies.

In one of the first studies of this type, Reedjik and coworkers used a carboxyfluorescein diacetate-tagged [$Pt(en)Cl_2$] complex and monitored localization of the compound within human osteosarcoma cells. In these experiments, cells were treated with the complex for 30 minutes, washed, and subsequently imaged. Initially observed throughout the cell, the Pt(II) complex accumulated in the nucleus after 1-2 h and after 6-8 h the compound started to migrate out of the nucleus and into Golgi bodies. These organelles seem to be the ultimate destination for this compound at extended time points. It is interesting to note that very little difference was observed in how this compound and similar fluorescently-labeled dinuclear Pt(II) compounds localized in an ovarian carcinoma cell line.[98,99]

Howell and coworkers have also used fluorescently-labeled Pt(II) compounds to study platination in a human ovarian carcinoma cell line. Following treatment with low micromolar concentrations of the complex, the Pt(II)-fluorophore is observed at the

periphery of the cellular membrane, in the nucleus, and in small vesicular structures scattered throughout the cytoplasm. Supporting biological assays show that while the Pt(II)-fluorophore conjugate is ~4-fold less potent that cisplatin, Pt(II)-resistant cell lines are similarly insensitive to the two complexes suggesting that the complexes may be similarly processed *in vivo*.[100] Further work by Howell and coworkers has used fluorescent Pt(II) complexes in concert with specific small molecule inhibitors to show that these compounds were first sequestered by lysosomes, subsequently transferred to Golgi apparatus and finally into secretory vesicles.[101] The accumulation of Pt(II) complexes in Golgi bodies has similarily been observed by Gottesman and coworkers using a different Pt(II) fluorophore-cisplatin conjugate in the course of studies which also identified platination occurring at nucleosomes and within the nucleolus.[102] In this case, the Pt(II)-fluorophore accumulated more in the cytosol than within the nucleus for a 2 h treatment.

This approach of fluorescently tagging Pt drugs has produced, over several studies, a more uniform picture of Pt(II)-conjugate localization than has been observed from the direct Pt(II) imaging-based techniques, although the influence of the attached fluorophore may affect the outcome of these studies. Nonetheless, these findings combined with those of the elemental imaging techniques are beginning to form a picture of the cellular components involved in platinum binding and processing, particularly for cancerous cells. Initially cisplatin and other Pt(II) drugs enter the cell and accumulate to varying degrees in the vesicles and organelles of the cytoplasm, including lysosomes, Gogi, and mitochondria. From there Pt enters and accumulates in the nucleus, often accumulating along the periphery of the nucleus and in nucleoli. Depending on the

treatment conditions and cell type this nuclear accumulation may become greater than cytoplasmic accumulation at 1-4 hr. Finally, export from the cell may involve the Golgi and vesicles of the secretory export pathway.

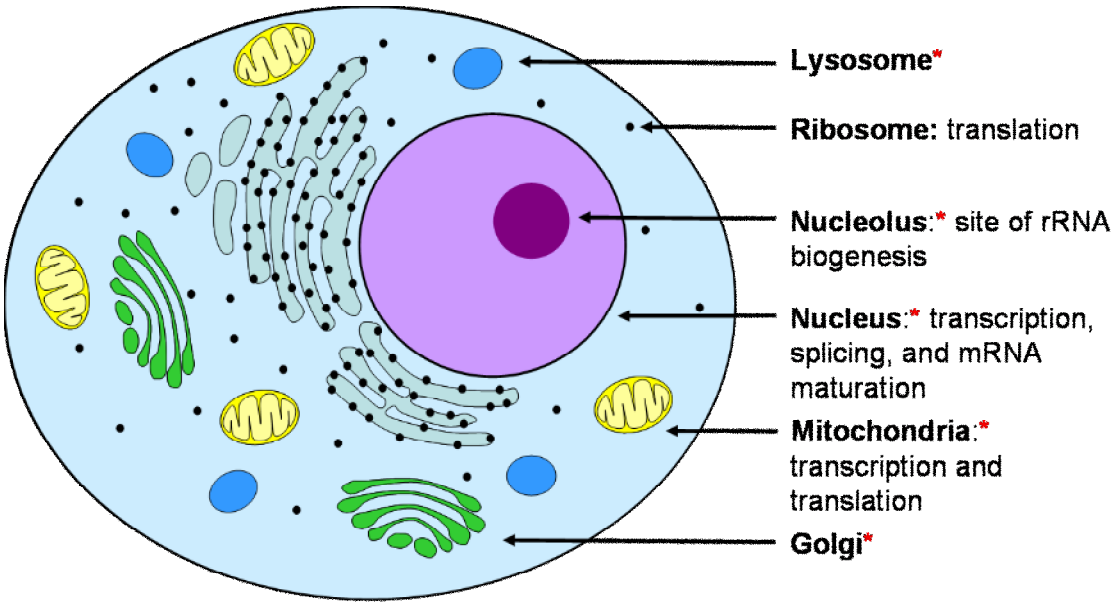

Figure 1.5. The organelles that accumulate Pt drugs in cancerous cells (indicated with a red star) and the locations of important RNA processes within the cell. References are given in Table 1.1.

Table 1.1. Organelles in Which Pt(II) Drug Accumulation Has Been Identified

Organelle	***Pt accumulation observed by elemental imaging***	***Pt accumulation observed by fluorescent label***
Nucleus	[87-93, 96]	[98, 100-102]
Nucleolus	[88-90, 94]	[102]
Mitochondria	[89, 90]	[101]
Lysosome	[97]	[101]
Golgi	Not observed	[98, 101, 102]

Given these sites of Pt accumulation (summarized in Figure 1.5 and Table 1.1), it likely that particular RNA targets for Pt(II) drugs are located in the cytoplasm at early timepoints and are then located in the nucleus, nucleolus, and mitochondria at later times. In these studies the nucleolus, the site of rRNA biogenesis, is a target that has a

particularly heavy Pt accumulation. In addition the transcription, splicing, and mRNA maturation that occur in the nucleus are also possible targets, as are the transcription and translation that occur in mitochondria. Pt complexation may disrupt any or all of these important RNA-based processes. In addition, because of their location in the cytoplasm, ribosomes, tRNA, and translation may be early targets even though they are not associated with sites of specific Pt accumulation.

NAMI-A

As mentioned above, ruthenium anticancer drugs in general have multiple oxidation states and favorable ligand exchange kinetics that take place on order of minutes to days, granting high kinetic stability.[8] Redox and ligand exchange chemistry are considered important to the mechanism of action of NAMI-A. When NAMI-A is dissolved in water it undergoes a series of aquation reactions in which the chloride, Im, and DMSO ligands all can be lost (Scheme 1.2).[103,104] Typically, when in the initial Ru(III) oxidation state the Im ligand is retained, while the chloride and DMSO ligands are lost.[103,104] There is some disagreement in the literature as to whether the chloride or DMSO ligand is lost first. Solution conditions such as pH and chloride concentration have an effect on the aquation as well. Aquation proceeds more rapidly at pH 7.4 than at 6.0, with a 20 min half-life for the first aquation reaction at pH 7.4 and a 2 h half-life at pH 6.0 (25 °C).[104] In addition, at pH 6.0 the DMSO is hydrolyzed first, while at pH 7.4 both the chloride and DMSO are hydrolyzed in the initial aquation step.[104] The presence of chloride can slow aquation, but this is a less pronounced effect than observed for cisplatin and high chloride concentrations cannot completely repress NAMI-A

aquation.[104] Once aquated, further complexity is added by the equibria between the aqua and hydroxo ligands, producing a wide range of possible active species in solution.

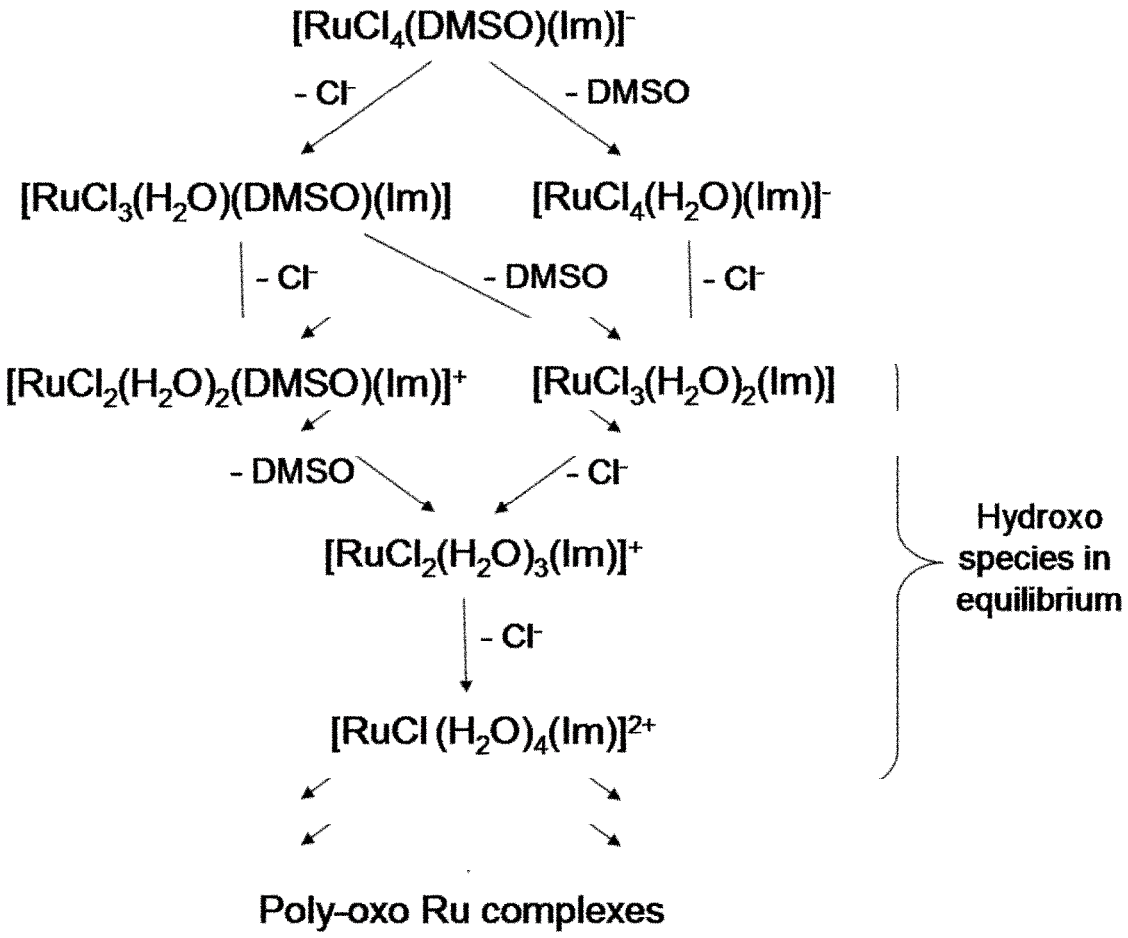

Scheme 1.2. The most commonly observed products of NAMI-A aquation.

The reduction potential of NAMI-A is +0.016 V vs. standard calomel electrode (SCE) in pH 7.4 phosphate buffer,[105] and as such, reduction from Ru(III) to Ru(II) is electrochemically attainable by the plasma and cellular reducing agents ascorbate and glutathione. The reduced Ru(II) species undergo aquation at a faster rate and demonstrate

a greater tendency to lose the chloride and Im ligands, while retaining the DMSO ligand.[106]

It is not know for certain which Ru species are responsible for the antimetastatic activity caused by NAMI-A treatment, but several aquated and reduced species, including $[Ru(III)Cl_4(H_2O)(Im)]^-$, have been shown to be active *in cellulo* and *in vivo*.[107] In addition, the tumor environment itself presents unique features. In tumors the density caused by the rapidly dividing cancer cells combined with insufficient blood flow creates a hypoxic[108,109] and acidic environment[110] which may cause drug activation via reduction.

Many ruthenium drugs also have the ability to mimic iron. NAMI-A is known to bind both transferrin (T_f) and human serum albumin (HSA), and it has been suggested that this is a mechanism by which it is transported to cancer cells, but there is debate about this.[111] In one case, both HSA and T_f heavily treated with NAMI-A (4:1 Ru to protein ratio) were shown to be ineffective at reducing lung metastasis in mice.[112]

NAMI-A exhibits low toxicity, high anti-metastatic activity, and a different mechanism of action than that of platinum drugs.[8] It causes transient tumor cell cycle arrest in the premitotic G2/M phase.[113] In addition, multiple other effects have been implicated in its antimetastatic activity, including interactions with the extracellular matrix, interactions with the cell surface, interference with NO metabolism, and effects on tumor metalloproteinases.[111,114]

NAMI-A is known to bind to DNA. NAMI, a highly related drug with a different counterion ([Na][*trans*-$Ru^{III}Cl_4$(DMSO)(Im)]), has been shown to cause a marked reduction of tumor nucleic acid content.[115] In addition, the cytotoxic activity of NAMI-A has been correlated with Ru-DNA adduct accumulation. However NAMI-A is much less

cytotoxic than cisplatin and, unlike the majority of other ruthenium based anticancer drugs, it is believed that NAMI-A's therapeutic action takes place by a mechanism other than DNA binding or direct cytotoxicity. This mechanism of action may involve tumor cell cycle arrest and binding to other cellular targets.[8,114]

No studies have been done on the effects of NAMI-A treatment on RNA, so it is completely unknown how many Ru adducts are accumulating on RNA, what their effect might be, or whether they may play a role in its mechanism of action. Some studies have been done on the effects of NAMI-A treatment on DNA and the subsequent products formed. Just as for cisplatin, the "soft," nucleophilic N7 site of purine bases, particularly guanine, is the main site of coordination for the hydrolysis products of NAMI-A.[116,117,104] Transcriptional mapping combined with denaturing agarose gel electrophoresis has been employed to discover that fewer intrastrand GG adducts were produced by NAMI-A treatment on double stranded DNA than from cisplatin treatment.[118] The other main adduct formed by NAMI-A in this study is most likely a monofunctional adduct. In addition, this study demonstrated that fewer interstrand cross-links were formed in dsDNA from NAMI-A treatment than from cisplatin treatment. *In vitro* studies have used calf thymus or plasmid DNA to compare the effects of NAMI-A and cisplatin treatment on global measures of DNA structure such as thermal denaturation or circular dichroism spectroscopic signatures. The results demonstrate less overall structural effects following NAMI-A treatment, which could be due to a greater number of Ru monoadducts formed.[119,120] The structural causes of this altered adduct profile are unknown. Taken together, these results suggest that for RNA a preference for purine bases can be expected, and that a different adduct pattern than that observed for cisplatin treatment

should be expected. Based on the DNA results, there could be a higher proportion of monofunctional adducts (which are expected to have less impact on RNA structure and function). However it is also possible that the wider variety of structures available in RNAs may offer binding geometries more suitable for the forming cross-links than those offered in canonical B-form DNA.

Bridge to Chapter II

In this dissertation the effects of anticancer metallodrugs on RNA were investigated with two drugs: cisplatin and NAMI-A. Cisplatin was chosen because it is the most studied anti-cancer therapeutic and it is known to bind to RNA. In addition cisplatin has been shown to be able to induce nuclear-independent apoptosis in endonucleated mouse proximal tubule cells, suggesting the presence of alternative targets from nuclear DNA.[121] NAMI-A is a particularly promising Ru anticancer drug which is in Phase Two of clinical trials. It was chosen because is known to bind to DNA (RNA binding has not been studied), but it has a different mechanism of action and different nucleic acid binding properties than cisplatin. Both *in vitro* and *in cellulo* studies were done to characterize the interaction of these drugs with RNA.

The following chapter focuses on cisplatin, describing *in vitro* kinetic and mapping studies of cisplatin induced cross-linking across an internal loop in a model of the active core of the spliceosome that were aimed at characterizing a novel RNA-platinum binding mode.

CHAPTER II

RAPID CROSS-LINKING OF AN RNA INTERNAL LOOP BY THE ANTICANCER DRUG CISPLATIN

This chapter covers kinetic studies comparing the platination rate of RNA and DNA oligonucleotides, mapping experiments that localized the platinum binding sites, and MALDI-MS data that demonstrate the stoichiometry of the platinated products. It includes important contributions from Dr. Erich G. Chapman and Prof. Victoria J. DeRose. I performed the kinetic studies, prepared the samples for the MALDI-MS experiments, and co-wrote the manuscript. Dr. Erich G. Chapman ran the MALDI-MS samples, performed the mapping experiments, and co-wrote the manuscript. Prof. Victoria J. DeRose guided this project and provided significant editorial feedback. This project was started by Prof. Victoria J. DeRose at Texas A&M University and the first studies were carried out by Dr. Janell E. Schaak. The main construct in this study, a model of a subdomain of the active core of the spliceosome, was designed and characterized by Sarah Tate and Dr. Janell E. Schaak. Reproduced with permission from Hostetter, A. A.; Chapman, E. C.; DeRose, V. J. *J. Am. Chem. Soc.* **2009**, *131*, 9250-9257. Copyright 2009 American Chemical Society.

Introduction

Cisplatin (*cis*-diamminedichloroplatinum(II)) is the flagship compound for a series of platinum(II) anti-tumor agents employed in the treatment of a wide range of cancers.[1-3] Cisplatin activity involves intracellular exchange of the labile chloride ligands

and ultimate coordination to "soft" biomolecular donor sites. *In vivo*, cisplatin is known to bind to multiple targets including DNA, RNA, proteins, and small-molecule ligands. Drug binding to adjacent purines on genomic DNA has been linked to the induction of apoptosis, a foundation of antitumor activity. Despite their prevalent use, a comprehensive understanding of additional drug-related biological processes is still forming for the platinum antitumor compounds.

Early studies that are often cited in identifying DNA as a target for cisplatin reveal that, on a per nucleotide basis, drug binding to DNA and RNA is roughly equivalent.[4,5] Additional studies have shown that platinum treatment is capable of interfering with transcription,[6-8] and that critical RNA-dependent activities such as splicing[9] and translation[5,10,11] are inhibited when measured in cell extracts. Combined, these studies suggest that cisplatin binding to RNA may contribute to the drug's *in vivo* effects. A limited number of studies have presented further details concerning interactions of cisplatin with RNA. Elmroth, Chow, and coworkers have previously communicated enhanced reactivity and more pronounced dependence of reaction rate on ionic conditions for the reaction of a 13nt RNA hairpin in comparison with a DNA analogue.[12] Elmroth and coworkers have additionally suggested binding locations for cisplatin near the G•U wobble pair in a $tRNA^{Ala}$ acceptor stem,[13,14] and have explored platinum-RNA adducts for directing RNA silencing.[15] Cisplatin has been shown by Danenberg and coworkers to inhibit *in vitro* activity of a Group I intron ribozyme.[16] Very recently, Rijal and Chow have reported cisplatin as a structural probe to identify accessible purine bases in bacterial ribosomes.[17] These studies suggest intriguingly selective cisplatin-RNA reactivity, and call for more detailed kinetic analyses and

comprehensive characterization of the nature of the platinated products in complex RNAs.

A common characteristic of naturally occurring metal sites in RNA is the involvement of ligands that are distant in primary sequence but brought into proximity in the folded RNA structure.[18-20] By cross-linking two such ligands, cisplatin-induced chelation, whether in naturally occurring metal sites or novel target sites, has the potential to inhibit activities that depend on the dynamic nature of RNA. The spliceosome is an example of an RNA machine that is dependent on dynamic rearrangements for function.[21,22] One key step in spliceosomal function is the formation of a complex between the U2 and U6 snRNAs that is implicated in the first step of the pre-mRNA splicing.[23] Here we provide an *in vitro* analysis of the reaction between aquated cisplatin and a 41nt RNA construct termed BBD (*b*ranch-*b*ulge *d*omain) that contains the purine-rich internal loop from U2 and U6 RNA strands (Figure 2.1).[24] We show that platinum forms a novel intrastrand cross-link across the internal loop of BBD and an interstrand cross-link in a two-piece construct. Additionally, we report that, under biologically pertinent ionic conditions, platination of both BBD and a related 40 nt RNA hairpin is ~5-fold faster than for a DNA hairpin analog. MALDI-MS data are presented that complement the conclusions from our biochemical studies. Taken together, these results indicate facile cisplatin-induced adduct formation across an RNA internal loop and fast platination kinetics of RNA oligonucleotides.

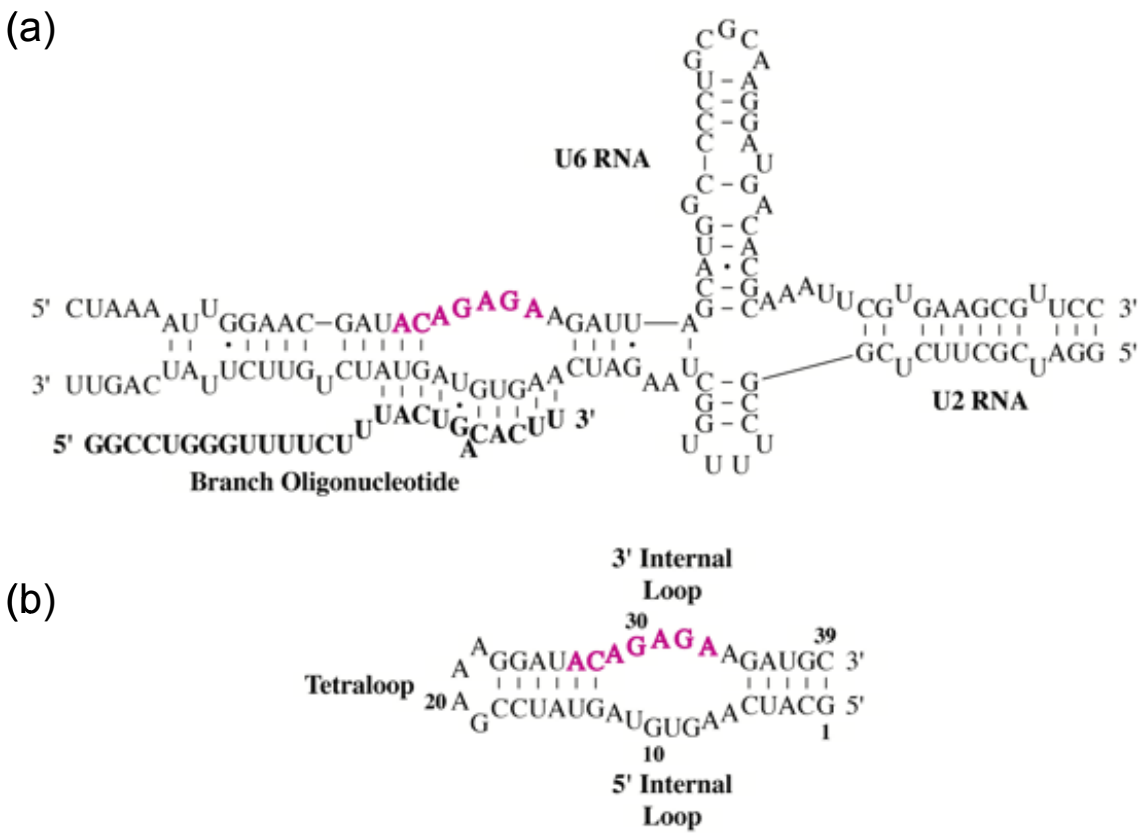

Figure 2.1. **(**a) The proposed secondary structure of a human U2:U6 snRNA core complex including bound branch oligonucleotide.[18] Conserved nucleotides are in pink. (b) Predicted secondary structure of the BBD RNA subdomain used in this study, with invariant nucleotides again highlighted in pink.

Evidence of Cisplatin-RNA Cross-Linking

RNA and DNA oligonucleotides used in this study are shown in Figure 2.2a. The BBD RNA subdomain contains a purine-rich internal loop flanked by helical regions, whereas the RNA and DNA hairpin sequences (RNA HP and DNA HP) are fully base-paired. In previous studies, reaction of RNA or DNA with cisplatin has resulted in product species that are typically observed to migrate more slowly when analyzed by denaturing polyacrylamide gel electrophoresis (dPAGE).[25,26] Slower migration of platinated oligonucleotides is likely due to added molecular weight and a decrease in the

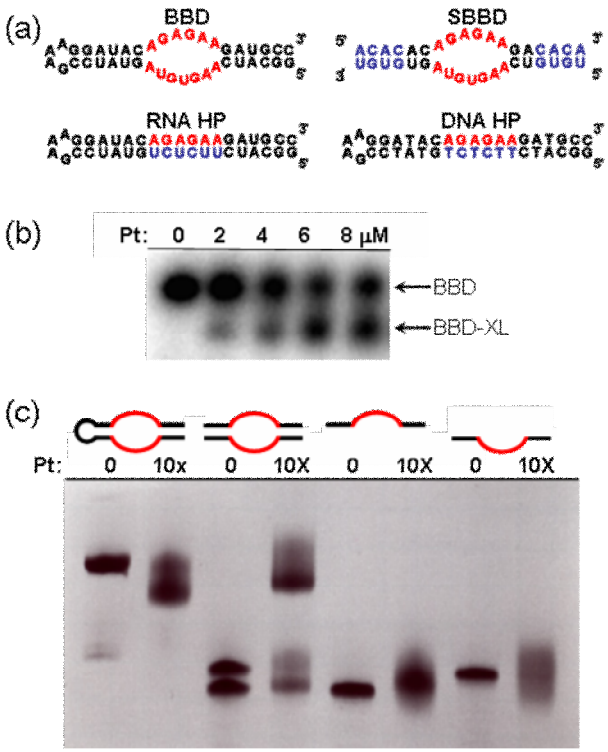

Figure 2.2. (a) Oligonucleotide sequences and predicted secondary structures. The BBD internal loop is highlighted in red. Differences in sequence relative to BBD are shown in blue. (b) Formation of a higher-mobility BBD product upon platination of BBD. (c) Confirmation of cisplatin-induced cross-linking in BBD internal loop sequence, showing products of platinum treatment with (i) BBD, (ii) SBBD hybrid, and (iii) individual strands of SBBD. Conditions: (b) 0.2 μM 5' ^{32}P-labeled BBD treated with indicated concentrations of cisplatin for 1.5 h in deionized water, analyzed by 18% dPAGE, and visualized by autoradiograph; (c) 20 μM (0.2 nmol) RNA reacted with 10x cisplatin (200 μM) in 5 mM TEA (pH 7.8), 12-15 hr, 37 °C, analyzed by 20% dPAGE, and visualized by staining with methylene blue.

overall charge of the nucleic acid through binding of a $[Pt(NH_3)_2]^{2+}$ fragment. By contrast, the reaction of cisplatin with BBD results in a product species with higher mobility (Figure 2.2b). Faster mobility under denaturing conditions may be caused by intrastrand cross-linking,[27,28] which was hypothesized to occur across the purine-rich internal loop region of the BBD RNA. In order to test this hypothesis, the BBD internal

loop sequence was embedded between two new duplex sequences, creating a two-piece "split" BBD duplex (SBBD, Figure 2.2a). Platination of SBBD results in cross-linking of the two strands, as observed unambiguously by dPAGE (Figure 2.2c). Platination of the individual upper or lower SBBD strands does not result in a cross-linked species, although the presence of secondary platination sites is indicated by the dispersion of the dPAGE product bands (Figure 2.2c). These data indicate that cisplatin creates a cross-link across the internal loop of BBD RNA.

Identification of Cross-Linked Nucleobases

In order to identify the specific bases involved in formation of an intrastrand cross-link, the proposed cross-linked product (BBD-XL) was isolated following dPAGE and mapped by partial alkali hydrolysis. Using 5' end-labeled RNA, normal hydrolysis products are expected to be observable up to the 5' side of the cross-linked site.[28-30] Hydrolysis products that contain the cross-linked site will result in significantly higher molecular weight species and unusual gel mobilities, leaving a gap in the hydrolysis ladder following the 5' cross-linked site.[28-30] As displayed in Figure 2.3, clear BBD-XL hydrolysis products are observed for nucleotides 3' to A_8 but not at G_9, identifying G_9 as the major 5' site involved in the internal cross-link. An additional faint band at U_{10} suggests G_{11} as a minor secondary site for platinum-induced cross-linking. In the cross-linked species generated using the two-piece SBBD complex, the site equivalent to G_9 was again identified as one major adduct site (Figure A.1, Appendix A). Using this SBBD construct, hydrolysis mapping also identified the site corresponding to G_{31} as the cross-linking partner on the other side of the internal loop (Figure A.2, Appendix A).

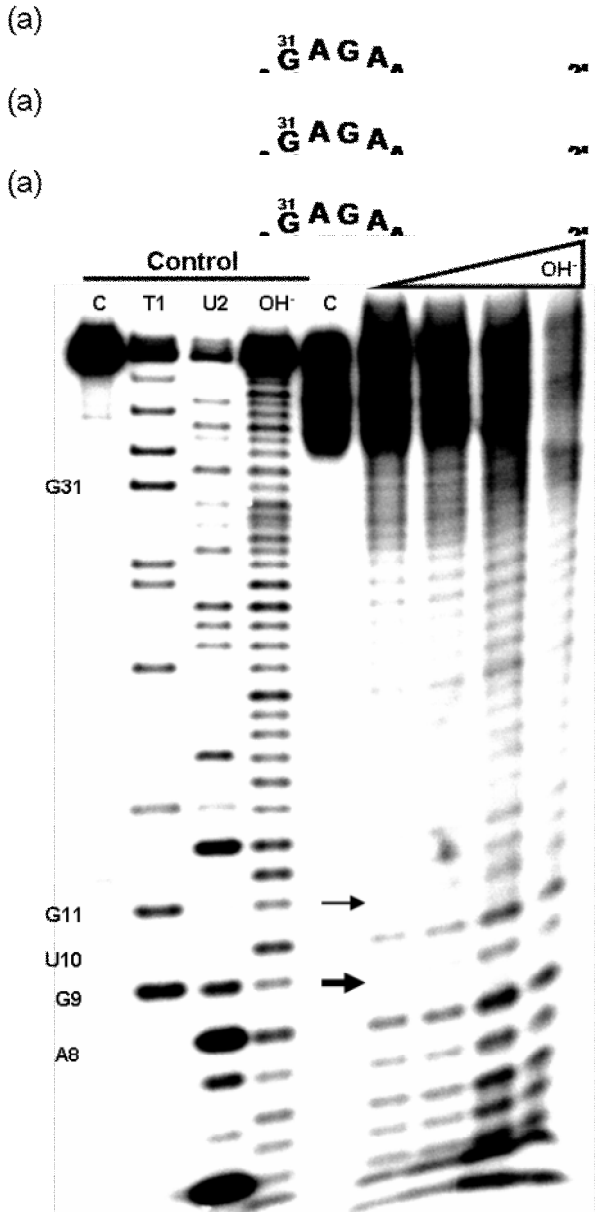

Figure 2.3. (a) Secondary structure of BBD representing the location of the cisplatin-induced cross-link found in BBD-XL. (b) Cleavage products produced by the alkali hydrolysis of isolated BBD-XL. Lanes from left to right. Control lanes (untreated BBD RNA)- **C:** control 5'-end-labeled untreated BBD. **T1:** G-specific sequence ladder generated by partial nuclease digestion by RNase T1. **U2:** A-specific sequence ladder generated by partial nuclease digestion by U2 RNAse. **OH^-:** Reference alkali hydrolysis ladder. BBD-XL lanes- **C:** dPAGE-isolated BBD-XL. **OH^- Lanes:** dPAGE-isolated BBD-XL treated under alkali hydrolysis conditions for increasing amounts of time (see Methods). Arrows indicate major (thick arrow, G_9) and minor (thin arrow, G_{11}) sites of platinum coordination.

The identification from dPAGE-isolated products of the intrastrand cross-link in BBD and the analogous interstrand cross-link in the SBBD hybrid strongly suggests that internal loop cross-linking is a major structural determinant for altered gel mobility upon platinum coordination to BBD.

Cisplatin-RNA Reaction Rates

The *in vivo* relevance of cisplatin-RNA reactions, including the internal loop cross-linking reaction observed here, depends in part on their rates relative to adduct formation with DNA or other cellular targets. In evaluating the reaction rates of cisplatin with the oligonucleotides of Figure 2.2a, kinetic studies were performed at 37 $^{\circ}$C and in a background of 0.1 M $NaNO_3$/1 mM $Mg(NO_3)_2$ in order to approximate cation competition *in vivo.* Nitrate salts were used instead of chloride salts to prevent bias of the observed reaction rates due to an increase in the cisplatin anation rate.[31] Because the aquation of cisplatin has been shown to be the rate-limiting step for reactions with oligonucleotides under similar conditions, cisplatin was aquated by reaction with $AgNO_3$ immediately before use.[32] RNA concentrations of 0.1 μM and platinum concentrations of at least 125-fold excess were used to ensure pseudo-first order conditions for the reaction (Figure A.4, Appendix A). Reaction products were analyzed following separation by dPAGE and autoradiography. Under these conditions, all data fit well to a single exponential function, indicating that a single rate-limiting step dominates the kinetics of product appearance in each case.

In addition to monitoring internal cross-link formation in BBD, reactions of aquated cisplatin with two related hairpin structures were monitored. RNA HP and DNA

HP (Figure 2.2a) retain the flanking helical and terminal loop sequences of BBD but replace the internal loop region with a fully base-paired sequence. These hairpin constructs provide control sequences having similar base composition, length, and terminal loops to those of BBD. Reaction of aquated cisplatin with both HP constructs results in products that migrate more slowly, in contrast to the faster-migrating cross-linked species produced with BBD (Figure 2.4a). As observed from Figures 2.4a and 2.4b, both RNA sequences (BBD and RNA HP) react at similar rates of k_{obs} = 9.8(1.0) × 10^{-5} and 8.3(2) × 10^{-5} s^{-1} respectively in 50 μM CP, pH 7.8 (Table A.1). Product formation for the DNA construct is 5-6 fold slower, with an observed rate constant of 1.7(2) × 10^{-5} s^{-1} under identical conditions. The calculated second-order rate constants are k_{rxn2} = 2.0(2), 1.7(3), and 0.33(3) M^{-1} s^{-1} for BBD, RNA HP, and DNA HP respectively.

Reaction rates were also investigated, under identical buffer conditions, for the two-stranded SBBD hybrid substrate for which product formation results in a clearly-separated cross-linked species (Figure A.1c and A.3, Appendix A). For the SBBD, a pseudo-first-order rate constant of k_{obs}= 5.2(3) × 10^{-5} s^{-1} and a calculated second-order rate constant of k_{rxn2}= 1.1(1) M^{-1} s^{-1} were obtained in 50 μM aquated cisplatin (Figure A.3 and Table A.1, Appendix A). These values are approximately 50% of those determined for BBD, but still reflect faster reaction rates than observed for the DNA HP. A likely explanation for the slower reaction rate observed for intermolecular cross-linking of the SBBD construct in comparison with intramolecular cross-linking in BBD is the incomplete hybridization of the SBBD strands under these reaction conditions (see Materials and Methods). Nonetheless, the fact that similar values are observed for cross-

linking in both BBD and the two-piece SBBD suggests that similar rate-limiting steps guide the internal loop cross-linking reaction regardless of RNA construct.

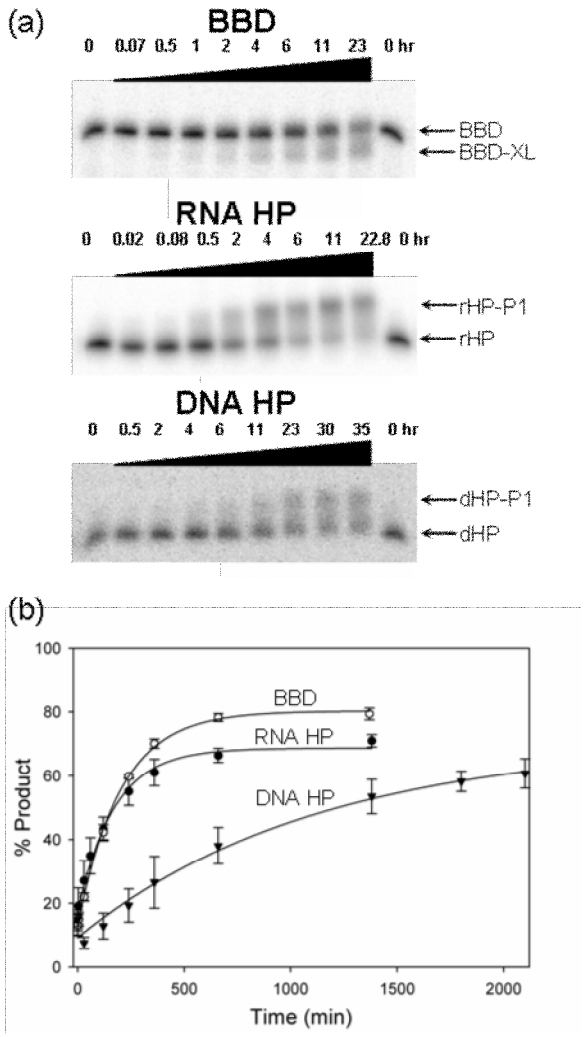

Figure 2.4. (a) Time-dependent product band appearance following treatment of radiolabeled RNA and DNA substrates with aquated cisplatin and analysis by dPAGE. Product bands are labeled BBD-XL, rHP-P1, and dHP-P1 for BBD, RNA HP (rHP), and DNA HP (dHP) respectively. (b) Comparison of the reaction rates of aquated cisplatin with BBD (open circles), RNA HP (filled circles), and DNA HP (triangles). Data are fit to a pseudo first-order rate expression as described in Materials and Methods. Conditions in (a): 0.1 μM oligonucleotide, 50 M aquated cisplatin, 100 mM $NaNO_3$, 1 mM $Mg(NO_3)_2$, and 5 mM TEA (pH 7.8) at 37 °C.

The reactions of aquated cisplatin with BBD and SBBD are pH-dependent, increasing in rate as the pH is lowered. At pH 6.8, second-order rate constants of 8.5(7) and 6.8(2) M^{-1} s^{-1} are measured for BBD and SBBD, respectively (Table A.1, Appendix A, data not shown). Based on known protonation equilibria for aquated cisplatin species, this rate enhancement likely reflects protonation of a cisplatin hydroxide ligand to aqua ligand on platinum(II), and is a closer approximation to rates that might be expected for *in vivo* conditions.

Analysis of Platinated RNAs by MALDI-MS

As described above, platination of the RNA and DNA domains used in this study results in products that have distinctly altered mobilities when analyzed by dPAGE. To further analyze these products, MALDI-MS was used to identify platinum-oligonucleotide species[33] in samples isolated from the dPAGE gels. MALDI-MS data for the RNA and DNA HP sequences reacted for 5 h at a ratio of 5:1 platinum/oligonucleotide are shown in Figure 2.5a. Products containing $[Pt(NH_3)_2]^{2+}$ adducts appear at the oligonucleotide mass plus increments of 229 amu. Additional lower-intensity peaks are often present at ~+17, +23 and +39 amu that are ascribed to residual $H_2O/OH/NH_4^+$, Na^+, and K^+, respectively. These features appear in untreated RNA as well as platinated RNA, and their presence along with the breadth of the features precludes identification of $[Pt(NH_3)_2X]$ (X = H_2O, OH^-, or Cl^-) species. Although MALDI-MS is not precisely quantitative, comparison of relative intensities within

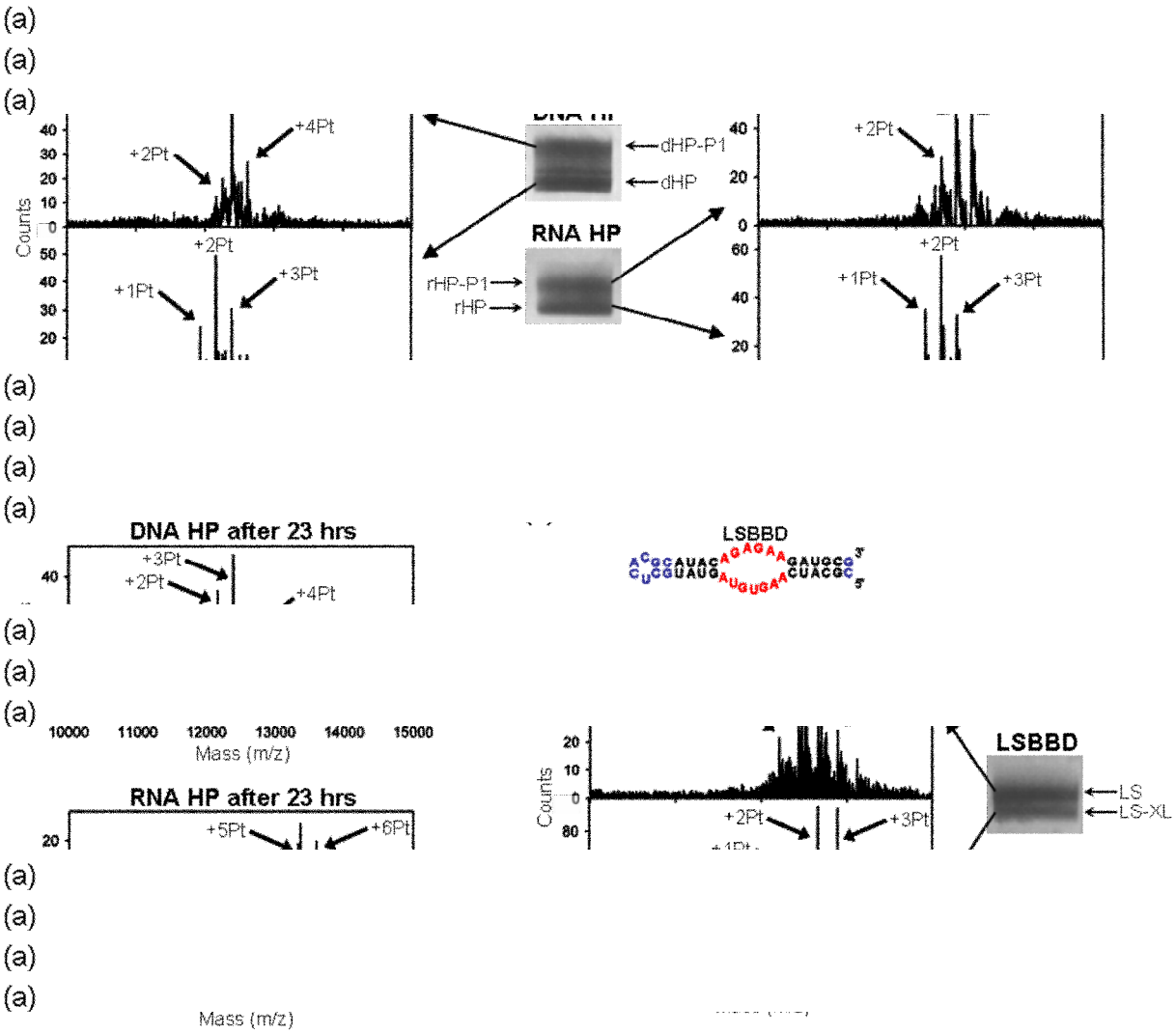

Figure 2.5. (a) Positive-ion mode MALDI mass spectra of products following aquated cisplatin treatment of the RNA HP and DNA HP and isolation via dPAGE. Product bands are labeled rHP-P1 and dHP-P1 for RNA HP (rHP), and DNA HP (dHP), respectively. (b) Positive-ion mode MALDI mass spectra of the products of 23 h reactions of RNA HP and DNA HP with cisplatin under the reaction conditions used for Figure 2.4. (c) Sequence and predicted secondary structure of LSBBD. The BBD internal loop is highlighted in red. Differences in sequence relative to BBD are shown in blue. Image and subsequent MALDI-MS of the two main electrophoretic bands resulting from cisplatin treatment of LSBBD (LS), with (LS) product band is labeled LS-XL. Conditions: (a) Reactions were performed with 30 M oligonucleotide, 150 M aquated cisplatin, 100 mM $NaNO_3$, 1 mM $Mg(NO_3)_2$, and 5 mM MOPS (pH 6.8) at 37 °C for 5 h. The bands were separated by 20% dPAGE, stained with methylene blue, and then excised. The MALDI was performed in 3-hydroxypicolinic acid. (c) Same as in (a), except that the reaction contained 90 M cisplatin.

identically treated samples provides qualitative information on relative populations of the major RNA-platinum adducts.

The data in Figure 2.5 show that RNA and DNA HP samples, treated under the reaction conditions described above, separate into upper and lower dPAGE bands that both contain platinated oligomers. As expected from their slower electrophoretic mobility, samples isolated from the upper band of these gels show a higher extent of platination. At a ratio of 5:1 Pt/oligomer, species with bound 1-3 $[Pt(NH_3)_2]^{2+}$ are present in the lowest-running dPAGE bands, whereas the higher bands contain oligomers with 2-4 bound $[Pt(NH_3)_2]^{2+}$ ions (Figure 2.5a). Consistent with the observation that RNA exhibits a faster reaction time, a higher population of the +4 $[Pt(NH_3)_2]^{2+}$ species is observed for the RNA HP sample than is found for the DNA analogue at the same time point. Faster reaction kinetics with RNA are also evident from bulk analysis of samples that are reacted for 23 hr in the high platinum/oligonucleotide ratios used for kinetic studies. In this case, the bulk DNA HP sample shows an overall adduct distribution that has major populations of 2-3 bound $[Pt(NH_3)_2]^{2+}$, distinctly fewer than the 5-6 $[Pt(NH_3)_2]^{2+}$ in the highest amplitude MALDI-MS peaks for the RNA HP sample treated under identical conditions (Figure 2.5b).

From these data, it is apparent that the products separated by dPAGE all contain multiple platinum adducts. In the case of the mainly helical hairpin samples, the major products quantified for kinetics analysis are separated as a lower-mobility species that contain on average one more $[Pt(NH_3)_2]^{2+}$ ion (Figure 2.5c). Although not a complete study, these data are broadly consistent with a model in which one site on the HP sequence reacts more quickly with cisplatin, and also causes a conformational change

resulting in a distinct lower-mobility species. Slower platination reactions occur at other sites, creating products that are not clearly separated by these dPAGE conditions.

The products of BBD platination were also analyzed by MALDI-MS. If a similar model holds in which one faster-reacting site results in altered gel mobility, then for the BBD reactions, it is predicted that the higher-mobility, cross-linked products will also contain on average one additional $[Pt(NH_3)_2]^{2+}$ ion. An alternative model for reactions of platinum with the BBD sequence is that the cross-linking and non-cross-linking sites react at equal rates, which would result in an equal distribution of platinum in both dPAGE bands. To simplify the MALDI-MS data, a modified BBD sequence that maintains the internal loop but reduces the number of other purine sites was employed (Figure 2.5b). MALDI-MS spectra of platinated LSBBD shows that peaks from the faster-migrating product band are indeed shifted by approximately + 1 $[Pt(NH_3)_2]^{2+}$ fragment (Figure 2.5c). Additional evidence that the gel bands observed for platinated BBD differ by one $[Pt(NH_3)_2]^{2+}$ fragment is provided by the dependence of reaction rates on platinum concentration. With platinum in large excess, the observed reaction rates vary linearly with a slope of 1.1 (r^2 = 1.0, Figure A.4, Appendix A), consistent with a 1:1 ratio between platinum and product.

Discussion

Understanding of the biological roles of RNA has vastly expanded over the last three decades.[34] RNA-based regulation is now known to occur through gene silencing and RNAi pathways,[35,36] as well as through specific binding of small molecules in the structured regions of riboswitches.[37-40] Complex RNA structures support catalytic active

sites,[41] and dynamic RNA-protein rearrangements take place throughout regulatory pathways[42-44] and in complex cellular machineries such as the spliceosome.[22] These factors serve as the basis for the recent push in advancing RNA as a drug target and spur interest in understanding how existing nucleic acid-targeted drugs might act in previously unidentified pathways.[45,46] Cisplatin provides an example of a known DNA-binding compound that might have unique interactions with complex RNA structures. Factors that may be relevant to structurally diverse RNAs have been encountered in studies of platinated DNA hairpins, platinum-cross-linked quadruplex structures, and platinated DNA-protein complexes.[47-53] Additionally, preliminary investigations have already begun to address cisplatin's use as a structural probe and as drug conjugate for targeting RNA.[15,17,54,55]

This report describes cisplatin cross-linking across the internal loop of a 41nt RNA branch-bulge subdomain (BBD) that is derived from the U2:U6 snRNA complex proposed to form the active core of spliceosome (Figure 2.1).[23,24] Cisplatin-induced intramolecular cross-linking takes place between G bases located in opposing sides of the BBD internal loop. In a cellular context, cross-linking of this type could have the potential to disrupt binding of the branch oligonucleotide or dissociation of the U2:U6 complex. It is interesting to note that the 3' side of the BBD internal loop corresponds to an invariant region of the U6 snRNA that is hypothesized to contain essential metal binding sites in the biological complex.[56,57] The ability of cisplatin to compete for pre-organized metal bind sites in RNA is unestablished and presents an interesting possibility for predicting *in vivo* drug binding locations. Further studies will also focus on the sequence requirements and generality of cisplatin-based drug interactions with structured

RNAs. Initial experiments indicate that this cross-linking reaction is tolerant of single base substitutions in the BBD internal loop, but that substitution of G31, the 3' partner in majority cross-link, with non metal-coordinating U results in a slightly different product as reflected by altered mapping data (data not shown). These limited studies indicate that platinum-induced cross-link formation is not strictly limited to internal loops with this exact BBD sequence and is likely to take place in other structured RNAs. In general, cisplatin cross-links in functional RNAs could disrupt a host of cellular processes that rely on RNA's dynamic structure.

Drug-binding kinetics may be an important factor governing the significance of cisplatin-RNA adducts *in vivo*. In order to begin to address this topic, here we compared the *in vitro* reaction rates of similar RNA and DNA oligomers with cisplatin. Somewhat surprisingly, the RNA constructs exhibit reaction rates that are 5-6 times faster than those measured for the DNA construct. In a related study, Elmroth and coworkers observed faster binding by other platinum(II) compounds to a 13nt RNA hairpin in comparison with its DNA analogue. Although that study used different reaction conditions than employed here, most notably lower ionic strength, the reported rate constants are within an order of magnitude of those in Table A.1.[12] Combined, these observations support RNA as a kinetically competitive target for cisplatin.

The application of polyelectrolyte theory to the platination of RNA or DNA suggests a model involving entry of a charged platinum species into the condensed cation atmosphere of a nucleic acid, followed by irreversible monoadduct and diadduct formation. [12,58-60] The range of literature values for the rate of monoadduct formation on duplex DNA by $[Pt(NH_3)_2Cl(OH_2)]^+$ vary from ~0.1-1 M^{-1} s^{-1}.[61-63] From this study, the

calculated second order rate constant for the platination of the DNA HP is 0.33(3) M^{-1} s^{-1} and lies within this range, while the rates observed for the RNA constructs are somewhat faster at ~2 M^{-1} s^{-1} (Table A.1). The observation that similar rates are obtained for monoadduct formation on two structurally distinct RNAs indicates that broader factors such as electrostatic potential and oligomer flexibility likely dictate enhanced reactivity when compared with DNA. Individual contributions of these factors are currently under investigation.

MALDI-MS allows identification of nucleic acids with bound $[Pt(NH_3)_2]^{2+}$ fragments[33] and was used to analyze bulk reaction mixtures and dPAGE isolated oligomers in this study. MALDI-MS analysis of platinated oligomers isolated from dPAGE shows an average of one additional $[Pt(NH_3)_2]^{2+}$ fragment in the product bands. This observation supports a model in which specific sites within each oligomer react quickly with cisplatin and are responsible for the structural distortions leading to altered gel mobility. Previous observations of kinetically preferred sites for platinum adduct formation on DNA have been reported. Enhanced reactivity can be based on electronegativity and target site geometry, as influenced by the nucleotide identity as well as oligonucleotide length, and secondary and tertiary structure.[49,53,64-71] Particularly relevant to this study is the observation of cross-strand adduct formation by $[Pt(NH_3)_2(OH_2)_2]^{2+}$ in telomeric DNA model sequences.[48,53] An even greater variety of platinum adducts might be expected for RNA based on its structural diversity and ability to specifically chelate divalent metals.[18-20]

The biological lifetime of each nucleic acid is an important factor in translating the faster *in vitro* rates observed for RNA in this study into a cellular context. In normal

human cells the most rapidly turned-over class of RNA is mRNA. Median mRNA lifetimes in human cell lines have been reported to be ~10 h, with a wide range of decay rates that vary by ~500-fold.[72] Both tRNA and rRNAs have significantly slower turnover rates, and lifetimes predicted to be on the order of days for average adults.* The lifetimes and abundance of cellular RNAs tsuggest that platinum drug binding could occur on a timescale allowing it to affect RNA processes within treated cells. The types of cellular RNAs that are sufficiently accessible for platinum adduct formation, and the range of cellular consequences that could result from cisplatin interactions with RNA including interstrand cross-linking such as is observed in this study, are topics that remain to be addressed.

Materials and Methods

Nucleic Acid Substrates

All RNAs, except BBD, were purchased from Dharmacon, Inc. DNA was purchased from Integrated DNA Technologies. BBD was transcribed *in vitro* from a plasmid template using T7 RNA polymerase. All nucleic acid substrates were purified by 20% dPAGE, eluted, then desalted and concentrated using Millipore YM-3 Centricon tubes. Subsequent buffer exchange and desalting was often accomplished using GE Healthcare G-25 Microspin Columns.

* Measured turnover rates range from 0.034-0.0048 mol/kg-day for rRNA and 0.46-0.88 mol/kg-day for tRNA.[73-76] Based on the calculation put forth by Petersen and coworkers,[74] this roughly corresponds to 12-29 days for rRNA and 17-29 for tRNA in average adults.

5' End-Labeling

Prior to radiolabeling, the 5' end of BBD was dephosphorylated using Antarctic phosphatase (New England Biolabs). 5'-OH Oligonucleotides were end-labeled with T4 polynucleotide kinase (USB) using γ^{32}P-ATP (Perkin Elmer). End-labeled oligonucleotides were purified by 20% dPAGE followed by overnight elution from excised gel bands. The resulting eluent was ethanol precipitated and desalted or buffer-exchanged as described above.

Cisplatin Aquation

Cisplatin (Sigma-Aldrich) was stored as a 1 mM solution in 10 mM NaCl in the dark at 4 °C. Immediately before use, cisplatin was aquated with 0.95 equivalents of 12 mM $AgNO_3$ (stored in the dark). The aquation reaction was incubated at 50 °C for 1 h, at which time AgCl was precipitated by centrifugation. The supernatant solution was removed and diluted accordingly. Based on ^{195}Pt NMR (data not shown), the main platinum species varied by pH: $[Pt(NH_3)_2Cl(OH_2)]^+$ for pH 6.8 and $[Pt(NH_3)_2ClOH]$ for pH 7.8.

Platination of BBD (Figure 2.2b)

A trace amount of 5'-end labeled BBD with 0.2 μM unlabeled BBD was annealed by heating to 90 °C for 90 s followed by cooling to room temperature, then reacted with 0-40 μM cisplatin in deionized water for 1.5 h at 37 °C. The bulk reaction mixtures were mixed with formamide loading buffer and immediately applied to 18% dPAGE. Results

were imaged using a Molecular Dynamics phosphor screen and scanned on a Molecular Dynamics Storm 860.

Comparative Platination of SBBD and BBD (Figure 2.2c)

Twenty micromolar (0.2 nmol) of BBD RNA, each individual SBBD strand, or the SBBD hybrid was annealed and rested on ice for 30 min. RNAs were then incubated in the presence or absence of 200 M cisplatin (added as a 1 mM solution with 8 mM NaCl) in 5 mm triethanolamine (TEA) for 12-16 hr at 37 °C. Reaction mixtures were analyzed on 20% dPAGE and visualized by staining with methylene blue.

Isolation of 5' End-Labeled, Cross-Linked RNAs

BBD: 5'End-labeled BBD in the presence of 0.1 μM unlabeled BBD was annealed and reacted with aquated cisplatin in 100 mM $NaNO_3$, 1mM $Mg(NO_3)_2$, and 5 mM 3-(N-morpholino)propanesulphonic acid (MOPS) (pH 6.8) at 37 °C for 23 h. Reaction products were isolated via excision from 18% dPAGE. RNA was eluted overnight into deionized water and desalted using in-house prepared G-25 sephadex spin columns (BioRad). SBBD: One 5'end-labeled strand was annealed in 10 μM of the unlabeled complement RNA in 12.5 mM NH_4NO_3 and reacted with 100 μM aquated cisplatin for 23 h. The cross-linked product was excised from 20% PAGE and eluted overnight into deionized water. Following speedvac concentration, SBBD cross-links were desalted using G-25 sephadex spin columns (GE Healthcare).

Hydrolysis Mapping of Cross-Linked RNAs

Trace 5' end-labeled, cross-linked RNAs were dried to completion in the presence of 0.2 pmol unlabeled RNA corresponding to the 5'end-labeled strand. Samples were then resuspended in 50 mM Na_2CO_3/$NaHCO_3$ (pH 9.5), 1 mM EDTA and reacted at 90 °C for times ranging from 5 to 25 min. The reaction was quenched by the addition of 8 M urea, 10 mM sodium citrate (pH 3.5), 0.005% (w/v) xylene cyanol loading buffer and held on dry ice until electrophoresis. The results were analyzed on 15 or 20% dPAGE (BBD and SBBD respectively) then visualized via phosphorimaging.

Reference lanes of 5' end-labeled un-cross-linked RNAs were generated from hydrolysis as above and by partial nuclease digestion by RNase T1 (Ambion) or U2 (Pierce/Thermo Scientific). Briefly, 5'-end-labeled RNA with 0.2 μM of the corresponding unlabeled RNA in 8 M urea, 10mM sodium citrate (pH 3.5), 0.005% (w/v) xylene cyanol was reacted for at 50 °C for 12-15 min with 1U T1 RNase, or 0.2U U2 RNase. Samples were then held on dry ice until electrophoresis.

Kinetic Analysis

Prior to kinetic analysis, 0.1 M oligonucleotide with trace 5'end-labeled material was annealed in buffered solution by heating to 90 °C for 90 s followed by gradual cooling to room temperature or, for the case of the SBBD hybrid, resting on ice for 30 min. Buffers included either 100 mM $NaNO_3$, 1 mM $Mg(NO_3)_2$, 5 mM triethanolamine (TEA) (pH 7.8) or 100 mM $NaNO_3$, 1 mM $Mg(NO_3)_2$, 5 mM MOPS (pH 6.8) depending on desired pH. Freshly aquated cisplatin was added to final concentrations of 13, 25, or 50 M, and the reactions incubated at 37 °C for times ranging from 1 min to 35 h.

Aliquots were removed and stopped by ethanol precipitation or dilution with formamide and freezing. These aliquots were applied to 18-19% dPAGE and visualized by autoradiography. Each kinetic experiment was repeated at least three times. Molecular dynamics ImageQuant software version 5.0 was used to quantify the reaction products from each kinetics experiment. Rate constants were generated from data analysis using SigmaPlot version 8.0.

MALDI-MS

Isolation of platinated oligonucleotides for MALDI-MS analysis: 30 M of an oligonucleotide was annealed in 100 mM $NaNO_3$, 1 mM $Mg(NO_3)_2$, 5 mM MOPS (pH 6.8) and reacted with either 90 M aquated cisplatin for LSBBD or 150 M for RNA HP and DNA HP. Samples were incubated at 37 °C for 5 h, at which time they were applied to 19% dPAGE. Products were stained with methylene blue and excised. Oligonucleotides were recovered via electroelution using a Schleicher and Schuell Elutrap electro-seperation system, concentrated, and desalted. Bulk time-course reactions for MALDI-MS analysis: 0.6 nmol of an oligonucleotide was reacted under identical conditions to those used in kinetics experiments (see above). Reactions were incubated for 1 or 23 h and stopped by ethanol precipitation, dryed, and desalted using G-25 sephadex spin columns.

Oligonucleotide samples (~50-100 pmol) were additionally desalted on C18 ZipTips (Millipore) following the manufacturer's protocol for RNA. RNA was eluted in a matrix solution containing 41 mg/mL 3-hydroxypiccolinic acid and 4.5 mg/mL diammonium citrate then applied to the sample plate. MALDI-MS analysis was

performed on a Waters QTof Premier mass spectrometer in positive ion mode using V-mode optics.

SBBD Thermal Denaturation

Thermal denaturation of SBBD, in a 'kinetics' buffer of 100 mM $NaNO_3$, 1 mM $Mg(NO_3)_2$, 5 mM TEA (pH 7.8), was monitored on a Varian Cary 300 Bio UV-visible spectrophotometer with multicell holder and temperature controller. These data were fit with the accompanying software, giving a T_m of 59 °C and a calculated K_d at 37 °C of 6.8×10^{-9}. Based on this K_d, approximately 60% of the SBBD hybrid would be formed during the kinetic analyses, which used a concentration of 0.1 μM for each SBBD strand.

Bridge to Chapter III

This chapter has described *in vitro* experiments characterizing a novel platinum-RNA cross-link in a subdomain of the active core of the spliceosome. The results of this study motivated us to explore cisplatin-induced RNA platination in the context of a cell. Chapter III describes *in cellulo* studies in *S. cerevisiae* in which Pt accumulation in yeast RNA species was quantified by ICP-MS, and the effects of cisplatin treatment on *S. cerevisiae* were examined using clonogenic and morphologic assays.

CHAPTER III

CHARACTERIZATION OF RNA-PT ADDUCTS IN *S. CEREVISIAE*

This chapter describes *in cellulo* studies of cisplatin treated *S. cerevisiae* in which Pt accumulation in yeast RNA was quantified by ICP-MS, the effects of cisplatin treatment on *S. cerevisiae* were examined using growth and clonogenic assays combined with DAPI and TUNEL staining, and specific platinum binding sites in ribosomes were located with mapping experiments. It includes important contributions from Maire F. Osborn and Prof. Victoria J. DeRose. I performed the ICP-MS experiments, the growth and clonogenic assays, the DAPI and TUNEL staining, and co-wrote the manuscript. Maire F. Osborn did the mapping experiments, and co-wrote the manuscript. Prof. Victoria J. DeRose guided this project and provided significant editorial feedback. This work is in preparation for submission to ACS Chemical Biology. Reproduced with permission from ACS Chemical Biology, in preparation. Unpublished work copyright 2011 American Chemical Society.

Introduction

Cisplatin (*cis*-diamminedichloroplatinum(II)) is a potent antitumor agent that has had a major clinical impact on the treatment of testicular and ovarian cancers since its introduction to the market in 1978. Currently, cisplatin and two other structurally related Pt(II) drugs, carboplatin and oxaliplatin, are used in the treatment regimes of 50-70% of cancer patients.[1] Despite the widespread prescription of cisplatin, a comprehensive description of the precise cellular mechanism of its cytotoxicity is still developing. *In*

vivo, cisplatin forms covalent adducts with multiple biomolecule targets including DNA, RNA, proteins, and small-molecule ligands.[2,3] Drug binding to adjacent purines on genomic DNA has been linked to cell cycle arrest at the G2 phase and the induction of programmed cell death, a foundation of antitumor activity.[4] However, cisplatin treatment has also been linked to the disruption of RNA-based processes such as splicing and translation.[5,6,7] To date, it is unknown if the targeting of non-DNA species by cisplatin, especially RNA, may contribute to or sensitize a cell to the downstream effects of this drug, including the induction of apoptosis.

RNA is chemically similar to DNA, but plays functionally diverse roles in cell regulation and gene expression. In addition to its well-defined functions in translation (mRNA, tRNA, and ribosomes), novel regulatory roles are continuously being defined.[8] These include the discovery of the regulatory roles of siRNA, microRNA, piwi-interacting RNA, and long noncoding RNAs in both transcription and translation. Previously it was thought that RNA damage, whether by free radicals or by anticancer agents, only led to RNA degradation. It is now known that RNA damage is an early event in the pathogenesis of many diseases and that specific kinds of RNA damage can trigger programmed cell death.[9-11] Two such examples are sarcin[10] and ricin,[11] toxic proteins that induce apoptosis through their interaction with the sarcin/ricin loop of the large subunit of the eukaryotic ribosome. Additionally, there is evidence that both ribosomes and tRNA may play specific roles in programmed cell death pathways.[12,13]

It is clear that drug binding to RNA has the potential to impact cell fate via downstream effects on RNA regulatory pathways. While studies with cisplatin show significant *in cellulo* drug accumulation in RNA as well as inhibition of RNA function in

extracts,[2,5-7] specific interaction sites have not been previously determined *in cellulo* in eukaryotes. Here we use *S. cerevisiae* for *in cellulo* analysis of Pt adduct formation on mRNA, rRNA, and total RNA and DNA. *S. cerevisiae* was chosen as a model because it has been used to study a range of anticancer drugs[14] and RNA pathways,[15,16] and is a genetically tractable system for future studies.[17] In this study, the action of cisplatin on *S. cerevisiae* in minimal media was established with full growth curves, clonogenic assays, and tests for apoptotic markers which determined that while cisplatin treatment is highly cytotoxic, under the conditions studied it is not inducing apoptosis. Under defined growth conditions, estimates of in-cell Pt concentrations and the platinum accumulation in mRNA, rRNA, total RNA, and DNA were determined using inductively coupled plasma mass spectrometry (ICP-MS). Interestingly, while similar Pt accumulation was observed in rRNA and total RNA, significantly less accumulated in mRNA. Mapping by reverse transcription demonstrates the formation of specific Pt adducts in ribosomes. Taken together, these data show both the specificity of Pt adduct formation on RNA following *in cellulo* treatment and important differences in the accumulation of Pt on different RNA species.

Cisplatin Treatment Causes Acute Cell Death in *S. cerevisiae*

We first sought to establish defined growth conditions for Pt quantification of RNA species following cisplatin treatment. *S. cerevisiae* has commonly been used as a model system for aspects of cisplatin toxicity, including drug transport, DNA repair, and the genes involved in drug resistance and sensitivity.[18-20] Within these reports, however, the sensitivity of *S. cerevisiae* to cisplatin treatment varies widely. In addition, although

cisplatin causes apoptosis in mammalian systems,[21] to our knowledge this topic had not been addressed for *S. cerevisiae* despite a growing body of work on yeast apoptotic-like cell death pathways.[22] Therefore, we characterized cisplatin cytotoxicity in *S. cerevisiae* (strain BY4741) by growth, survival, and tests for apoptotic markers.

Typically, in human patients cisplatin activation occurs through hydrolysis of the labile chloride ligands and is triggered upon moving from relatively high bloodstream Cl^- concentrations to relatively low intracellular Cl^- concentrations.[23] For cultured cells, however, significant amounts of aquation may take place in the media. In many yeast studies with Pt(II) drugs, growth curves have been established from cultures grown in YEPD (yeast extract peptone dextrose) or other rich media.[24] Under these conditions the highly reactive aquation products of cisplatin may interact with soft sulfur- and nitrogen-containing nucleophiles within the media to effectively sequester the drug, resulting in higher IC_{50} measurements than those observed in mammalian and cancer cell lines (for example, 500 μM in *S. cerevisiae* in YEPD media[20] as compared to 2-40 μM for human cancer cell lines[25,26,27]). To reduce drug sequestering by the media, we assayed drug toxicity in minimal SD (synthetic dextrose) liquid media between 1 and 29 h using 100 μM and 200 μM cisplatin. Full growth curves are shown in Figure 3.1a, demonstrating a moderate (76 ± 8% of control at 29 h) and severe (36 ± 1% of the control at 29 h) reduction in culture density for 100 μM and 200 μM drug, respectively.

The effect of cisplatin on BY4741 cells was also monitored through a clonogenic assay. Following incubation with cisplatin for 1 to 29 h in minimal media, BY4741 cells were plated on drug-free YEPD and colonies were counted following 3 days of growth (Figure 3.1b). The results show a marked decrease in cell viability for both cisplatin

treatment concentrations, being more rapid and severe for 200 µM cisplatin treatment. Although there is a loss of viability after just 1 h of incubation in the drug, the majority of irreversible cisplatin toxicity coincides with the onset of exponential growth. From this standpoint, we have chosen 6 h (Table 3.1) as a relevant timepoint to investigate the distribution of cisplatin-derived Pt species on different RNAs within the cell.

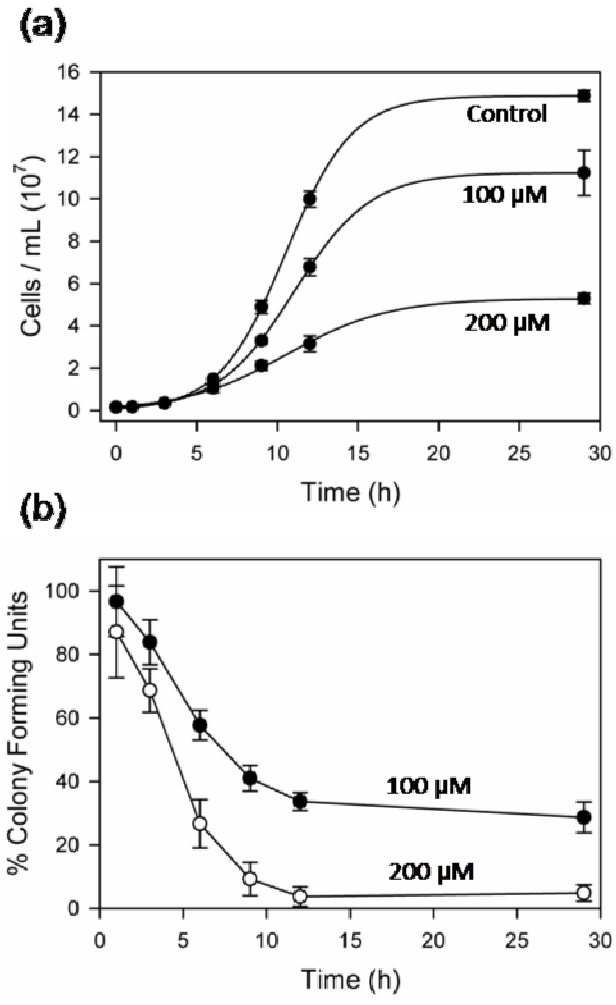

Figure 3.1. (a) Exponential growth curves of yeast continuously treated with 0, 100, and 200 µM cisplatin. Results are averaged from four independent experiments. (b) Survival of yeast treated with cisplatin for the indicated time, measured as percentage colony-forming units (cfu). Results are averaged from three independent experiments.

Table 3.1. Influence of Cisplatin on *S. cerevisiae* at 6 Hours as Compared to the Control

Cisplatin Concentration	100 µM	200 µM
Culture Density	87 ± 6%	71 ± 12%
Cell Viability	58 ± 5%	27 ± 8%

Cisplatin-Induced Cell Death Does Not Proceed Through Apoptosis in BY4741

Cisplatin induces apoptosis in mammalian cells.[21] Cell death via apoptotic pathways has been reported for *S. cerevisiae* when treated with other agents including hydrogen peroxide, acetic acid, ethanol, aspirin, arsenic, and anticancer drugs (bleomycin, valproate, etc.), however it has not been reported for metallodrugs such as cisplatin.[22,28] In order to gain more information about toxicity pathways induced by these drugs, we assayed cell cultures for hallmarks of apoptosis after continuous treatment with cisplatin for 6-12 h. Similar to mammalian systems, yeast apoptosis has been demonstrated to result in chromatin condensation and DNA fragmentation.[29] DAPI DNA staining of BY4741 cells treated with 200 µM cisplatin for 6 h showed significant changes in chromatin morphology from the control (Figure 3.2a). In almost all samples, nuclei were either fragmented and diffuse, or abnormally enlarged. These findings are consistent with an activation of apoptosis, but could be consistent with other forms of programmed cell death.[30] Interestingly, we were directly able to observe cells undergoing cell cycle arrest, a previously observed characteristic of cisplatin treatment in both yeast and mammalian systems.[31,32] Here, cell cycle arrest is defined by an increase in parent cell size in conjunction with an increase in bud size. This is in contrast to the reduction in cell size and daughter size at birth that are typically observed for yeast that are undergoing slow cell division due to metabolic factors.[33] However, it is important to note

that oncosis (increase in parent cell volume) is generally associated with necrotic cell death,[34] with some exceptions.[35]

In addition to DAPI staining, apoptotic DNA cleavage is usually assayed through terminal dUTP nick-end labeling (TUNEL).[29] The reactive 3'-OH species generated by apoptosis-induced cleavage are detected by d-UTP labeling with terminal deoxynucleotide transferase. Although cell and chromatin morphologies were disrupted, BY4741 cells were TUNEL-negative following treatment with 200 μM cisplatin for both 6 h (Figure 3.2b) and 12 h (data not shown). This suggests that although cisplatin treatment may disrupt normal chromatin segregation, it is not sufficient to initiate an apoptotic signal culminating in DNA strand breaks in BY4741 under these conditions.

An apoptotic signal, once triggered, is potentiated through a caspase-like family of signaling proteins, including YCA1, which belongs to the type 1 family of metacaspases. Yeast apoptosis can also proceed through an independent pathway mediated by AIF1, a homolog of mammalian apoptosis-inducing factor.[22] To determine if cisplatin-induced toxicity proceeds through either of these programmed cell death pathways which are involved with the majority of yeast apoptosis[29] we assessed the cell viability of *YCA1* and *AIF1* deletion mutants treated with 200 μM cisplatin for 6 h. In these cell lines, each disrupted gene was replaced with a KanMX module and tagged with a unique primer sequence for identification (Saccharomyces Genome Deletion Project). For both Δ*YCA1* and Δ*AIF1*, no differences in cell viability were observed, indicating that neither protein is involved in translating drug treatment into downstream cytotoxicity in yeast (Figure 3.2c). Based on these results, the cells treated with these specific concentrations of cisplatin are likely undergoing a form of necrosis, but whether it is

uncontrolled necrosis or a programmed necrosis cannot be determined by the present data.[34]

A variety of antitumor agents, such as the DNA fragmenting bleomycin, the microtubule directed paclitaxel, and the ribosome targeting toxin ricin have been shown to induce apoptotic markers in yeast.[28,36] There are two main explanations for a lack of apoptotic markers upon cisplatin treatment in the current experiments. The first is that cisplatin may induce apoptosis in yeast, but not under the conditions studied here. There are many cases in the literature in which a stimulus can induce yeast apoptosis at low doses and necrosis at high doses.[35,37] It is also possible that unlike the case for other toxins, yeast lacks a key component of a pathway through which cisplatin treatment triggers apoptosis. In mammalian cells the tumor suppressor protein p53 is a central player in the induction of apoptosis, but there is no p53 homologue in yeast.[18] Mismatch repair pathways have been linked to p53-induction of apoptosis in mammalian cell lines, but deletion of MMR components in yeast does not influence cisplatin sensitivity.[18] Thus, in the absence of p53, different cisplatin-induced cell toxicity pathways appear to be present in yeast that result in cell cycle arrest and disrupt chromatin morphologies, but not the hallmark DNA cleavage events associated with apoptosis. Similar phenotypes have been observed in *S. cerevisiae* following treatment with tunicamycin, an X-type agent that also causes cell-cycle arrest and the unfolded protein response, but death by non-apoptotic methods.[38]

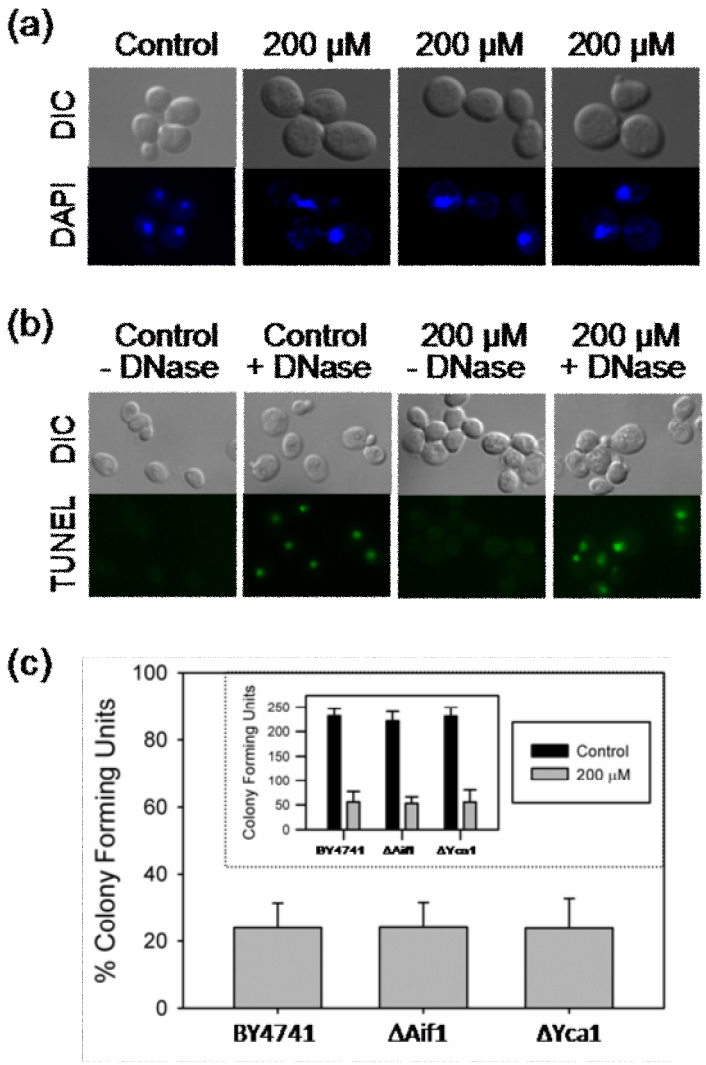

Figure 3.2. (a) DAPI staining of yeast treated with 0 and 200 µM cisplatin for 6 h. (b) TUNEL assay of yeast treated with 0 and 200 µM cisplatin for 6 h. Positive controls were obtained by treating fixed, permeabilized cells with 5 U DNase I. (c) Survival of BY4741, ΔAif1 and ΔYca1 treated with 200 µM cisplatin for 6 h, measured as percent of control colony-forming units (cfu). Inset: average cfu counts for both the control and cisplatin treated cultures. Results were averaged from three independent experiments presented as the means ± SD.

Cisplatin Treatment Causes an Exponential Increase in the In-Cell Pt Concentration

The concentration of Pt species inside a cell following cisplatin treatment is affected by a complex set of dynamics including passive diffusion, active transport into

the cell, and active efflux from the cell.[23] In order to assess the drug concentrations that cellular RNA are exposed to at each timepoint the accumulation of Pt in whole yeast cells was measured by ICP-MS. An exponential increase in the amount of Pt per cell was observed from 1 to 12 h (Figure B.1, Appendix B), with an estimated $7.0 \pm 0.3 \times 10^5$ and $1.2 \pm 0.1 \times 10^6$ Pt/cell measured at 1 h and $1.7 \pm 0.4 \times 10^6$ and $3.5 \pm 0.2 \times 10^6$ Pt/cell measured at 6 h for 100 and 200 μM treatment concentrations, respectively. These numbers are in line with those measured previously for 130 μM cisplatin-treated yeast at 18 h[39,40] and in cisplatin treated HeLa cells when differences in cell volume are taken into account.[27,41]

Because cisplatin treatment causes an increase in yeast cell size a clearer picture of the in-cell Pt concentration affecting the cellular RNA can be gained by taking the volumes of drug treated yeast cells into account. Yeast cell radii were measured from differential interference contrast (DIC) images and the volumes were estimated by treating the yeast as spheres. Interestingly, the average size of the 200 μM cisplatin-treated yeast continuously increases, while the average size of the 100 μM cisplatin-treated yeast remains roughly steady after 6 h, possibly representing differences in the viability of the cells in these two cultures at later time points (Figure 3.3a). The average volume of the yeast calculated for the control sample is ~ 40 fL, a value consistent with other measurements for the volume of a haploid yeast cell.[33,42]

Figure 3.3b shows estimated in-cell Pt concentrations using the calculated average cell volumes at each treatment concentration. Doubling the cisplatin treatment concentration results in a doubling of the measured cellular Pt concentration when it is calculated in this manner, with 47 ± 10 and 84 ± 5 μM measured at 6 h for 200 and 100

μM respectively. It is worth noting that at 12 h the in-cell Pt concentration is higher than the concentration of cisplatin in the media. This effect has been seen before for other anticancer metallodrugs[43] and is consistent with an active transport process[44] and also the fact that these drugs produce kinetically inert adducts when bound to cellular targets, putting drug binding under kinetic rather than thermodynamic control.[45]

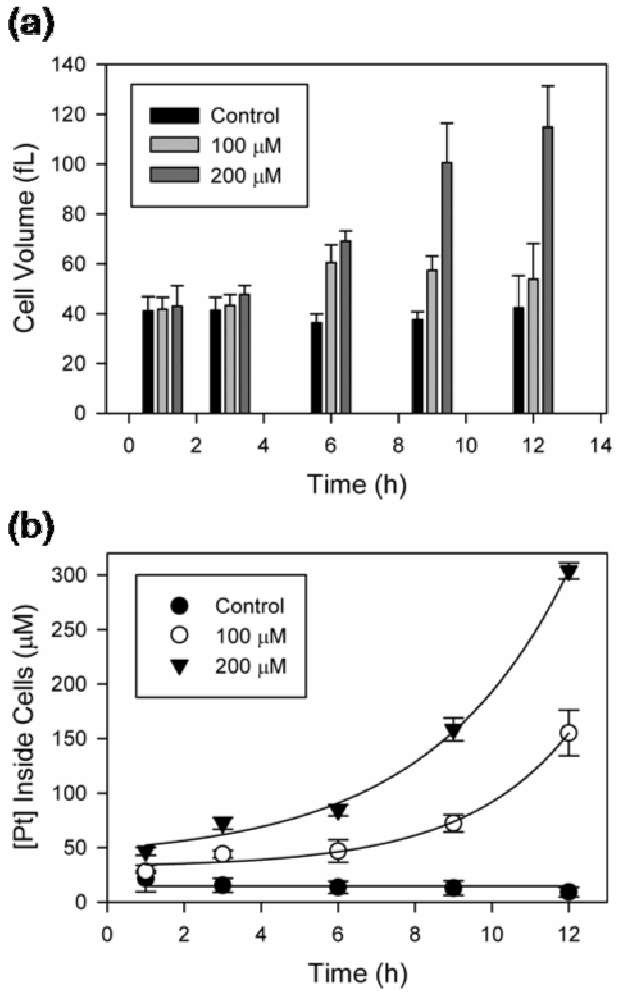

Figure 3.3. (a) Average estimated cell volumes (see Methods). (b) Calculated in-cell Pt concentrations based on Pt / cell ICP-MS measurements and the average estimated cell volumes. Results were averaged from at least three independent experiments presented as the means ± SD.

Pt Accumulates to a Different Extent in rRNA, mRNA, Total RNA, and DNA

In order to elucidate the effect of cisplatin treatment on yeast cellular RNA as a whole, ICP-MS was used to quantify the Pt accumulation in total RNA isolated from 100 and 200 μM cisplatin treated yeast. For both concentrations an exponential increase in Pt content was observed from 1 to 12 h (Figure 3.4a), roughly matching the exponential increase in Pt cellular concentration. This indicates that accumulation of Pt in RNA is roughly proportional to accumulation of Pt in the whole cell. At 6 h the Pt accumulation corresponds to one Pt every 14,600 ± 1,500 and 5760 ± 580 nt for 100 and 200 μM cisplatin treatments, respectively. As a comparison of target size, the yeast ribosome is roughly 5600 nt.[46]

Pt accumulation on whole-cell RNA and DNA were tested at 12 h of treatment with cisplatin (see Methods). Both cisplatin concentrations yield ~ 3-fold more Pt bound to the DNA than the RNA on a per nucleotide basis (Figure 3.4b). However, there is 10-50 fold more RNA in a yeast cell than DNA,[47,48] and so when the whole cell is considered there is ~4-20 fold more Pt accumulation in the total cellular RNA than in the total cellular DNA (Table 3.2). This result is interesting because cisplatin cellular distribution studies done in human cell lines have observed an accumulation of Pt in the nucleus and nucleolus.[49] The higher per nucleotide Pt accumulation in DNA could be an indication that this is taking place.

In order to compare the Pt accumulation in mRNA and rRNA, total cellular RNA was harvested from yeast after 6 h of continuous cisplatin treatment. Messenger RNA was extracted with the GenElute mRNA Miniprep Kit from Sigma while 25S and 18S rRNA was isolated by gel purification. Pt accumulated in the rRNA and total RNA to a

similar extent, while significantly less accumulated in mRNA (Figure 3.4c). Given that yeast RNA is 80% ribosomes, 15% tRNA, and 5% mRNA,[48] it seems likely that the Pt content in the total RNA is largely due to accumulation in rRNA. Assuming a statistical distribution of Pt adducts, these data indicate an average of 1 and 2 Pt adducts for every 3 ribosomes for 6-hr treatments with 100 and 200 μM cisplatin respectively.

Translation in both yeast and mammalian cells is tightly controlled, and, in particular, messenger RNA has a high rate of surveillance.[50] In addition, mRNA may take on more extended structures than the compact, highly-charged ribosome. Differences in structure and protein content are expected to cause each RNA species to present a different electrostatic surface to the reactive cationic aquation products of cisplatin. Therefore, the lower Pt accumulation in mRNA could be due to either lower initial Pt accumulation on mRNA or rapid detection and degradation of Pt-bound mRNAs, or a combination of these two effects.

Platinum Accumulation on Ribosomal RNA Is Directly Observed *In Cellulo*

The specific location of stable platinum adducts within *S. cerevisiae* ribosomal RNA was probed by 5' end-labeled primer extension analysis. Reverse transcriptase, as well as several other RNA processing enzymes, is directly inhibited by the formation of kinetically inert Pt-RNA species.[51,52] RT-primer extension can be used to map reactive platinum binding sites *in cellulo* to single nucleotide resolution. Information gained from these experiments lends insight into the solvent accessibility and electrostatic potential of specific RNA motifs within the ribosome. In addition, we hope to use these data to

distinguish platinum adducts whose formation may have downstream consequences from those whose accumulation may be more tolerated.

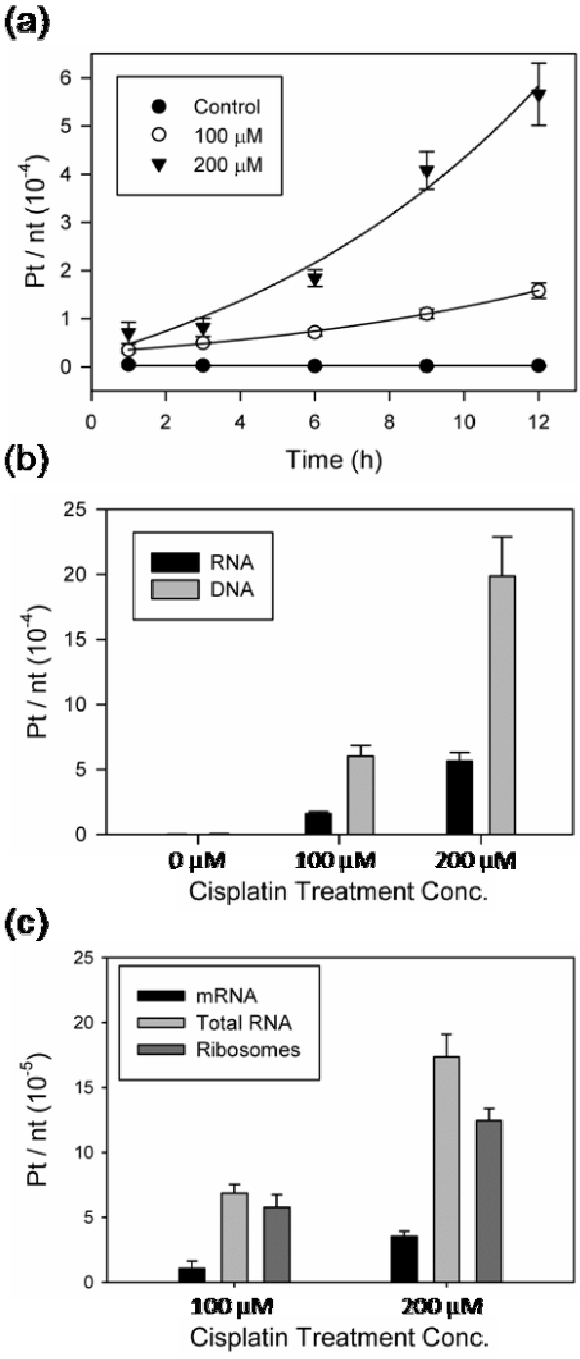

Figure 3.4. (a) Accumulation of Pt atoms in total RNA from yeast treated with cisplatin for 1, 3, 6, 9, and 12 h. (b) Accumulation of Pt in total RNA and genomic DNA at 12 h on a per nucleotide basis. (c) Accumulation of Pt in mRNA, total RNA, and rRNA at 6 h on a per nucleotide basis. Results averaged from at least three independent experiments.

Table 3.2. Number of Pt Atoms Estimated to Accumulate in the Total RNA or Genomic DNA of One Yeast Cell[a]

Cisplatin Concentration	100 μM	200 μM
DNA (10^4)	1.5	4.8
RNA (10^4)	7-34	24-120

[a]Calculations are based on the genome size of *S. cerevisiae*[58], the mass of RNA in one haploid *S. cerevisiae* cell[57], and the variance of cellular RNA content over the growth cycle[47], treating the mass of RNA measured for one haploid cell as a maximum number.

Using a similar methodology, Rijal and Chow reported on the locations of platinum binding sites within helix 24 of the *E. coli* small ribosomal subunit.[53] Their *in cellulo* results revealed strong cisplatin binding to two adjacent guanines at positions 799 and 800. Secondary binding was observed at A792, adjacent to a G in the terminal loop of helix 24. From these experiments, it was concluded that cisplatin was an effective probe for reactive RNA sites that may become targets for *de novo* antibiotic drug design. As an ideal antibiotic drug differentially targets bacterial and eukaryotic ribosomes, we became interested in the formation of platinum adducts within this particular helix in *S. cerevisiae*. Importantly, the sequence (helix 18 in yeast) is fully conserved between yeast and humans. Reverse transcription experiments were performed on total yeast RNA extracted from cultures treated with 0-150 μM cisplatin for 6 h. Under these conditions, significant platination occurs at the capping loop of helix 18, as evidenced by two major stops in the sequencing gel at positions A792 (***) and A790 (***), as seen in Figure 3.5. Although it is expected for reverse transcriptase to stop or be stalled at the nucleotide 3' to the platinum adduct, the two additional minor stop sites observed occur directly on purine residues G797 and G786. Intriguingly, the presence of a C-G wobble base pair at position 801 in yeast precludes platinum binding and is sufficient to switch the major stop site from position U801 in *E. coli* to A792 in *S. cerevisiae*. These findings demonstrate

that although aquated cisplatin products are highly reactive, they are remarkably sequence-specific.

The ICP-MS data described above could be used to predict an average coverage of approximately one platinum adduct per three ribosomes following treatment with 100 µM cisplatin over a 6 h time period, but it is reasonable to expect that certain sites will be more accessible and/or reactive. The data of Fig. 5 suggest several platination sites near helix 18, with an onset at concentrations as low as 50 µM after 6 h. This cluster of targets

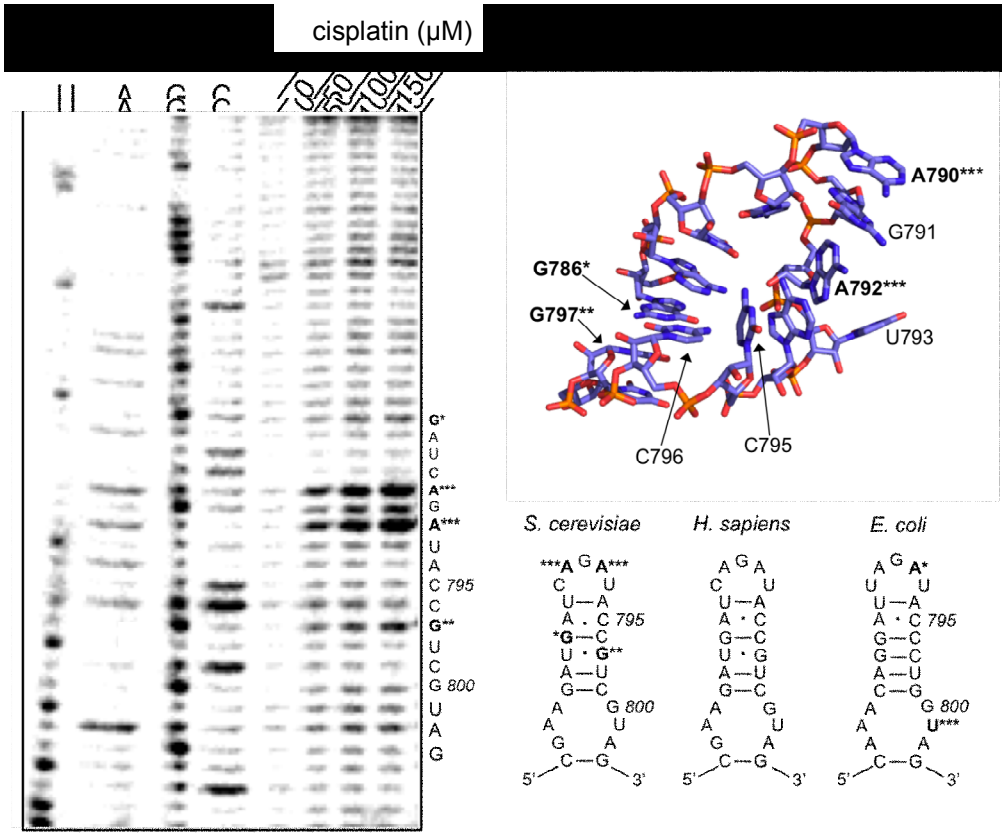

Figure 3.5. Primer extension analysis of RNA isolated from 6 h cisplatin-treated BY4741 (left) shows a dosage-dependant increase in termination intensity at indicated sites. A dideoxy sequencing ladder is denoted by U, A, G, and C. Major (***) and minor (*, **) bands which represent positions adjacent to a platination site are highlighted in the secondary structure diagram (right, lower panel) and the crystal structure (right, upper panel, PDB 3O30). Experimental results from Rijal and Chow[53] are summarized in the *E.* coli secondary structure model (far right, lower panel). The *E. coli* numbering is used for all structures here as a basis of comparison.

may reflect the solvent accessibility of this loop (Figure B.2, Appendix B). Future studies will examine the accumulation of cisplatin-derived reactive species at less accessible sites within this macromolecule.

Conclusions

The action of cisplatin on *S. cerevisiae* was characterized with full growth curves in minimal media and clonogenic assays that assessed cell viability. The majority of cisplatin toxicity coincided with the onset of exponential growth, at 6 h. Although DAPI staining indicated that the nuclei of some cisplatin treated cells are diffuse and enlarged, both the absence of DNA fragmentation (measured by TUNEL staining), and fact that *YCA1* and *AIF1* do not play a role in translating drug treatment into downstream cytotoxicity indicate that apoptosis is not taking place under the conditions of this study. The amount of Pt per cell increased exponentially from 1 to 12 h. At 6 h the in-cell Pt concentrations, calculated using estimated yeast volumes, are 47 ± 10 and 84 ± 5 μM for 200 and 100 μM respectively. The exponential increase in the Pt accumulation in total RNA indicates that the accumulation of Pt in RNA is roughly proportional to accumulation of Pt in the whole cell. Comparison of Pt accumulation in RNA and DNA at 12 h show ~ 3-fold more Pt bound to the DNA than the RNA on a per nucleotide basis, however, taking into account the overabundance of RNA in *S. cerevisiae* this value represents ~4-20 fold more Pt accumulation in the total cellular RNA than in the total cellular DNA. Pt accumulated in the rRNA and total RNA to a similar extent, while significantly less accumulated in mRNA. Mapping by reverse transcription demonstrates the formation of specific Pt adducts in ribosomes. Taken together, these data show both

the specificity of Pt-RNA adduct formation in a eukaryotic cell and important differences in the resulting in-cell adducts for specific RNA species.

Materials and Methods

Cell Cultures and Treatments

The *S. cerevisiae* strains used in this study, BY4741 (MATa; *his3*Δ1; *leu2*Δ0; *met15*Δ0; *ura3*Δ0), *yca1*Δ (BY4741 *yca1*::kanMX4) and *aif1*Δ (BY4741 *aif1*::kanMX4), were gifts from the Stevens laboratory at the University of Oregon. All liquid cultures were grown on Synthetic Complete medium (SC) consisting of 0.67% yeast nitrogen base and 2% glucose as a carbon source supplemented with amino acids and nucleotide bases. Plated cells were grown on YEPD agar plates (1% yeast extract, 2% peptone, 2% glucose, and 2% agar). Liquid culture growth was maintained in the dark at 30 °C with shaking at 200 rpm. A 5 mM cisplatin (Sigma Aldrich) stock in 100 mM NaCl (no more than a week old, stored in the dark at room temperature) was used for all yeast treatments. Yeast cultures were pregrown to an OD_{600} of 5 then inoculated into media at 30 °C to an OD_{600} of 0.075 and treated with the given concentrations of cisplatin.

Measurement of Culture Growth, Cell Survival, and Cell Size

Culture growth was measured as the optical density at 600 nm (conversion factor OD_{600}; 1 $AU_{600} = 2.0 \times 10^7$ cells/mL). Cell viability was measured by plating serial dilutions of treated and untreated yeast onto drug-free YEPD agar plates (~250 cells/plate) and counting the number of colonies formed after 3 d at 30 °C. The number of colony-forming units (cfu) was determined by dividing the cfu counts of treated cultures

by those of untreated cultures, which were assumed to be 100%. Yeast cell radii were measured from differential interference contrast (DIC) images were obtained on a Carl Zeiss Axioplan 2 fluorescence microscope using a 100× objective and AxioVision software (Carl Zeiss, Thornwood, NY) and the volumes were calculated by treating the yeast as spheres. Data was graphed using SigmaPlot 11.0.

Extraction and Purification of Nucleic Acids

For measurements of Pt in total RNA ~1.2×10^8 cisplatin treated yeast cells were pelleted and RNA was extracted using the MasterPure RNA Purification Kit (Epicentre) according to manufacturer's specifications. For both mRNA and rRNA samples total RNA was extracted from cisplatin treated cells (~4×10^8 cells/extraction) according to the method of Motorin *et al.*.[54] The mRNA was isolated using GenElute mRNA Miniprep Kit (Sigma), doing the bind and wash steps twice to ensure maximum mRNA purity. Ribosomal RNA was isolated from total RNA run on an 8% denaturing polyacrylamide gel. The 25S and 18S bands were visualized by light staining with methylene blue, cut out and eluted with an Elutrap Electroelution System (Whatman), then desalted on 3k Microsep Centrifugal Devices (Pall). DNA samples were purified from ~2×10^9 cell pellets according to the method of Rose *et al.* including the optional RNase A treatment.[55] All pellets were collected at 4 °C and washed 3 times with deionized H_2O before further processing. DNA was extracted at 12 h, a time at which it is much easier to obtain a suitably pure DNA sample due to the 4-5 fold lower RNA content of the yeast cell.[47] Typically, RNase A treatment is a standard way to ensure DNA purity when DNA is extracted at timepoints with higher proportions of RNA, however Pt adducts on RNA are

known to inhibit RNase activity,[51] and extensive RNase treatment may result in an enrichment of Pt content on residual RNA carried through the procedure, thus biasing the results. Data was graphed using SigmaPlot 11.0.

Measurement of Pt Content in Whole Cells and Extracted Nucleic Acids

For whole cell Pt accumulation ~2×10^7 cells were pelleted and washed as described above. The RNA and DNA was then desalted on in-house prepared G-25 sephadex spin columns (BioRad) and quantified by absorbance at 260 nm [extinction coefficient]. The whole cell, rRNA, DNA, and some of the total RNA samples were digested in 70% nitric acid (trace select, Fluka) for 2 hours at 65^{o}C then diluted to 2% (v/v) nitric acid with milli-Q H_2O. Pt content was determined by Inductively Coupled Plasma Mass Spectrometry (ICP-MS) using a Thermo VG PQExcell quadrupole ICP-MS equipped with a Gilson 222 autosampler at the W. M. Keck Collaboratory for Plasma Spectrometry (Oregon State University, Corvallis, Oregon). The instrument was calibrated , for ^{194}Pt, ^{195}Pt and ^{196}Pt by developing standard curves from a Ru standard (High Purity Standards). All measurements were done in triplicate using ^{115}In as an internal standard. Data was graphed using SigmaPlot 11.0.

Tests for Apoptotic Markers

Terminal deoxynucleotidyl transferase-mediated dUTP nick end labeling (TUNEL) was performed according to the method of Madeo et. al.[56] with some modification. Briefly, 3.0×10^7 yeast cells were pelleted, washed 3x with PBS, fixed with 3.7% formaldehyde for 2 h at 24 °C, and then digested with 2.5 U zymolyase 100T (US

biological) for 30 min at 30 °C in 1 mL sorbitol buffer (1.2 M sorbitiol, 0.5 mM $MgCl_2$, 35 mM phosphate buffer pH 6.8). A portion of the sample was applied to a polylysine-coated slide and let dry for 1 hr at 37 °C. The slides were incubated with freshly prepared permiabilization solution (0.1% Triton X-100, 0.1 sodium citrate) for 1 min at 4 °C, then rinsed 3x with PBS. Positive control samples were incubated with 0.2, 1, and 5 U DNase I (Fermentas) for 1 hr at 37 °C in the rxn buffer provided by the manufacturer. Samples were incubated with 10 μM TUNEL reaction mixture (in situ cell death detection kit, fluorescein, Roche) for 30 min at 37 °C in the dark, rinsed 3x with PBS. Images were acquired on a Carl Zeiss Axioplan 2 fluorescence microscope using a 100× objective and AxioVision software (Carl Zeiss, Thornwood, NY). DAPI staining was performed by pelleting 1.0×10^7 yeast cells, washing 3x with PBS, fixing in 70% EtOH for 30 min at room temperature, washing with PBS, and then incubating with 0.5 μg/mL DAPI for 20 min at room temperature in the dark. The samples were then washed 3x with PBS and visualized immediately on the Carl Zeiss Axioplan 2 fluorescence microscope.

5' End-Labeling

The DNA primer designed for reverse transcription of helix 18 of the small yeast ribosomal subunit was purchased from Integrated DNA Technologies. γ-^{32}P 5' end-labeling was performed with T4 polynucleotide kinase (Fermentas) according to the manufacturer's protocol. Labeled primer was gel purified by 20% PAGE. Bands were visualized using a GE phosphor screen in conjunction with a Molecular Dynamics Storm 860 imaging system and analyzed with Molecular Dynamics ImageQuant software

(version 5.0). The correct bands were excised and eluted overnight in deionized water. The resulting eluent was desalted (G25 sephadex) and concentrated by SpeedVac.

Reverse Transcription of Helix 18 of the Small Ribosomal Subunit

Total RNA extracted from yeast cells treated with cisplatin was used as a template for reverse transcription to monitor platination *in cellulo*. Briefly, a solution of 5×10^6 cells/mL was grown for 6 h in SD-URA in the presence of 0-300 μM cisplatin. Total RNA was isolated using a MasterPure Yeast RNA Extraction kit (Epicentre) and resuspended in 10 mM Tris-HCl pH 7.5 and 1mM EDTA pH 7.5 to a final concentration of 10 μg/μL. Primer extension analysis was catalyzed by Avian Myeloblastosis Virus reverse transcriptase (Fermantas). 1 μg of RNA template was annealed to 100 pmol of the specified 5' end-labeled primer in the manufacturer's supplied reaction buffer and subsequently incubated in the presence of enzyme for 1 hour and 45 minutes at 42°C. The resulting cDNA products were diluted in loading buffer containing 0.005% (w/v) xylene cyanol and bromophenol blue and analyzed by 8% PAGE. Bands were visualized as described previously.

Bridge to Chapter IV

Chapters II and III describe *in vitro* and *in cellulo* experiments investigating cisplatin-induced RNA platination. The results of these studies motivated us to broaden our investigations to other anticancer metallodrugs. The following chapter describes the results of a collaboration with Prof. Karen L. McFarlane Holman at Willamette

University (Salem, Oregon) in which we performed both *in vitro* and *in cellulo* investigations of Ru-RNA binding induced by NAMI-A treatment.

CHAPTER IV

RU BINDING TO RNA FOLLOWING TREATMENT WITH THE ANTI-METASTATIC DRUG NAMI-A IN *S. CEREVISIAE* AND *IN VITRO*

This chapter describes *in cellulo* studies of NAMI-A treated yeast and *in vitro* MALDI-MS experiments comparing binding to RNA and DNA oligonucleotides under different solution conditions. It includes important contributions from Michelle L. Miranda, Prof. Victoria J. DeRose, and Prof. Karen L. McFarlane Holman. I performed the *in vitro* studies, and wrote the majority of the manuscript. The *in cellulo* studies were done by Michelle L. Miranda under my direction and according to protocols that I developed. Michelle L. Miranda also provided an initial draft of the results from the *in cellulo* studies. Both Prof. Victoria J. DeRose and Prof. Karen. L. McFarlane Homan provided guidance for this project and contributed significant editorial feedback. Reproduced with permission from Biochemistry, submitted for publication. Unpublished work copyright 2011 American Chemical Society.

Introduction

Current metal-based anticancer therapeutics such as cisplatin are effective against primary tumors, but suffer from several drawbacks: severe side effects, the development of resistance, and only minimal antimetastatic activity.[1] Research efforts to find more successful treatments have led to a number of promising new drugs. One ruthenium-based complex has received particular attention and is currently in Phase Two of clinical trials: [ImH][*trans*-$Ru^{III}Cl_4$(DMSO)(Im)](Im = imidazole), or NAMI-A (Figure 1.2).[2,3] This complex has shown low toxicity and remarkable efficacy against metastases,

especially among lung carcinomas. Multiple effects may be involved in this antimetastatic activity, including interactions with the extracellular matrix and the cell surface, interference with NO metabolism, effects on tumor metalloproteinases, and transport into tumors through binding to serum proteins such as transferrin.[4,5] NAMI-A also causes transient tumor cell cycle arrest in the premitotic G2/M phase.[6] In addition, the highly related NAMI, [Na][*trans*-$Ru^{III}Cl_4$(DMSO)(Im)], has been shown to cause a marked reduction of tumor nucleic acid content.[7] This effect and its consequences have not yet been explored for NAMI-A. In short, NAMI-A is an extremely attractive drug candidate due to both its antimetastatic activity and low toxicity to healthy cells, but much remains to be determined regarding its mechanism of action.

Redox and ligand exchange chemistry are also considered important to the mechanism of action of NAMI-A, and the *in vivo* effectiveness of aquated and reduced drug products have led to the conceptualization of NAMI-A as a prodrug.[8] The reduction potential of NAMI-A is +0.016 V vs. standard calomel electrode (SCE) in pH 7.4 phosphate buffer,[9] and as such, reduction from Ru(III) to Ru(II) is electrochemically attainable by the plasma and cellular reducing agents ascorbate and glutathione. In addition to the presence of ubiquitous reducing agents, rapidly dividing cancer cells provide a hypoxic environment[10,11] accompanied by low pH levels[12] that affect reduction and subsequent reactivity. Furthermore, several pH-dependent equilibria are possible *in vivo* and, as such, there are expected to be multiple Ru species present, many of which have the potential to be therapeutically active.[8]

Ru anticancer therapeutics are known to bind to DNA *in vitro* and *in cellulo*.[13,14] Indeed, treatment with NAMI-A results in Ru-DNA adducts. Similar to the case of

cisplatin, the cytotoxic activity of NAMI-A has been correlated with Ru-DNA accumulation in several cancer cell lines.[15] Results from *in vitro* studies using calf thymus or plasmid DNA to investigate the consequences of NAMI-A treatment on global measures of DNA structure such as thermal denaturation or circular dichroism spectroscopic signatures suggest less overall structural effects for NAMI-A than with cisplatin, which could be due to the types of adducts formed or less accumulation for a given treatment method.[16,17] The "soft," nucleophilic N7 site of guanine is the main site of coordination for cisplatin-derived Pt(II), with coordination to the N7 adenine also observed.[18] Similarly, a hydrolysis product of NAMI-A, $[trans\text{-}RuCl_4(H_2O)(Im)]^-$, has been observed binding to the N7 of 9-methyladenine by NMR.[19] Ru-binding to GMP following NAMI-A treatment has been documented by capillary electrophoresis coupled with inductively coupled plasma mass spectrometry (ICP-MS), and a strong preference for guanine over adenine bases was confirmed by electrospray ionization mass spectrometry (ESI-MS).[20,21] Because of their different propensities for mono- and diaddut formation, the *in vivo* adduct profiles produced by NAMI-A and cisplatin are expected to be different. This has been shown *in vitro* for NAMI, where transcriptional mapping combined with denaturing agarose gel electrophoresis was employed to discover that fewer intrastrand GG adducts were produced on double stranded DNA.[22] A minor amount of interstrand cross-links were formed (also fewer than for cisplatin). The other adducts formed were most likely monofunctional adducts. To our knowledge the specific geometries and percent occurrences of the different DNA adducts formed following NAMI-A treatment are not known.

RNA is chemically similar to DNA, but plays diverse roles in cell regulation and gene expression. In addition to well-known functional roles in translation (mRNA, tRNA, and ribosomes) a great deal is now being learned about the regulatory roles carried out by RNAs such as siRNA, microRNA, piwi-interacting RNA, and long noncoding RNA in both transcription and translation.[23] Consistent with these regulatory roles, the integrity of cellular RNA is monitored. RNA damage is linked to disease and can trigger programmed cell death.[24-26] Two such examples are sarcin[25] and ricin,[26] toxic proteins that induce apoptosis through their interaction with the sarcin/ricin loop of the large subunit of the eukaryotic ribosome. In addition, there is evidence that both ribosomes and tRNA may play specific roles in programmed cell death pathways.[27,28]

Drug binding to RNA could impact cell fate via downstream effects on a wide range of RNA and regulatory pathways. Studies with cisplatin show significant drug accumulation in RNA as well as inhibition of RNA function in extracts.[29-31] This could be true for other DNA binding drugs such as NAMI-A. To our knowledge, the effect on RNA of treatment with NAMI-A has not been previously studied. Here we use *S. cerevisiae* for *in cellulo* analysis of drug accumulation on RNA, and we perform *in vitro* analysis of binding to RNA and DNA oligonucleotides. *S. cerevisiae* was chosen as a model system because it has been used to study a range of anticancer drugs.[32] and RNA pathways,[33,34] and is a genetically tractable system for future studies.[35] When *S. cerevisiae* is treated with NAMI-A, growth inhibition and accumulation of Ru in whole cells and cellular RNA is observed. *In vitro* drug binding occurs with model DNA and RNA oligonucleotides. The extent of Ru-nucleotide binding depends on both pH and reduction by ascorbate, where enhanced binding occurs under acidic, reducing conditions

similar to those found in solid tumors. Taken together, these studies demonstrate the binding of NAMI-A or its aquated and reduced derivatives to RNA *in vitro* and *in cellulo*, and enhanced binding with nucleic acids targets in a tumor-like environment.

Growth Inhibition and Cell Viability Following NAMI-A Treatment

Yeast in SC media were continuously treated with freshly dissolved NAMI-A for 1 to 24 h. Concentrations below 100 μM NAMI-A did not result in significant change in culture density by 6 h treatment, while treatments of 100-300 μM showed a gradual decrease in cell density, making 100 μM a threshold concentration above which decreases in culture density are clearly observable (Figure C.1a, Appendix C). Full growth curves for 0, 150, and 450 μM NAMI-A are shown in Figure 4.1, demonstrating a moderate (63 ± 7% of control at 24 h) and severe (12 ± 3% of the control at 24 h) reduction in culture density for 150 and 450 μM, respectively.

To discriminate between slow and/or reversibly inhibited cell division and full loss of cell viability due to NAMI-A treatment, cell survival was measured by clonogenic assay. After 6 h of drug treatment, NAMI-A treated yeast were plated on drug-free YEPD and allowed to grow for 3 days, at which time the number of resultant colonies were compared to the control. The results for four concentrations of NAMI-A ranging from 150 to 600 μM show a moderate decrease in cell viability that does not scale linearly with treatment concentration (Figure 4.1b). Tripling the NAMI-A dose from 150 to 450 μM results in a doubling of the number of non-viable cells (viable cells going down from 80 ± 8% to 59 ± 4%) and a somewhat higher loss in cell culture density (from of 88 ± 20% to 53 ± 14%, Table 4.1). This relatively low loss of viability contrasts with the properties

of the more cytotoxic cisplatin, which after 6 h at a 200 µM treatment concentration results in a culture density of 72 ± 14%, but only 27 ± 8% viable cells in comparison with controls (Hostetter, Osborn, and DeRose, *in preparation*). Taken together these results indicate that the reduced culture density of NAMI-A treated yeast is due to a combination of cell death and slowed growth. Typically yeast that are undergoing slower cell division due to general metabolic factors have a smaller average cell size.[38] Yeast treated with NAMI-A, however, exhibit an increased average cell size (Figure C.1b, Appendix C) which might be indicative of cell cycle arrest.

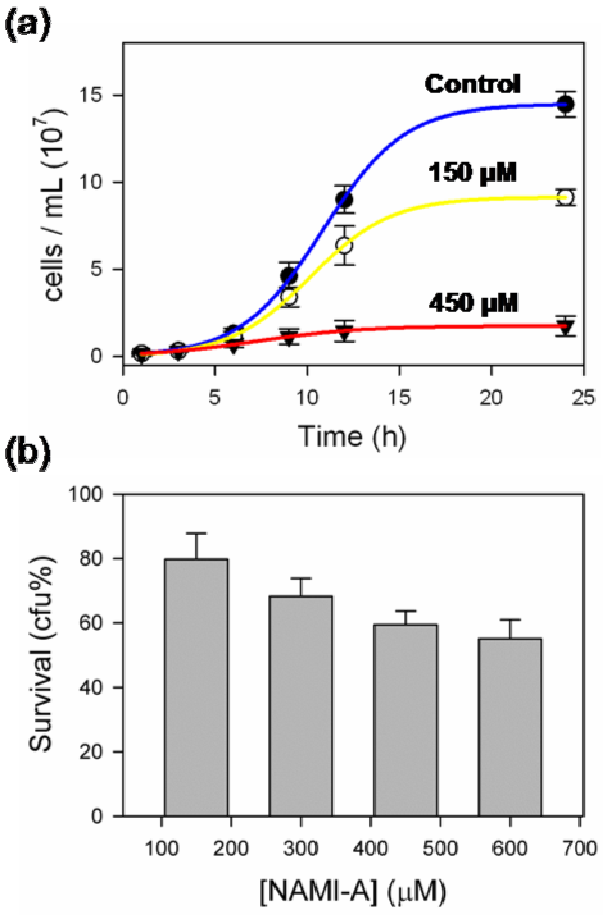

Figure 4.1. (a) Exponential growth curves of yeast treated with 0, 150, and 450 µM NAMI-A. (b) Survival of yeast treated for 6 h with NAMI-A measured as percentage colony-forming units (cfu) after 3 d in drug-free media. Results were averaged from three independent experiments presented as the means ± SD.

Accumulation of Ru in Yeast Cells and Cellular RNA

The Ru content of whole cells and of total RNA isolated from yeast treated for 6 hrs with 0, 150, and 450 μM NAMI-A were quantified by ICP-MS. Results for both whole cells and total RNA show significant Ru accumulation that is proportional to the treatment concentration, roughly tripling when the treatment concentration is tripled (Figure 4.2). Very approximate average cellular Ru concentrations of ~370 μM and 1200

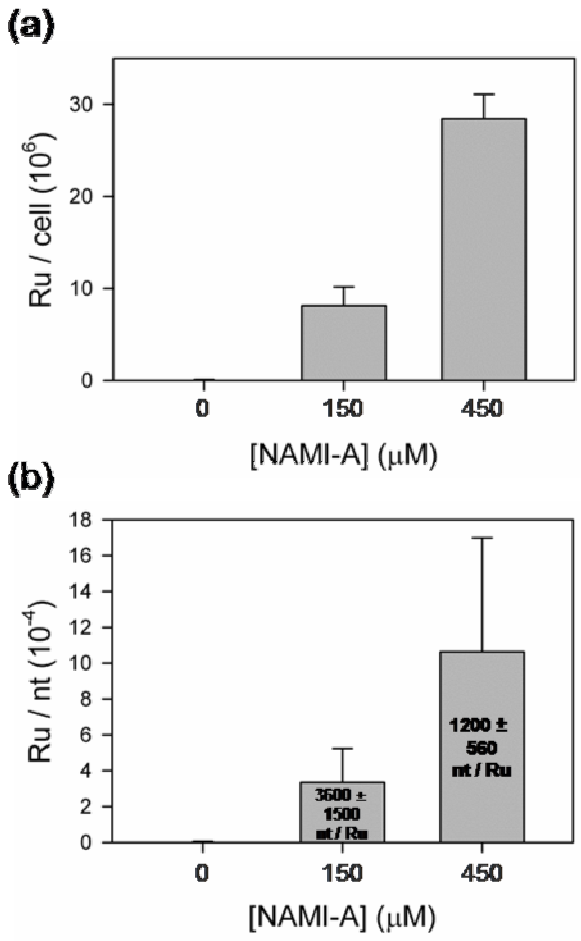

Figure 4.2. (a) Accumulation of Ru atoms per cell in yeast treated with NAMI-A for 6 h. (b) Accumulation of Ru atoms in total RNA from yeast treated with NAMI-A for 6 h depicted as Ru per nucleotide with the average number of nucleotides per Ru atom given in text. Each result was averaged from three independent experiments and presented as the mean ± SD.

μM (for 150 μM and 450 μM NAMI-A treatment, respectively) can be calculated based on these results and estimates for the average volume of growing yeast (see Methods); these values are approximate upper limits, since as noted above, yeast cell sizes increase with treatment. Although cells were washed in triplicate before analysis, an influence from extracellular accumulation of Ru on cell walls cannot be excluded. Nonetheless, the proportional increase in Ru content for both whole cells and extracted RNA indicates that under these conditions cellular uptake of NAMI-A is not saturated and that Ru accumulation in RNA is proportional to the cellular Ru accumulation.

Table 4.1. Effects of NAMI-A on Yeast at 6 Hours

NAMI-A Concentration	150 μM	450 μM
Culture Density	88 ± 20%	53 ± 14%
Cell Viability	80 ± 8%	59 ± 4%

Ru Adduct Formation on RNA and DNA Oligonucleotides Following *In Vitro* Treatment with NAMI-A

Measurements from the *in cellulo* studies above indicate significant accumulation of Ru on cellular RNA following 6 h of NAMI-A exposure in a yeast cell environment. To provide context for these results, the reactivity of NAMI-A with RNA and DNA oligonucleotides was examined *in vitro*. NAMI-A was incubated with single-stranded RNA and DNA oligonucleotides in an ionic background similar to biological conditions (100 mM $NaNO_3$ and 2 mM $Mg(NO_3)_2$). Comparative studies were performed at pH 6.0, chosen to simulate the lower pH often found in tumor tissue[12] and pH 7.4 (blood and healthy cells). A strong preference for Ru coordination to G has been previously observed

for DNA,[21] and so a simple model containing a single GG site embedded in a sequence of U or T nucleotides (U_6GGU_5 and T_6GGT_5) was chosen for this study.

Figure 4.3 shows the Matrix-Assisted Laser Desorption/Ionization Time-of-Flight (MALDI-TOF) mass spectra following oligonucleotide treatment with NAMI-A for 24 hrs at pH 6.0. Due to the natural abundances of Ru isotopes, in which there are six isotopes that have more than 5% natural abundance (with ^{101}Ru having the highest abundance at 31.6%),[41] the product peaks appear broad and short. In addition to the parent DNA or RNA oligonucleotide ion, the major +1 Ru products are assigned as [oligo + 1Ru] and [oligo + 1Ru(Im)]. Minor peaks for all three +2 Ru product species are also present, corresponding to binding at either both Gs or to one G and one U/T. As

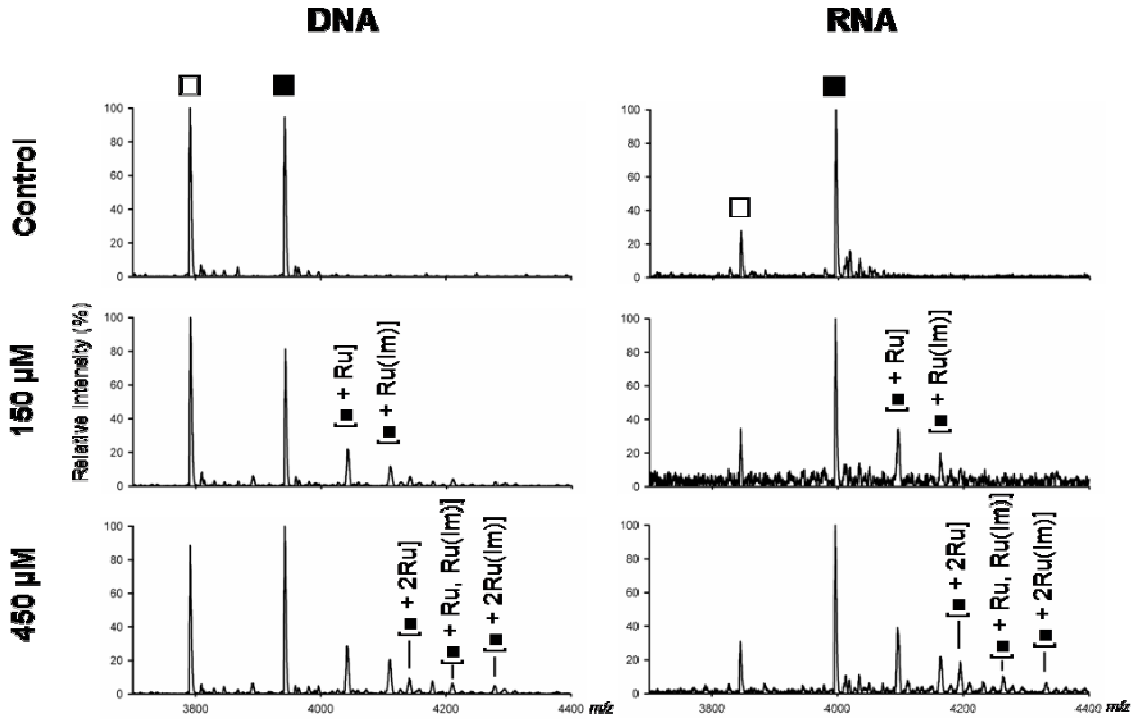

Figure 4.3. Representative MALDI-TOF spectra of the products of the incubation of 0, 150, and 450 µM NAMI-A with 20 µM DNA T_6GGT_5 or RNA U_6GGU_5 for 24 h at 37 °C and pH 6.0 in 100 mM $NaNO_3$ and 2 mM $Mg(NO_3)_2$. Filled squares denote unmodified, full-length T_6GGT_5 and U_6GGU_5 and open squares denote singly depurinated oligonucleotides.

expected, the relative amount of these +2 Ru products increases with an increase in NAMI-A concentration from 150 to 450 μM. No chloride, aqua, hydroxo, or DMSO ligands are observed in these mass spectra, indicating loss of all but the least exchangeable ligands. This matches previous observations of the loss of labile ligands in both ESI and MALDI-TOF mass spectra for other metallodrugs bound to oligonucleotides.[21,39,42]

In these mass spectra the overall amount of Ru adduct formation appears to be similar with RNA and DNA oligonucleotides. MALDI-MS spectra are not quantitative due to varying ionization efficiencies, but qualitative conclusions can be drawn from similar experiments performed with the same oligonucleotides, ionic conditions, and matrix protocols as were used for the data in Figure 4.3. A more exact comparison between RNA and DNA products is not possible because the absolute ratio of product to starting material may be influenced by differential ionization, and is additionally difficult due to the high amount of depurination observed for the DNA oligonucleotide strand.

Interestingly, the apparent increase in the amount of +Ru product species with treatments of 150 to 450 μM NAMI-A is modest, and a comparison of reaction products at 6 and 24 h shows that the reaction has run to completion by 6 h (Figures 4.3, 4.4, and Figure C.2a, Appendix C). This is surprising as it appears that a significant amount of unreacted oligonucleotides remain despite the 7.5 to 22.5-fold excess of NAMI-A. Less reaction is observed for A_5CCA_6 when compared to T_6GGT_5 in a side-by-side study, suggesting that the preference for G previously observed in the literature is observed under these conditions as well (Figure C.2b, Appendix C).[21]

Effects of pH and Ascorbate on Ru-Oligonucleotide Formation Following *In Vitro* Treatment with NAMI-A

Oligonucleotide reactivity at pH 6.0 (simulation of tumor tissue pH) and pH 7.4 (blood and healthy cells) were compared and a slight increase of reactivity at lower pH was observed (Figure 4.4). The addition of 2.5 mM ascorbate to the reaction, however, greatly enhanced the reactivity at both pH values, leading to a nearly complete loss of unreacted oligonucleotides, in particular at pH 6.0. Treatment with ascorbate also causes

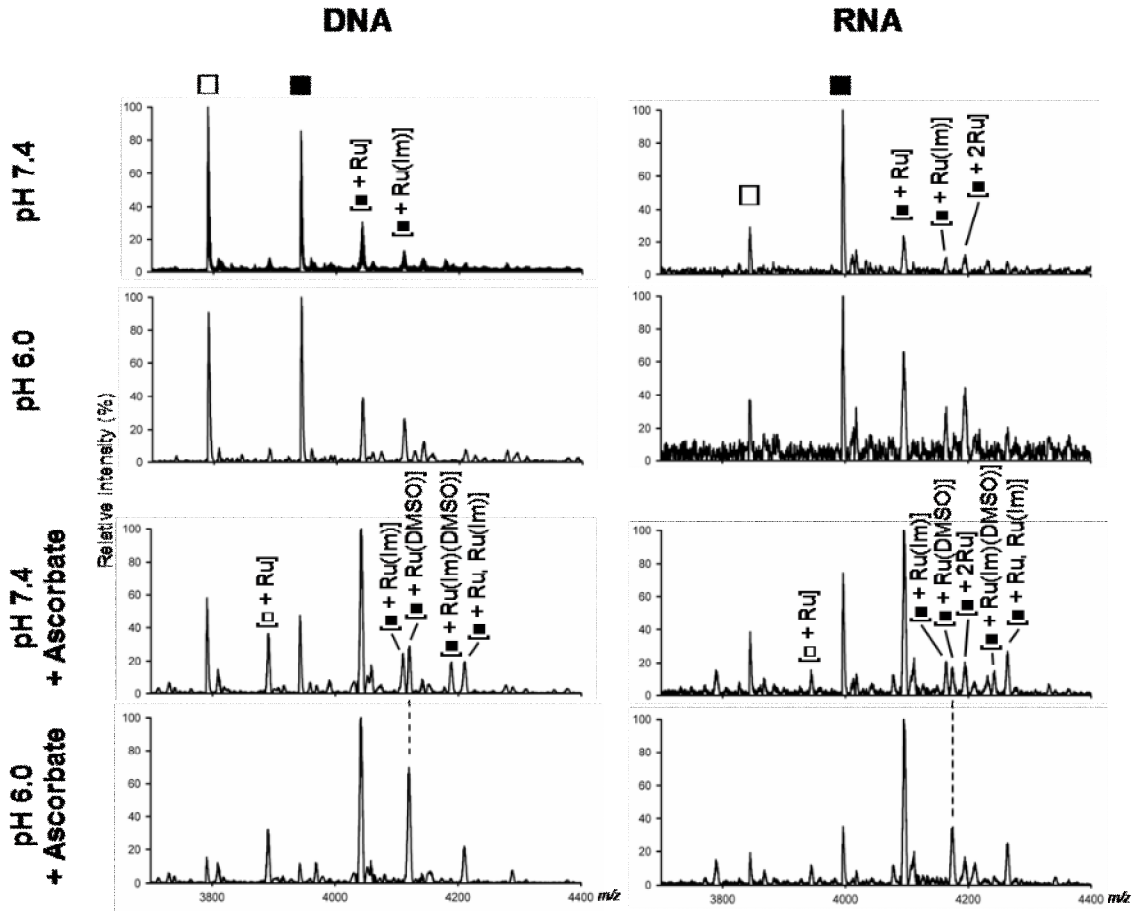

Figure 4.4. Representative MALDI-TOF spectra of the products of the incubation of 450 μM NAMI-A with 20 μM DNA T_6GGT_5 or RNA U_6GGU_5 at pH 6.0 and 7.4, with and without 2.5 mM ascorbate. Reactions were run for 6 h at 37 °C in 100 mM $NaNO_3$ and 2 mM $Mg(NO_3)_2$. Filled squares denote the unmodified, full-length T_6GGT_5 and U_6GGU_5 strands and open squares denote singly depurinated oligonucleotides strands.

a change in the observed product species, favoring the inclusion of [oligo + 1Ru(DMSO)] and [oligo + 1Ru(DMSO)(Im)], especially at pH 6.0 (Figure 4.4). The changes observed upon treatment with ascorbate are consistent with reduction of Ru(III) to Ru(II) leading to greater oligonucleotide binding and retention of the DMSO ligand.

Discussion of Ru Accumulation Following NAMI-A Treatment *In Cellulo*

Growth, viability, and accumulation of Ru in cells and cellular RNA were characterized following treatment with 150 and 450 μM NAMI-A, concentrations that produce a moderate and severe reduction in culture density respectively. Based on whole-cell ICP-MS measurements, growth for 6 hr in these conditions resulted in estimated intracellular Ru concentrations of ~370 μM and 1200 μM, indicating uptake of Ru from the media. As a basis of comparison, in a Phase I clinical trial the mean maximum Ru concentration observed in patient blood was 183 ± 17.3 μg/mL (1800 μM) for the maximum recommended dose (300 mg/m^2/day, on day 5, course 1).[3] Both the 150 and 450 μM NAMI-A treatments caused a decrease in the number of viable yeast cells, but this loss is modest in comparison with the more cytotoxic cisplatin, indicating that in the case of NAMI-A a significant portion of the decreased culture density is due to reversible growth inhibition. Indeed, transient cell cycle arrest in human tumor cell lines at the G2/M phase has been seen following treatment with NAMI-A.[6] The relatively high threshold of 100 μM NAMI-A that is required to clearly observe decreases in budding yeast culture density is consistent with previous observations. For example, a threshold of 100 μM NAMI-A was necessary to cause cell cycle effects in the KB tumor cell line, in which a "significant increase of cells in the S and G2/M phases" was observed 24 h after

exposure.[43] The observed increases in yeast cell size also indicate a halting of the cell cycle. Taken together, it is likely that a portion of the reduced culture growth in NAMI-A treated budding yeast is due to transient cell cycle arrest.[38]

In both total RNA and whole yeast cells Ru accumulated in a dose-dependent manner indicating that drug uptake is not saturated at 450 μM and that drug accumulation on RNA is proportional to cellular accumulation. This result is consistent with the lack of saturation of Ru accumulation observed in human tumor cell lines treated with NAMI-A at concentrations up to 600 μM.[15] In treated yeast, a significant amount of Ru accumulated on RNA: one Ru every 3500 ± 1500 and 1100 ± 550 nucleotides for 150 and 450 μM NAMI-A, respectively. Assuming that yeast ribosomes, which are 80% of total cellular RNA in log-phase growth, accumulate the same amount of Ru as total RNA, there would be on average 2 or 5 Ru bound per ribosome.[44] RNA binding of this scale has the potential to cause significant downstream effects and may be involved in the mechanism of cell cycle arrest. A growing body of knowledge connects ribosomal stress (such as the disruption of ribosome biogenesis) to p53 activation and cell cycle arrest in humans.[45] In addition, the elucidation of the nonfunctional rRNA decay pathway in yeast is revealing connections between cellular response to RNA damage and DNA damage.[46] To our knowledge this is the first study of both the effect of NAMI-A on the genetically tractable *S. cerevisiae* and the result of NAMI-A treatment on RNA alone. The results establish yeast as a model system for studying the effects of NAMI-A on RNA, observing a significant level of drug accumulation that has the potential to cause disruption of RNA function.

Discussion of Ru-Oligonucleotide Adduct Formation Following NAMI-A Treatment *In Vitro*

When NAMI-A is dissolved in water it undergoes a series of aquation reactions in which the chloride, Im, and DMSO ligands can be lost.[47,19] The aqua derivates of the complex can also be in equilibrium with the hydroxo species, producing a wide range of possible active species in solution. The first aquation reaction has been measured to take place with a half life of 20 min at pH 7.4 and 2 h at pH 6.0 (25 °C).[19] Despite the faster aquation at pH 7.4, MALDI-TOF mass spectra showed that both RNA and DNA oligonucleotides with a single GG site demonstrated a greater extent of reaction at pH 6.0 than 7.4 when reacted for 6 h in a physiological salt background. This could be due to the greater exchangeability of Ru-aqua ligands as compared to hydroxo ligands, which would be expected to form more readily at higher pH, or due to formation of unreactive Ru-hydroxo polymers at higher pH values.[8,19]

The reduction of NAMI-A or its aqua derivatives by ascorbate has been measured to take place in seconds at pH 7.4 (37 °C) and significantly increases the rate of subsequent aquation reactions.[47,48] For the DNA and RNA oligonucleotides examined here, the presence of ascorbate caused a significant increase in the extent of reaction along with changes in the observed products in the MALDI-TOF mass spectra. Without ascorbate, the main observed products had a single bound Ru or Ru(Im). At pH 6.0 the ascorbate-treated samples showed mainly a single bound Ru or Ru(DMSO). At pH 7.4 both Ru(Im) and Ru(DMSO)-bound products were present. The increased resiliency of the Ru-DMSO bond following reduction to Ru(II) is likely due to the greater extent of $d\pi$-S backbonding that tends to occur in Ru(II)-DMSO complexes as compared to

Ru(III).[49] This increased retention of the DMSO ligand as compared to Im is consistent with previous studies by Bacac *et al.*[9] and Brindell *et al.*,[48] both of which observed Im hydrolysis following reduction of NAMI-A, but to different extents. Our observations indicate that ascorbate-induced reduction is taking place and that reduced Ru(II) species are binding to the oligonucleotides.[49]

In summary, our investigations of the effect of NAMI-A treatment on RNA *in cellulo* and *in vitro* adds a new piece to the growing understanding of ruthenium-based anti-cancer drugs. Firstly, we observe a nonlinear decrease in cell viability in *S. cerevisiae* with increasing NAMI-A concentration that corresponds with a moderate decrease in the number of viable cells. We quantified accumulation of Ru within the cells and found that hydrolysis products of NAMI-A bind to intracellular RNA in numbers large enough to cause 2-5 Ru bound per ribosome. Secondly, to support our *in cellulo* studies, we carried out *in vitro* treatment of DNA and RNA oligonucleotides with NAMI-A both in physiological (7.4) and cancer cell (6.0) pH, and in normal and reducing environments. The greatest extent of Ru-RNA adduct formation was observed in the acidic, reducing environment which is analogous to that of tumor tissue,[10-12] giving a strong indication that NAMI-A can become activated to react with nucleic acids in the environment of a tumor.

Materials and Methods

Cell Cultures and Treatments

The *S. cerevisiae* strain used in this study was BY4741, a gift from the Stevens laboratory at the University of Oregon. All liquid cultures were grown on Synthetic

Complete medium (SC) consisting of 0.67% yeast nitrogen base and 2% glucose as a carbon source supplemented with amino acids and nucleotide bases. Plated cells were grown on YEPD agar plates (1% yeast extract, 2% peptone, 2% glucose, and 2% agar). Liquid culture growth was maintained in the dark at 30 °C with shaking at 200 rpm. For each yeast treatment a 10 mM NAMI-A stock was prepared fresh in 50 mM $NaHPO_4$ (pH 7.4) with 0.1 M NaCl exactly 10 minutes before the start. Yeast cultures were pregrown to an OD_{600} of 5 then inoculated into media at 30 °C to an OD_{600} of 0.075 and treated with the given concentrations of NAMI-A.

Synthesis and Characterization of NAMI-A

The two-step procedure described in the international patent held by Mestroni et al.[36] was followed with slight modifications, as follows. In step two, 0.782 g of $[(DMSO)_2H][trans\text{-}RuCl_4(DMSO)_2]$ was dissolved in 15 mL of acetone and stirred for fifteen minutes to allow the counter ion to dissolve before adding 0.391 g of imidazole. The suspension was then heated and stirred at 30 °C for 21 hours. Product was collected via vacuum filtration, washing with acetone and ethyl ether and drying under vacuum. The final product was recrystallized by dissolving crude NAMI-A in DMSO to form a saturated paste, and then acetone was added to precipitate out the product. NAMI-A was characterized using FTIR, Raman and UV-Vis spectroscopy. Spectra were in agreement with results from samples that were characterized via XRD.[37]

Measurement of Culture Growth and Cell Survival

Culture growth was measured as the optical density at 600 nm (conversion factor OD_{600}; 1 AU_{600} = 2.0 x 10^7 cells/mL). Cell viability was measured by plating serial dilutions of treated and untreated yeast onto drug-free YEPD agar plates (~200 cells/plate) and counting the number of colonies formed after 3 d at 30 °C. The number of colony-forming units (cfu) was determined by dividing the cfu counts of treated cultures by those of untreated cultures, which were assumed to be 100%.

Measurement of Ru Content in Whole Cells and Extracted RNA

NAMI-A treated yeast cultures were pelleted (6 x 10^7 cells for whole cell measurements and 1.2 x 10^8 cells for RNA extraction) at 4 °C and washed 3 times with milli-Q H_2O. RNA was extracted using the MasterPure RNA Purification Kit (Epicentre) according to manufacturer's specifications. The RNA was then desalted on in-house prepared G-25 sephadex spin columns (BioRad) and quantified by absorbance at 260 nm [extinction coefficient]. Both RNA and whole cell samples were digested in 70% nitric acid (trace select, Fluka) for 2 hours at 65^{o}C then diluted to 2% (v/v) nitric acid with milli-Q H_2O. Ru content was determined by Inductively Coupled Plasma Mass Spectrometry (ICP-MS) using a Thermo VG PQExcell quadrupole ICP-MS equipped with a Gilson 222 autosampler at the W. M. Keck Collaboratory for Plasma Spectrometry (Oregon State University, Corvallis, Oregon). The instrument was calibrated for ^{99}Ru, ^{101}Ru and ^{102}Ru by developing standard curves from a Ru standard (High Purity Standards). All measurements were done in triplicate using ^{115}In as an internal standard. Intracellular Ru content was estimated using an average volume of 36.6 fL calculated for

a wild-type haploid strain of *S. cerevisiae* grown on YEPD media,[38] whose cell size matches estimates for control samples from this study (Figure C.1, Appendix C, and data not shown).

In Vitro *Oligonucleotide Treatment with NAMI-A*

RNA (Dharmacon, Inc.) and DNA (IDT) oligonucleotides (T_6GGT_5, U_6GGU_5, and A_5CCA_6) were heated to 90 °C for 90 s, cooled to room temperature, and then incubated with 0, 150, and 450 μM NAMI-A (freshly dissolved in the appropriate buffer immediately before use) in 25 mM phosphate buffer (pH 6.0 or 7.4) at 37 °C in the dark. All reactions were carried out for 6 or 24 h in 100 mM $NaNO_3$ and 2 mM $Mg(NO_3)_2$. Ascorbate was freshly dissolved in water immediately before use and added to the buffered oligonucleotide samples (final concentration 2.5 mM) immediately before NAMI-A. Samples were desalted using in-house prepared G-25 sephadex spin columns (BioRad) to stop the reaction.

MALDI-TOF Analysis

RNA and DNA samples were purified using C18 ZipTips (Millipore) with a procedure modified by Champan *et al.*[39] from the manufacturer's protocol for RNA.[40] ZipTips were washed by aspiration three times with 1:1 MeCN/H_2O, and equilibrated by washing three times with 0.1% trifluoroacetic acid (TFA). RNAs were bound to the tip by repeated aspiration of the analyte solution. Bound RNA was washed three times by aspiration with 0.1% TFA, three times with milli-Q water, and then eluted from the column using two washes of 1:1 MeCN/H_2O. The eluent was dried to completion by

SpeedVac and resuspended in a matrix consisting of 375 mM 2',4',6'-trihydroxyacetophenone (THAP, Sigma-Aldrich, puriss. p.a., matrix substance for MALDI-MS), 30 mM diammonium citrate in 3:1 EtOH/H_2O, with added NH_4^+ loaded Dowex cation exchange beads (Aldrich) and applied to the sample plate. MALDI-MS analysis was performed on a Waters QToF Premier mass spectrometer in positive-ion mode using V-mode optics.

Bridge to Chapter V

Chapters II, III, and IV describe *in vitro* and *in cellulo* experiments investigating cisplatin induced Pt-RNA binding and NAMI-A induced Ru-RNA binding. The following chapter pulls this information together in order to compare what has been learned about the RNA-binding abilities of the two drugs and discuss future directions for research on the interactions of anticancer metallodrugs with RNA.

CHAPTER V

CONCLUSIONS AND FUTURE DIRECTIONS

This chapter pulls together the knowledge gained so far and discusses questions for future investigation. All of the writing in this section was done by me, however many people have contributed to the ideas herein, including Prof. Victoria J. DeRose, Dr. Erich G. Chapman, Maire F. Osborn, and the other members of the DeRose lab.

Introduction

There is growing knowledge of both the importance RNA processes and the connections between RNA and other significant cellular processes such as cell cycle control and apoptosis. Despite this, and the fact that antitumor metallodrugs are known to bind to nucleic acids, little study has gone into investigating the roles that RNA-binding can play in the mechanisms of these and related drugs. This is a gap that the research presented in this dissertation addresses through both *in vitro* and *in cellulo* studies of the effects of cisplatin and NAMI-A treatment on RNA. As discussed in Chapter I cisplatin and NAMI-A were chosen because they are two anticancer metallodrugs that are both known to bind to DNA and that have different mechanisms of action. The research presented here aims to answer basic questions about the reactivity of these drugs (or their aquated products) with RNA *in vitro* and *in cellulo*, the kinds of adducts that are formed, and the types of RNA species that are targeted. Because this is an area of research that is largely unexplored every question that is answered leads to at least five new questions to explore. As is true for any exciting field full of thought-provoking questions and

possibilities, there are far too many questions here for any one person to answer in a single dissertation. As such, the following sections discuss both the conclusions drawn so far and the questions that these results have opened up for further research, beginning with a brief discussion of the relevant properties of cisplatin and NAMI-A.

Cisplatin and NAMI-A

Cisplatin is the best studied of the anticancer metallodrugs. It is a Pt based drug that exerts significant cytotoxicity against a range of primary tumors, and it is believe that binding to DNA at the N7 site of purine bases is an important part of its mechanism. When inside a cell, the low chloride concentration induces it to undergo aquation of its labile chloride ligands, producing aqua species that can react with cellular targets. Cisplatin inhibits tumor growth, but has little effect against metastasis.[1]

NAMI-A is a promising Ru-based anticancer drug currently in Phase Two of clinical trials. It has low general toxicity in patients and a much lower cytotoxicity than cisplatin. Rather than being effective against primary tumors, NAMI-A has strong antimetastatic effects. Although NAMI-A treatment forms DNA adducts at the N7 of purine bases, those adducts cause less structural distortion than those caused by cisplatin (likely due to the formation of different types of adducts). Therefore, it is not surprising that DNA adduct formation is not believed to be a major part of NAMI-A's mechanism of action. In addition, NAMI-A is known to undergo both aquation and reduction in biological conditions.[2]

***In Vitro* Studies**

Chapter II focused on the *in vitro* reactions of aquated cisplatin with RNA and DNA hairpins, including an RNA hairpin model, termed BBD, containing an internal loop that was derived from the active core of the spliceosome. Treatment of BBD with aquated cisplatin formed a novel cross-link across this internal loop. Kinetic studies determined that both BBD and a completely basepaired RNA hairpin react with aquated cisplatin 5-6 fold faster than a DNA hairpin. Interestingly, the rate of these reactions increases at lower pH. MALDI-MS analysis demonstrated that for all of these oligonucleotide constructs many Pt adducts were forming (as many as 7 $[Pt(NH_3)_2]^{2+}$ adducts were observed under some conditions). Collectively these data support a model in which there are kinetically preferred platinum binding sites, such as the cross-link across BBD, that compete with less reactive sites in oligonucleotide structures.

Chapter IV includes *in vitro* experiments in which single-stranded RNA and DNA oligonucleotides with a simple U_6GGU_5 or T_6GGT_5 sequence were treated with NAMI-A and then analyzed by MALDI-MS. The results demonstrate significant Ru binding to RNA *in vitro*, which goes to the furthest extent in an acidic, reducing environment like that found in a tumor. Although a direct comparison between the reactivity of RNA and DNA was not possible, all changes in drug concentration and solution conditions produced similar effects on both the RNA and DNA constructs studied, implying that Ru binding to RNA and DNA are comparable.

From these results it is clear that the RNA-binding caused by cisplatin and NAMI-A treatment shares some common features: both drugs can cause multiple RNA adducts to be formed (even when the simple U_6GGU_5 was used with NAMI-A), binding

is enhanced when the pH is lowered, and similar or better reactivity is observed for RNA when compared to DNA. The main difference observed between the cisplatin and NAMI-A in these studies is that NAMI-A can be activated toward RNA binding through reduction, while it is known that cisplatin is not reduced *in vivo*.

These comparisons lead to several interesting questions: How do the RNA adduct profiles and reaction rates produced by cisplatin and NAMI-A treatment compare? Is NAMI-A treatment capable of producing the same type of interstrand cross-link that is formed in BBD with cisplatin treatment? It has been shown with DNA that NAMI-A treatment causes less structural distortion, possibly due to the formation of a greater number of monoadducts.[3] Are these differences in adduct profile and structural impact true for RNA as well? This is particularly interesting in light of the *in cellulo* data reviewed below that shows that NAMI-A treatment results in greater uptake and higher numbers of RNA-adducts while causing lower cytotoxicity. Perhaps there are different toxicities for the adducts formed by each drug, in which those produced by NAMI-A treatment cause less structural distortion and inhibition of function. This leads to the question: What effects do the Ru-RNA adducts produced by NAMI-A treatment have on RNA structure and function? This question can be addressed by further *in vitro* studies, beginning with tests of the both ability of Ru to form interstrand cross-links and of exo- and endo-nucleases to degrade the Ru-RNA adducts.

In Cellulo* Studies in *S. Cerevisiae

Chapter III discussed *in cellulo* experiments using cisplatin-treated *S. cerevisiae.* At cisplatin treatment concentrations that caused moderate and severe culture growth

inhibition at 29 h, large decreases in cell viability were observed at 6 h. Morphological studies of cisplatin-treated yeast showed increased cell size and tests for apoptotic markers indicated that apoptosis is not taking place. In-cell Pt concentrations and Pt accumulation on RNA are roughly proportional when measured by ICP-MS. At 12 h a higher Pt per nucleotide ratio was measured in DNA than RNA, but because there is much more RNA than DNA per cell, the total number of Pt bound to cellular RNA is higher than the total number of Pt bound to cellular DNA for each yeast cell. Interestingly, Pt accumulation in gel-isolated rRNA was close to that accumulated in total cellular RNA, while the amount of Pt in mRNA was substantially lower.

Chapter IV covered studies on NAMI-A treated *S. cerevisiae*. When compared to cisplatin, it takes significantly higher doses of NAMI-A to inhibit yeast culture growth. At doses that cause both moderate and severe inhibition of culture growth at 24 h, only a moderate loss in cell viability was observed at 6 h. This matches literature reports indicating that NAMI-A is much less cytotoxic than cisplatin.[4] When the Ru accumulation in whole cells and cellular RNA was measured by ICP-MS it was found that, just as for cisplatin, the accumulation of Ru in RNA is proportional to the accumulation of Ru in whole cells. Significantly, it was also observed that more drug adducts accumulate per cell for NAMI-A treated yeast than for yeast treated with similar concentrations of cisplatin, while causing lower toxicity.

It is not yet known if different types of cellular RNA accumulate different amounts of Ru, nor is it known what type of cell death NAMI-A induces in *S. cerevisiae*, though preliminary studies indicate that apoptosis is not induced (data not shown). These interesting lines of investigation lead to several big questions. The first is “Do the adducts

formed by cisplatin and NAMI-A treatment accumulate to the same extend in mRNA, rRNA, tRNA, and snRNA?" Fundamentally, this question asks both how accessible different types of cellular RNA are to metal-based drugs and how the drug-adducts formed on those different RNA species are processed. For yeast cultures continuously treated with antitumor metallodrugs the processes of accumulation and removal are difficult to separate. However, these two important processes could be teased apart by studies following the removal of drug adducts from RNA. In these studies, drug treatment would be discontinued after a period of time and then the rate of adduct removal for each type of RNA could be observed as a function of time. This would tell us if drug adducts on mRNA are, in fact, being removed much more quickly than those on rRNA (and thus responsible for the differences in observed Pt accumulation). The comparison of adduct accumulation and removal between cisplatin and NAMI-A would provide interesting information about how general these processes are for different metallodrugs. A related research question would be to probe which pathways are responsible for removing Pt and Ru adducts using the library of deletion strains available from the *Saccharomyces* Genome Deletion Project to knock out one degradation pathway at a time and observe changes in drug adduct accumulation.

Future Possibilities

There is a great deal still being learned about RNA degradation, repair, and the connections between RNA processes, cell cycle control, and apoptosis. In addition, very little is known about the effect of anticancer metallodrugs on RNA, leaving numerous future research possibilities wide open. Mapping experiments could be done to locate

specific drug binding sites in cellular RNAs. All of the *in cellulo* experiments described above would be very interesting to try in HeLa cells, especially if the RNA degradation pathways responsible for clearing most of the RNA drug adducts could be first located in *S. cerevisiae*. The contributions of drug adduct formation on RNA to the mechanism of action of cisplatin and NAMI-A could be tested using the connections between RNA and apoptosis that have been uncovered so far. For example, can cisplatin or NAMI-A treated tRNA still bind to cytochrome c and inhibit the initiation of apoptosis?[5] In addition, other nucleic acid binding anticancer drugs with both similar and different mechanisms of action to cisplatin and NAMI-A could be tested to build up both a picture of RNA accessibility to metallodrugs and the impacts of drug binding on RNA structure and function.

If I had the time I could easily do five more dissertations on this topic and I wouldn't be anywhere near done answering all of these questions. That is why this is such an exciting area of research. It is largely unexplored and full of intriguing questions and fascinating possibilities. I am grateful to have had the opportunity to spend my time at the University of Oregon exploring it.

APPENDIX A

SUPPORTING INFORMATION FOR CHAPTER II: RAPID CROSS-LINKING OF AN RNA INTERNAL LOOP BY THE ANTICANCER DRUG CISPLATIN

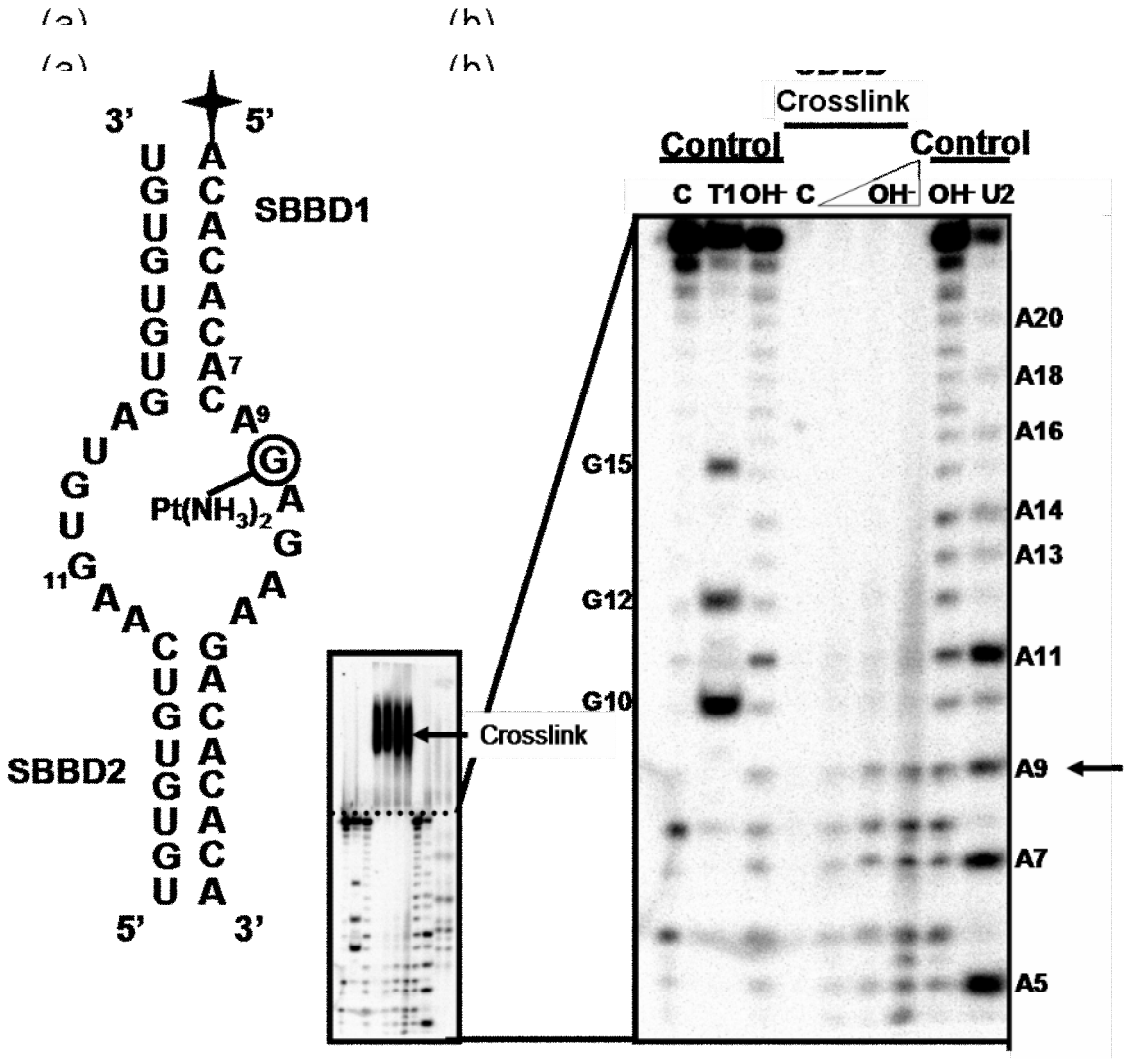

Figure A.1. (a) The predicted secondary structure of hybridized SBBD1 and SBBD2 RNAs with the location of the major platinum induced cross-link on the SBBD1 strand highlighted. (b) 20% dPAGE analysis of the products of partial alkali hydrolysis of the SBBD cross-link with 5'-end-labeled SBBD1. Lanes: Control- **C:** 5' end-labeled SBBD1. **T1:** G specific sequence ladder generated by partial nuclease digestion of SBBD1 RNA by T1 RNase. **U2:** A specific sequence ladder generated by partial nuclease digestion of SBBD1 RNA by U2 RNAse. **OH^-:** Reference alkali hydrolysis ladder for SBBD1. SBBD Cross-link Samples- **C:** dPAGE-isolated SBBD cross-link. **OH^- Lanes:** dPAGE-isolated SBBD cross-link treated under alkali hydrolysis for increasing amounts of time.

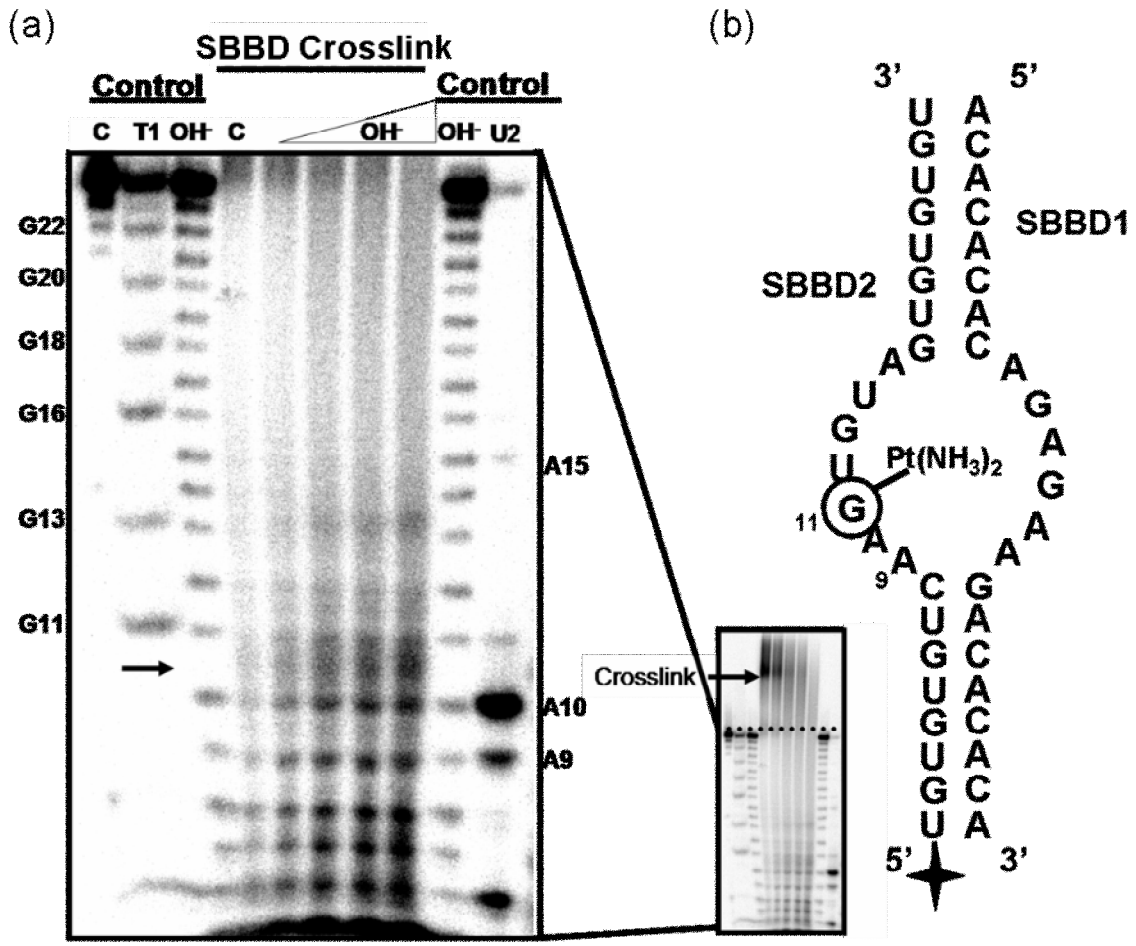

Figure A.2. (a) 20% denaturing PAGE analysis of the products of partial alkali hydrolysis of the SBBD cross-link with 5'-end-labeled SBBD2. Lanes: Control- **C:** 5' end-labeled SBBD2. **T1:** G specific sequence ladder generated by partial nuclease digestion of SBBD2 RNA by T1 RNase. **U2:** A specific sequence ladder generated by partial nuclease digestion of SBBD2 RNA by U2 RNAse. **OH^-:** reference alkali hydrolysis ladder for SBBD2. SBBD cross-link Samples- **C:** dPAGE-isolated SBBD2 cross-link. **OH^- Lanes:** dPAGE-isolated SBBD cross-link treated under alkali hydrolysis for increasing amounts of time. (b) The predicted secondary structure of hybridized SBBD1 and SBBD2 RNAs with the location of the major $[Pt(NH_3)_2]^{2+}$ on the SBBD2 strand highlighted.

(a)

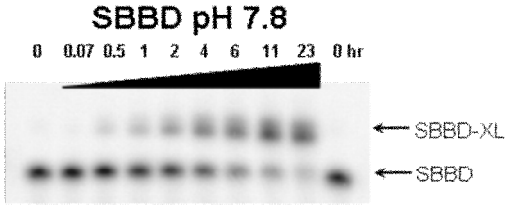

(a)

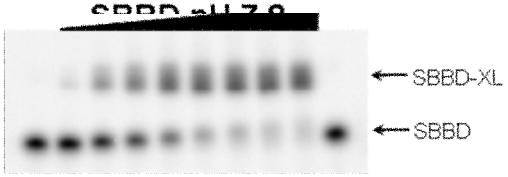

(b)

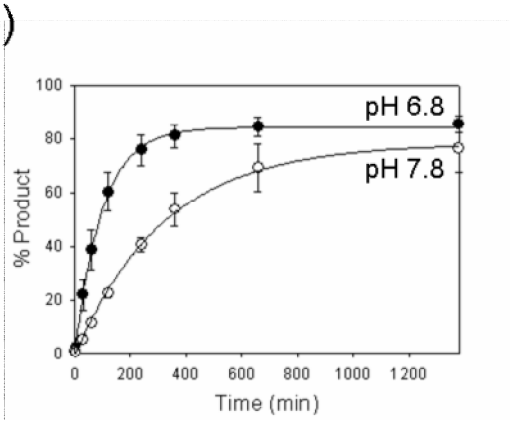

Figure A.3. (a) dPAGE radiograms depicting products of cisplatin binding to SBBD in pH 6.8 and 7.8 over time. (b) Comparison of the reaction rates of SBBD in pH 6.8 (filled circles) and 7.8 (open circles). Conditions: (a) Reactions were performed with 0.1 M SBBD duplex with either 50 M aquated cisplatin in 5 mM TEA (pH 7.8) or 25 M aquated cisplatin in 5 mM MOPS (pH 6.8). Both reactions were in 100 mM $NaNO_3$, 1 mM $Mg(NO_3)_2$, and at 37 °C. Reactions analyzed by 20% dPAGE.

(a)

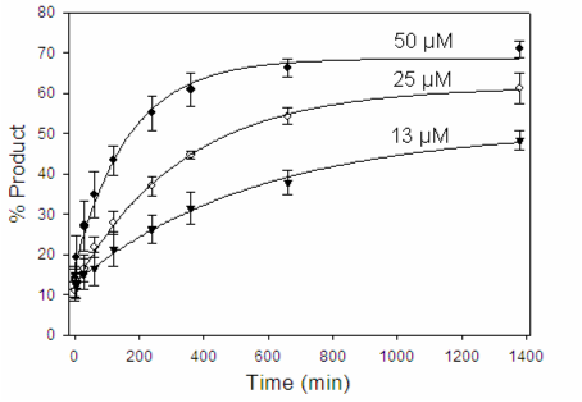

(b)

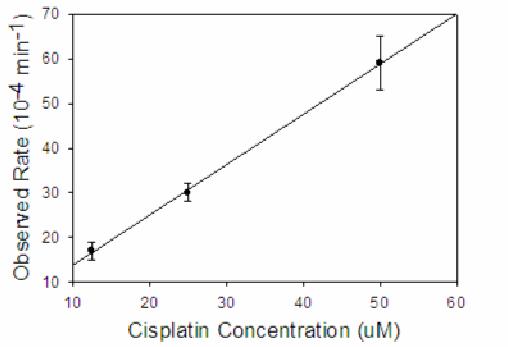

Figure A.4. (a) BBD kinetics with 50 M (filled circles), 25 M (open circles), and 12.5 M (triangles) aquated cisplatin. (b) Observed rate constant (k_{obs}) versus cisplatin concentration. Conditions: Reactions were performed in 100 mM $NaNO_3$, 1 mM $Mg(NO_3)_2$, and 5 mM TEA (pH 7.8) at 37 °C.

Table A.1. Platination Rates of Oligonucleotide Constructs[a]

Construct	M Pt	pH	k_{obs} (10^{-5} s^{-1})	k_{rxn2} (M^{-1} s^{-1})[b]
BBD	50	7.8	9.8(1.0)	2.0(2)
BBD	25	7.8	5.0(3)	2.0(1)
BBD	12.5	7.8	2.8(3)	2.3(2)
BBD	25	6.8	21.3(1.8)	8.5(7)
RNA HP	50	7.8	8.3(2)	1.7(3)
DNA HP	50	7.8	1.7(2)	0.33(3)
SBBD	50	7.8	5.2(3)	1.1(1)
SBBD	25	6.8	17.0(5)	6.8(2)

a All experiments used 0.1 M oligonucleotide (or 0.1 μM SBBD duplex) and were performed at 37 °C with 100 mM $NaNO_3$ and 1 mM $Mg(NO_3)_2$. Trials at pH 7.8, and 6.8 were done in 5 mM TEA and MOPS respectively.

b Because all kinetics were performed under pseudo-first order conditions, second order rate constants were obtained by dividing k_{obs} by the concentration of aquated cisplatin used.

APPENDIX B

SUPPORTNG INFORMATION FOR CHAPTER III: CHARACTERIZATION OF RNA-PT ADDUCTS IN *S. CEREVISIAE*

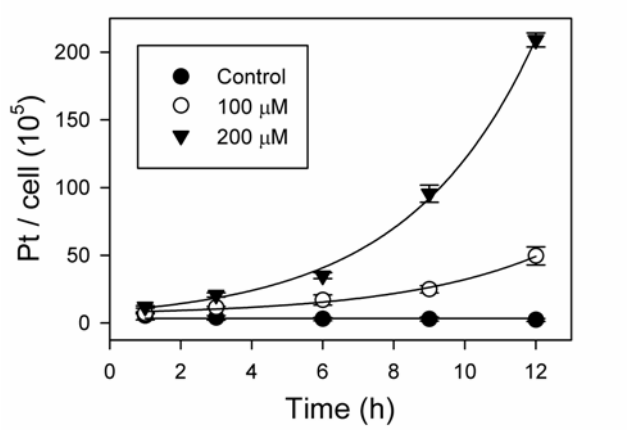

Figure B.1. Accumulation of Pt atoms per yeast cell in yeast treated with cisplatin for 1, 3, 6, 9, and 12 h. Results averaged from four independent experiments, presented as the means ± SD.

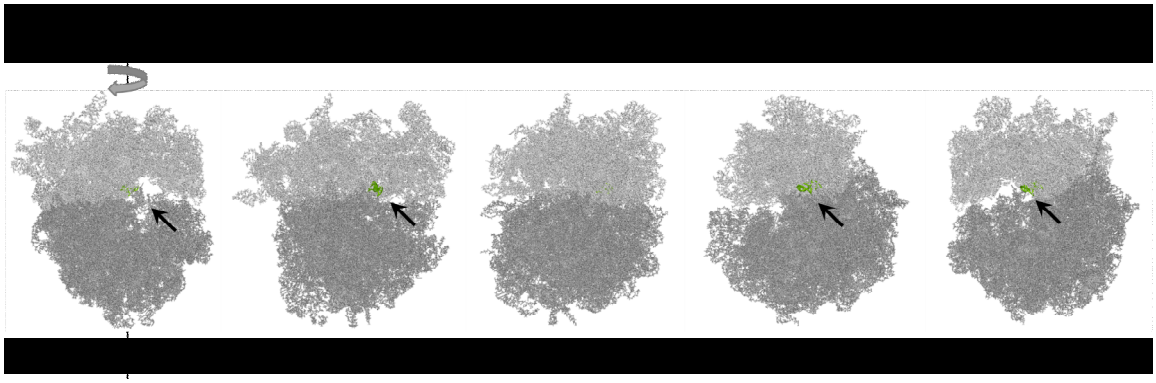

Figure B.2. Helix 18 of the yeast ribosome (green) is located in close proximity to the peptidyltransferase center within the small ribosomal subunit (light gray). Image created with PyMol from PDB files 3O30 and 3O5H.

APPENDIX C

SUPPORTING INFORMATION FOR CHAPTER IV: RU BINDING TO RNA FOLLOWING TREATMENT WITH THE ANTI-METASTATIC DRUG NAMI-A IN *S. CEREVISIAE* AND *IN VITRO*

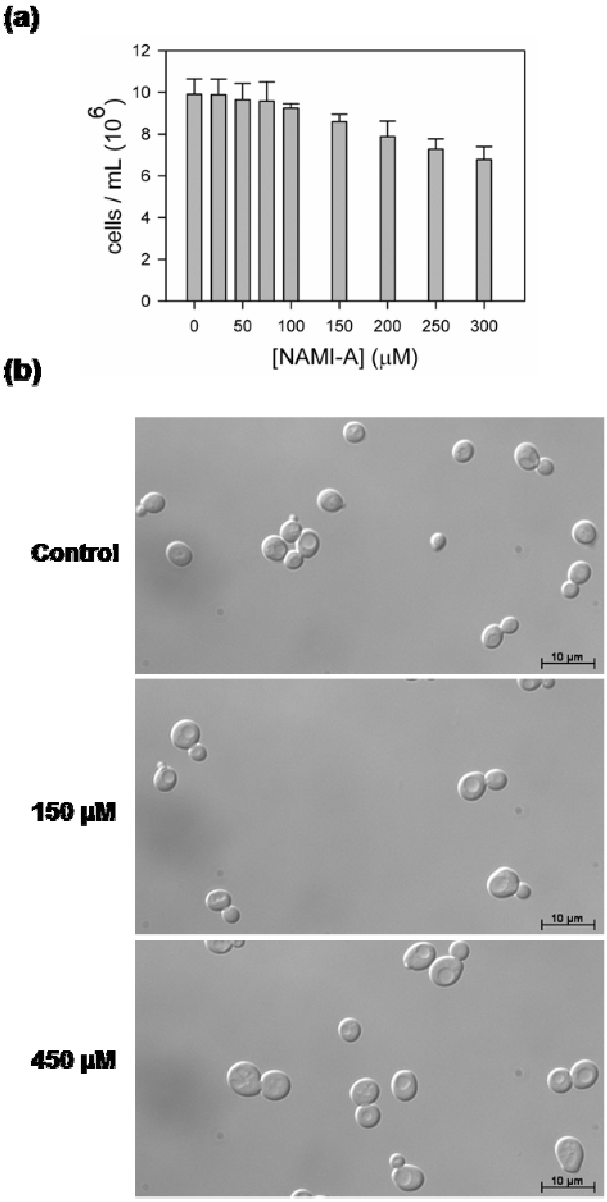

Figure C.1. (a) Yeast culture growth after 6 h of continuous NAMI-A treatment. Results were averaged from three independent experiments presented as the means ± SD. (b) Differential interference contrast images of NAMI-A treated yeast at 6 h. Images were acquired on a Carl Zeiss Axioplan 2 fluorescence microscope using a 100× objective and AxioVision software (Carl Zeiss, Thornwood, NY).

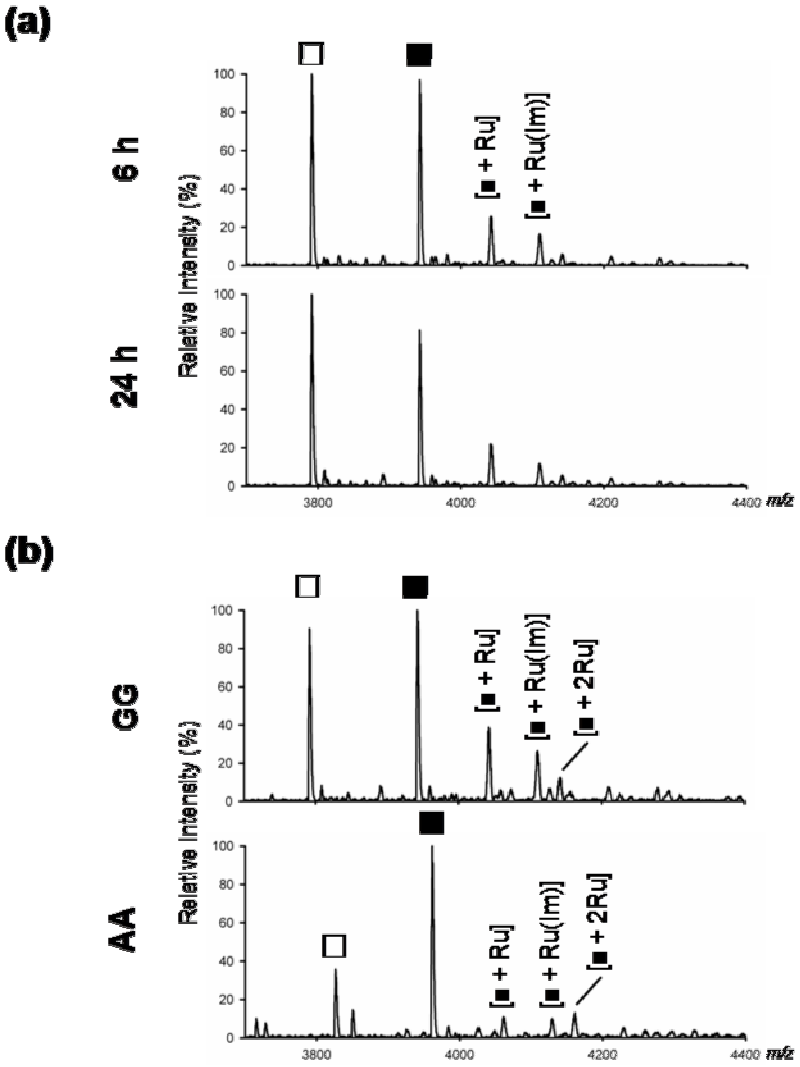

Figure C.2. Representative MALDI-TOF spectra of the products of the incubation of NAMI-A with (a) DNA T_6GGT_5 for 6 and 24 h in 150 μM NAMI-A and (b) DNA T_6GGT_5 and A_5CCA_6 for 6 h in 450 μM NAMI-A (comparison of GG and AA binding sites). Reactions were run with 20 μM oligonucleotides at pH 6.0 in 100 mM $NaNO_3$ and 2 mM $Mg(NO_3)_2$ at 37 °C. Filled squares denote the unmodified, full-length T_6GGT_5 and A_5CCA_6 strands and open squares denote singly depurinated oligonucleotides strands.

REFERENCES CITED

Chapter I

(1) Dyson, P. J.; Sava, G. *Dalton Trans.* **2006**, 1929-1933.

(2) Jung, Y.; Lippard, S. J. *Chem. Rev.* **2007**, *107*, 1387-1407.

(3) Hannon, M. J. *Pure Appl. Chem.* **2007**, *79*, 2243-2261.

(4) Boulikas, T.; Vougiouka, M. *Oncol. Rep.* **2003**, *10*, 1663-1682.

(5) Heffeter, P.; Jungwirth, U.; Jakupec, M.; Hartinger, C.; Galanski, M.; Elbling, L.; Micksche, M.; Keppler, B.; Berger, W. *Drug Resist. Update.* **2008**, *11*, 1-16.

(6) Page, S. M.; Boss, S. R.; Barker, P. D. *Future Med. Chem.* **2009**, *1*, 541-559.

(7) Clarke, M. J.; Zhu, F.; Frasca, D. R. *Chem. Rev.* **1999**, *99*, 2511-2533.

(8) Antonarakis, E. S.; Emadi, A. *Cancer Chemother. Pharmacol.* **2010**, *66*, 1-9.

(9) Qureshi, I. A.; Mehler, M. F. *Arch. Neurol.* **2010**, *67*, 1435-1441.

(10) Mattick, J. S. *Nat. Rev. Genet.* **2004**, *5*, 316-323.

(11) Jamieson, E. R.; Lippard, S. J. *Chem. Rev.,* **1999**, *99*, 2467-2498.

(12) Schmittgen, T. D.; Ju, J.-F.; Danenberg, K. D.; Danenberg, P. V. *Int. J. Oncol.* **2003**, *23*, 785-789.

(13) Rosenberg, J. M.; Sato, P. H. *Mol. Pharmacol.* **1993**, *43*, 491-497.

(14) Burda, J. V.; Zeizinger, M.; Leszczynski, J. *J. Comput. Chem.* **2005**, *26*, 907-914.

(15) Davies, M. S.; Berners-Price, S. J.; Hambley, T. W. *Inorg. Chem.* **2000**, *39*, 5603-5613.

(16) Davies, M. S.; Berners-Price, S. J.; Hambley, T. W. *J. Inorg. Biochem.* **2000**, *79*, 167-172.

(17) Bancroft, D. P.; Lepre, C. A.; Lippard, S. J. *JACS* **1990**, *112*, 6860-6870.

(18) Gerweck, L. E., Vijayappa, S., and Kozin, S. (2006) Tumor pH controls the in vivo efficacy of weak acid and base chemotherapeutics. *Mol. Cancer Ther. 5*, 1275–1279.

(19) Berners-Price, S. J.; Frenkiel, T. A.; Frey, U.; Ranford, J. D.; Sadler, P. J. *J. Chem. Soc., Chem. Commun.* **1992**, 789-791.

(20) Hambley, T. W. *Dalton Trans.* **2001**, 2711-2718.

(21) Elmroth, S. K. C.; Lippard, S. J. *Inorg. Chem.* **1995**, *34*, 5234-5243.

(22) Monjardet-Bas, V.; Elizondo-Riojas, M. A.; Chottard, J. C.; Kozelka, J. *Angew. Chem., Int. Ed.* **2002**, *41*, 2998-3001.

(23) Snygg, A. S.; Brindell, M.; Stochel, G.; Elmroth, S. K. C. *Dalton Trans.* **2005**, 1221-1227.

(24) Fuertes, M. A.; Castilla, J.; Nguewa, P. A.; Alonso, C.; Perez, J. M. *Medicinal Chemistry Reviews* **2004**, *1*, 187-198.

(25) Baik, M.-H.; Friesner, R. A.; Lippard, S. J. *JACS* **2003**, *125*, 14082-14092.

(26) Garnier, I. O.; Bombard, S. *J. Inorg. Biochem.* **2007**, *101*, 514-524.

(27) Gonnet, F.; Reeder, F.; Kozelka, J.; Chottard, J.-C. *Inorg. Chem.* **1996**, *35*, 1653-1658.

(28) Monjardet-Bas, V.; Chottard, J.-C.; Kozelka, J. *Chem. Eur. J.* **2002**, *8*, 1144-1150.

(29) Mattick, J. S. *Nat. Rev. Genet.* **2004**, *5*, 316-323.

(30) Warner, J. R. *Trends Biochem. Sci.* **1999**, *24*, 437-440.

(31) Hamilla, S.; Wolina, S. L.; Reinischa, K. M. *P. Natl. Acad. Sci. USA* **2010**, *107*, 15045-15050.

(32) Isken, O.; Maquat, L. E. *Genes Dev.* **2007**, *21*, 1833-3856.

(33) Lafontaine, D. L. J. *Trends Biochem. Sci.* **2009**, *35*, 267-277.

(34) Chernyakov, I.; Whipple, J. M.; Kotelawala, L.; Grayhack, E. J.; Phizicky, E. M. *Genes Dev.* **2008**, *22*, 1369-1380.

(35) Aas, P. A.; Otterlei, M.; Falnes, P. O.; Vagbo, C. B.; Skorpen, F.; Akbari, M.; Sundheim, O.; Bjoras, M.; Slupphaug, G.; Seeberg, E.; Krokan, H. E. *Nature* **2003**, *421*, 859-863.

(36) Reichert, A. S.; Morl, M. *Nucleic Acids Res.* **2000**, *28*, 2043-2048.

(37) Kong, Q.; Lin, C.-L. G. *Cell. Mol. Life Sci.* **2010**, *67*, 1817-1829.

(38) Olmo, N.; Turnay, J.; González de Buitrago, G.; López de Silanes, I.; Gavilanes, J. G.; Lizarbe, M. A. *Eur. J. Biochem.* **2001**, *268*, 2113-23.

(39) Jetzt, A. E.; Cheng, J. S.; Tumer, N. E.; Cohick, W. S. *Int. J. Biochem. Cell B.* **2009**, *41*, 2503-2510.

(40) Hinnebusch, A. G. *Genes Dev.* **2009**, *23*, 891-895.

(41) Horn, H. F.; Vousden, K. H. *Oncogene* **2007**, *26*, 1306-1316.

(42) Holzel, M.; Burger, K.; Muhl, B.; Orban, M.; Kellner, M.; Eick, D. *OncoTarget* **2010**, 43-47.

(43) Zhang, F.; Hamanaka, R. B.; Bobrovnikova-Marjon, E.; Gordan, J. D.; Dai, M. S.; Lu, H.; Simon, M. C.; Diehl, J. A. *J. Biol. Chem.* **2006**, *281*, 30036-30045.

(44) Deisenroth, C.; Zhang, Y. *Oncogene* **2010**, *29*, 4253-4260.

(45) Thompson, D. M.; Parker, R. *Cell* **2009**, *138*, 215-219.

(46) Mroczek, S.; Kufel, J. *Nucleic Acids Res.* **2008**, *36*, 2874-2888.

(47) Degen, W. G. J.; Pruijn, G. J. M.; Raats, J. M. H.; van Venrooij, W. J. *Cell Death Differ.* **2000**, *7*, 616-627.

(48) Mei, Y. D.; Yong, J.; Liu, H. T.; Shi, Y. G.; Meinkoth, J.; Dreyfuss, G.; Yang, X. L. *Mol. Cell* **2010**, *37*, 668-678.

(49) Hoffmann, R.L. *Tox. & Env. Chem.,* **1988** *17*, 139-151.

(50) Harder, H. C.; Rosenberg, B. *Int. J. Cancer* **1970**, *6*, 207-215.

(51) Jung, Y.; Lippard, S.J. *J. Biol. Chem.* **2006,** *281***,** 1361-1370.

(52) Jordan, P.; Carmo-Fonseca, M. *Nuc. Acids Res.* **1998**, *26*, 2831-2836.

(53) Tornaletti, S.; Patrick, S. M.; Turchim, J. J.; Hanawalt, P. C. *J. Biol. Chem.* **2003**, *287*, 35791-35797.

(54) Ang, W. H.; Myint, M.; Lippard, S. J. *J. Am. Chem. Soc.* **2010**, *132*, 7429-7435.

(55) Danenberg, P. V.; Shea, L. C. C.; Danenberg, K. D.; Horikoshi, T. *Nucleic Acids Res.* **1991**, *19*, 3123-3128.

(56) Rosenberg, J.; Sato, P. *Mol. Pharmacol.* **1988**, *33*, 611-616.

(57) Heminger, K. A.; Hartson, S. D.; Rogers, J.; Matts, R. L. *Arch. Biochem. Biophys.* **1997**, *344*, 200-207.

(58) Houseley, J.; Tollervey, D. *Cell* **2009**, *136*, 763-776.

(59) Phizicky, E. M.; Hooper, A. K. *Genes Dev.* **2010**, *24*, 1832-1860.

(60) Chapman, E. G.; DeRose, V. J. *J. Am. Chem. Soc.* **2010**, *132*, 1946-1952.

(61) Rijal, K.; Chow, C. S. *Chem. Comm.* **2009**, 107-109.

(62) Hostetter, A. A.; Chapman, E. G.; DeRose, V. J. *J. Am. Chem. Soc.* **2009**, *131*, 9250-9257.

(63) Hagerlof, M.; Papsai, P.; Chow, C. S.; Elmroth, S. K. C. *J. Biol. Inorg. Chem.* **2006**, *11*, 974-990.

(64) J. R. Rubin, M. Sabat and M. Sundaralingam, *Nuc. Acids Res.*, 1983, **11**, 6571-6586.

(65) J. C. Dewan, *J. Am. Chem. Soc.*, 1984, **106**, 7239-7244.

(66) Papsai, P.; Aldag, J.; Persson, T.; Elmroth, S. K. C. *J. Chem. Soc., Dalton Trans.* **2006**, 3515-3517.

(67) Papsai, P.; Snygg, A. S.; Aldag, J.; Elmroth, S. K. C. *Dalton Trans.* **2008**, 5225-5234.

(68) Pascoe, J. M.; Roberts, J. J. *Biochem. Pharmacol.* **1974**, *23,* 1345-1357.

(69) Akoboshi, M.; Kawai, K.; Maki, H.; Akuta, K.; Ujeno, Y.; Miyahara, T. *Jpn. J. Cancer Res.* **1992**, *83*, 522-526.

(70) Akoboshi, M.; Kawai, K.; Maki, H.; Akuta, K.; Ujeno, Y.; Ono, K.; Miyahara, T. *Nuc. Med. Biol.* **1994**, *20*, 389-393.

(71) Esteban-Fernández, D.; Verdaguer, J. M.; Ramírez-Camacho, R.; Palacios, M. A.; Gómez-Gómez, M. M. *J. Anal. Toxicol.* **2008**, *32*, 140-146.

(72) Kabolizadeh, P.; Ryan, J.; Farrell, N. *Biochem. Pharmacol.* **2007**, *73*, 1270-1279.

(73) Song, I.-S.; Savaraj, N.; Siddik, Z. H.; Liu, P.; Wei, Y.; Wu, C. J.; Kuo, M. T. *Mol. Cancer Ther.* **2004**, *3*, 1543-1549.

(74) Zhang, J.; Zhao, X. *Eur. J. Med. Chem.* **2007**, *42*, 286-291.

(75) Goodman, J.; Hagrman, D.; Tacka, K. A.; Souid, A.-K. *Cancer Chemother. Pharmacol.* **2006**, *57*, 257-267.

(76) Gabano, E.; Colangelo, D.; Ghezzi, A. R.; Osella, D. *J. Inorg. Biochem.*, **2008**, *102*, 629-635.

(77) Kitada, N.; Takara, K.; Minegaki, T.; Itoh, C.; Tsujimoto, M.; Sakaeda, T.; Yokoyama, T. *Cancer Chemother. Pharmacol.* **2008**, *62*, 577-584.

(78) Martelli, L.; Di Mario, F.; Ragazzi, E.; Apostoli, P.; Leone, R.; Perego, P.; Fumagalli, G. *Biochem. Pharmacol.* **2006**, *72*, 693-700.

(79) Gemba, M.; Nakatani, E.; Teramoto, M.; Nakano, S. *Toxicol. Lett.* **1987**, *38*, 291-297.

(80) Yang, Z.; Schumaker, L. M.; Egorin, M. J.; Zuhowski, E. G.; Guo, Z.; Cullen, K. J. *Clin. Cancer Res.* **2006**, *12*, 5817-5825.

(81) Giurgiovich, A. J.; Diwan, B. A.; Olivero, O. A.; Anderson, L. M.; Rice, J. M.; Poirier, M. C. *Carcinogenesis* **1997**, *18*, 93-96.

(82) Olivero, O. A.; Semino, C.; Kassim, A.; Lopez-Larraza, D. M.; Poirier, M. C. *Mutat. Res.* **1995**, *346*, 221-230.

(83) Lindauer, E.; Holler, E. *Biochem. Pharmacol.* **1996**, *52*, 7-14.

(84) Samimi, G.; Katano, K.; Holzer, A. K.; Safaei, R.; Howell, S. B. *Mol. Pharmacol.* **2004**, *66*, 25-32.

(85) Samimi, G.; Safaei, R.; Katano, K.; Holzer, A. K.; Rochdi, M.; Tomioka, M.; Goodman, M.; Howell, S. B. *Clin. Cancer Res.* **2004**, *10*, 4661-4669.

(86) Klein, A. V.; Hambley, T. W. *Chem. Rev.* **2009**, *109*, 4911-4920.

(87) Beretta, G. L.; Righetti, S. C.; Lombardi, L.; Zunino, F.; Perego, P. *Ultrastruct. Pathol.* **2002**, *26*, 331-334.

(88) Khan, M. U. A.; Sadler, P. J. *Chem.-Biol. Interact*. **1978**, *21*, 227-232.

(89) Kiyozuka, Y.; Takemoto, K.; Yamamoto, A.; Guttmann, P.; Tsubura, A.; Kihara, H. *X-ray Microscopy: Proceedings of the Sixth International Conference* **2000**, 153-158.

(90) Meijer, C.; van Luyn, M. J. A.; Nienhuis, E. F.; Blom, N.; Mulder, N. H.; de Vries, E. G. E. *Biochem. Pharmacol.* **2001**, *61*, 573-578.

(91) Ortega, R.; Moretto, P.; Fajac, A.; Bénard, J.; Llabador, Y.; Simonoff, M. *Cell. Mol. Biol.* **1996**, *42*, 77-88.

(92) Hall, M. D.; Dillon, C. T.; Zhang, M.; Beale, P.; Cai, Z.; Lai, B.; Stampfl, A. P. J.; Hambley, T. W. *J. Biol. Inorg. Chem.* **2003**, *8*, 726-732.

(93) Hall, M. D.; Alderden, R. A.; Zhang, M.; Beale, P. J.; Cai, Z.; Lai, B.; Stampfl, A. P. J.; Hambley, T. W. *J. Struct. Biol.* **2006**, *155*, 38-44.

(94) Berry, J. P.; Galle, P.; Viron, A.; Kacerovská, H.; Macieira-Coelho, A. *Biomed. Pharmacother.* **1983**, *37*, 125-129.

(95) Kirk, R. G.; Gates, M. E.; Chang, C.-S.; Lee, P. *Exp. Mol. Pathol.* **1995**, *63*, 33-40.

(96) Makita, T.; Itagaki, S.; Ohokawa, T. *Jpn. J. Cancer Res.* **1985**, *76*, 895-901.

(97) Berry, J. P.; Brille, P.; LeRoy, A. F.; Gouveia, Y.; Ribaud, P.; Galle, P.; Mathé, G. *Cancer Treat. Rep.* **1982**, *66*, 1529-1533.

(98) Molenaar, C.; Teuben, J.-M.; Heetebrij, R. J.; Tanke, H. J.; Reedijk, J. *J. Biol. Inorg. Chem.* **2000**, *5*, 655-665.

(99) Kalayda, G. V.; Zhang, G.; Abraham, T.; Tanke, H. J.; Reedijk, J. *J. Med. Chem.* **2005**, *48*, 5191-5202.

(100) Katano, K.; Safaei, R.; Samimi, G.; Holzer, A.; Tomioka, M.; Goodman, M.; Howell, S. B. *Clin. Cancer Res.* **2004**, *4578*, 4578-4588.

(101) Safaei, R.; Katano, K.; Larson, B. J.; Samimi, G.; Holzer, A. K.; Naerdemann, W.; Tomioka, M.; Goodman, M.; Howell, S. B. *Clin. Cancer Res.* **2005**, *756*, 756-767.

(102) Liang, X.-J.; Shen, D.-W.; Chen, K. G.; Wincovitch, S. M.; Garfield, S. H., Gottesman, M. M. *J. Cell. Physiol.* **2005**, *202*, 635-641.

(103) Brindell, M.; Stawoska, I.; Supel, J.; Skoczowski, A.; Stochel, G. van Eldik, R. *J. Biol. Inorg. Chem.* **2008**, *13*, 909-918.

(104) Bacac, M.; Hotze, A. C. G.; van der Schilden, K.; Haasnoot, J. G.; Pacor, S.; Alessio, E.; Sava, G.; Reedijk, J. *J. Inorg. Biochem.* **2004**, *98*, 402-412.

(105) Ravera, M.; Baracco, S.; Cassino, C.; Zanellos, P.; Osella, D. *Dalton Trans*. **2004**, 2347-2351.

(106) Brindell, M.; Piotrowska, D.; Shoukry, A. A.; Stochel, G.; van Eldik, R. *J. Biol. Inorg. Chem*. **2007**, *12*, 809–818.

(107) Sava, G.; Bergamo, A.; Zorzet, S.; Gava, B.; Casarsa, C.; Cocchietto, M.; Fulani, A.; Scarcia, V.; Serli, B.; Iengo, E.; Alessio, E.; Mestroni, G. *Eur. J. Cancer* **2002**, *38,* 427-435.

(108) Gullino, P.M. *Adv. Exp. Biol. Med.* **1976**, *75*, 521–536.

(109) Richard, D. E.; Berra, E.; Pouyssegur, J. *Biochem. Biophys. Res. Commun.* **1999**, *266,* 718–722.

(110) Gerweck, L. E.; Vijayappa, S.; Kozin, S. *Mol. Cancer Ther.* **2006**, *5*, 1275–1279.

(111) Levina, A.; Mitra, A.; Lay, P. A. *Metallomics* **2009**, *1*, 458-470.

(112) Bergamo, A.; Messori, L.; Piccoli, F.; Cocchietto, M.; Sava, G. *Inv. New Drugs* **2003**, *21*, 401–411.

(113) Bergamo, A.; Gagliardi, R.; Scarcia, V.; Furlani, A.; Alessio, E.; Mestroni, G.; Sava, G. *J. Pharmacol. Exp. Ther.* **1999**, *289*, 559-564.

(114) Kostova, I. *Curr. Med. Chem.* **2006**, *13*, 1085-1107.

(115) Sava, G.; Capozzi, I.; Bergamo, A.; Gagliardi, R.; Cocchietto, M.; Masiero, L.; Onisto, M.; Alessio, E.; Mestroni, G.; Garbisa, S. *Int. J. Cancer* **1996**, *68*, 60-66.

(116) Schluga, P.; Hartinger, C. G.; Egger, A.; Reisner, E.; Galanski, M.; Jakupec, M. A.; Keppler, B. K. *Dalton Trans.* **2006**, 1796-1802.

(117) Groessl, M.; Tsybin, Y. O.; Hartinger, C. G.; Keppler, B. K.; Dyson, P. J. *J. Biol. Inorg. Chem.* **2010**, *15*, 677-688.

(118) Malina, J.; Novakova, O.; Keppler, B. K.; Alessio, E.; Brabec, V. *J. Biol. Inorg. Chem.* **2001**, *6*, 435-445.

(119) Galori, E.; Vettori, C.; Alesso, E.; Vilchez, F. G.; Vilaplana, R.; Orioli, P.; Casini, A.; Messori, L. *Arch. Biochem. Biophys.* **2000**, *376*, 156-162.

(120) Messori, L.; Casini, A.; Vullo, D.; Haroutiunian, S. G.; Dalian, E. B.; Orioli, P. *Inorg. Chim. Acta* **2000**, *303*, 283-286.

(121) Yu, F.; Megyesi, J.; Price, P. *Am. J. Physiol. Renal. Physiol.* **2008**, *295*, F44-F52

Chapter II

(1) Jung, Y.; Lippard, S. J. *Chem. Rev.* **2007**, *107*, 1387-1407.

(2) Wang, D.; Lippard, S. J. *Nat. Rev. Drug Discovery* **2005**, *4*, 307-320.

(3) Reedijk, J. *PNAS* **2003**, *100*, 3611-3616.

(4) Akaboshi, M.; Kawai, K.; Maki, H.; Akuta, K.; Ujeno, Y.; Miyahara, T. *Jpn. J. Cancer Res.* **1992**, *83*, 522-526.

(5) Pascoe, J. M., Roberts, J. J. *Biochem. Pharmacol.* **1974**, *23*, 1345-1357.

(6) Harder, H. C.; Rosenberg, B. *Int. J. Cancer* **1970**, *6*, 207-216.

(7) Jung, Y.; Lippard, S. J. *J. Biol. Chem.* **2006**, *281*, 1361-1370.

(8) Damsma, G. E.; Alt, A.; Brueckner, F.; Carell, T.; Cramer, P. *Nat. Struct. Mol. Biol.* **2007**, *14*, 1127-1133.

(9) Schmittgen, T. D.; Ju, J. F.; Danenberg, K. D.; Danenberg, P. V. *International Journal Of Oncology* **2003**, *23*, 785-789.

(10) Rosenberg, J. M.; Sato, P. H. *Mol. Pharmacol.* **1993**, *43*, 491-497.

(11) Rosenberg, J.; Sato, P. *Mol. Pharmacol.* **1988**, *33*, 611-616.

(12) Hagerlof, M.; Papsai, P.; Chow, C. S.; Elmroth, S. K. C. *J. Biol. Inorg. Chem.* **2006**, *11*, 974-990.

(13) Papsai, P.; Snygg, A. S.; Aldag, J.; Elmroth, S. K. C. *Dalton Trans.* **2008**, 5225-5234.

(14) Papsai, P.; Aldag, J.; Persson, T.; Elmroth, S. K. C. *Dalton Trans.* **2006**, 3515-3517.

(15) Hagerlof, M.; Papsai, P.; Hedman, H. K.; Jungwirth, U.; Jenei, V.; Elmroth, S. K. C. *J. Biol. Inorg. Chem.* **2008**, *13*, 385-399.

(16) Danenberg, P. V.; Shea, L. C. C.; Danenberg, K. D.; Horikoshi, T. *Nucleic Acids Res.* **1991**, *19*, 3123-3128.

(17) Rijal, K., Chow, C. S. *ChemComm* **2009**, 107-109.

(18) DeRose, V. J. Burns, S; Kim, N-K; Vogt, M. In *Comprehensive Coordination Chemistry II*; Elsevier: St. Louis, 2003, p 787-813.

(19) Pyle, A. M. *J. Biol. Inorg. Chem.* **2002**, *7*, 679-690.

(20) Klein, D. J.; Moore, P. B.; Steitz, T. A. *RNA* **2004**, *10*, 1366-1379.

(21) Wahl, M. C.; Will, C. L.; Luhrmann, R. *Cell* **2009**, *136*, 701-718.

(22) Smith, D. J.; Query, C. C.; Konarska, M. M. *Mol. Cell* **2008**, *30*, 657-666.

(23) Wachtel, C.; Manley, J. L. *Mol. Biosyst.* **2009**, *5*, 311-316.

(24) Valadkhan, S.; Manley, J. L. *Nature* **2001**, *413*, 701-707.

(25) Hagerlof, M. P., P.; Chow, C. S.; Elmroth, S. K. C. *J. Biol. Inorg. Chem.* **2006**, *11*, 974-990.

(26) Ouliac-Garnier, I.; Bombard, S. *J. Inorg. Biochem.* **2007**, *101*, 514-524.

(27) Sigurdsson, S. T.; Eckstein, F. *Anal. Biochem.* **1996**, *235*, 241-242.

(28) Huggins, W.; Shapkina, T.; Wollenzien, P. *Rna-A Publication Of The Rna Society* **2007**, *13*, 2000-2011.

(29) Behlen, L. S.; Sampson, J. R.; Uhlenbeck, O. C. *Nucleic Acids Res.* **1992**, *20*, 4055-4059.

(30) Butcher, S. E.; Burke, J. M. *Biochemistry* **1994**, *33*, 992-999.

(31) Davies, M. S. B.-P., S. J.; Hambley, T. W. *J. Inorg. Biochem.* **2000**, *79*, 167-172.

(32) Bancroft, D. P. L., C. A.; Lippard, S. J. *JACS* **1990**, *112*, 6860-6870.

(33) Chifotides, H. T.; Koomen, J. M.; Kang, M. J.; Tichy, S. E.; Dunbar, K. R.; Russell, D. H. *Inorg. Chem.* **2004**, *43*, 6177-6187.

(34) Green, R.; Doudna, J. A. *Acs Chemical Biology* **2006**, *1*, 335-338.

(35) Valencia-Sanchez, M. A.; Liu, J.; Hannon, G. J.; Parker, R. *Genes Dev.* **2006**, *20*, 515-524.

(36) Farazi, T. A.; Juranek, S. A.; Tuschl, T. *Development* **2008**, *135*, 1201-1214.

(37) Serganov, A.; Patel, D. J. *Nat. Rev. Genet.* **2007**, *8*, 776-790.

(38) Montange, R. K.; Batey, R. T. *Ann. Rev. Biophys.* **2008**, *37*, 117-133.

(39) Bayne, E. H.; Allshire, R. C. *Trends Genet.* **2005**, *21*, 370.

(40) Mandal, M.; Breaker, R. R. *Nat. Rev. Mol. Cell Biol.* **2004**, *5*, 451-463.

(41) Strobel, S. A.; Cochrane, J. C. *Curr. Opin. Chem. Biol.* **2007**, *11*, 636-643.

(42) Mansfield, K. D.; Keene, J. D. *Biol. Cell* **2009**, *101*, 169-181.

(43) Grundy, F. J.; Henkin, T. M. *Crit. Rev. Biochem. Mol. Biol.* **2006**, *41*, 329-338.

(44) Lukong, K. E.; Chang, K. W.; Khandjian, E. W.; Richard, S. *Trends Genet.* **2008**, *24*, 416-425.

(45) Thomas, J. R.; Hergenrother, P. J. *Chem. Rev.* **2008**, *108*, 1171-1224.

(46) Hermann, T.; Tor, Y. *Expert Opin. Ther. Pat.* **2005**, *15*, 49-62.

(47) Legendre, F.; Kozelka, J.; Chottard, J. C. *Inorg. Chem.* **1998**, *37*, 3964-3967.

(48) Redon, S.; Bombard, S.; Elizondo-Riojas, M. A.; Chottard, J. C. *Nucleic Acids Res.* **2003**, *31*, 1605-1613.

(49) Monjardet-Bas, W.; Chottard, J. C.; Kozelka, J. *Chem.--Eur. J.* **2002**, *8*, 1144-1150.

(50) Danford, A. J.; Wang, D.; Wang, Q.; Tullius, T. D.; Lippard, S. J. *Proc. Natl. Acad. Sci. U. S. A.* **2005**, *102*, 12311-12316.

(51) Ober, M.; Lippard, S. J. *J. Am. Chem. Soc* **2008**, *130*, 2851-2861.

(52) Zhang, C. X.; Chang, P. V.; Lippard, S. J. *J. Am. Chem. Soc* **2004**, *126*, 6536-6537.

(53) Garnier, I. O.; Bombard, S. *J. Inorg. Biochem.* **2007**, *101*, 514-524.

(54) Bombard, S.; Kozelka, J.; Favre, A.; Chottard, J. C. *Eur. J. Biochem.* **1998**, *252*, 25-35.

(55) Boer, J.; Blount, K. F.; Luedtke, N. W.; Elson-Schwab, L.; Tor, Y. *Angewandte Chemie-International Edition* **2005**, *44*, 927-932.

(56) Yu, Y. T.; Maroney, P. A.; Darzynkiewicz, E.; Nilsen, T. W. *Rna-A Publication Of The Rna Society* **1995**, *1*, 46-54.

(57) Fabrizio, P.; Abelson, J. *Nucleic Acids Res.* **1992**, *20*, 3659-3664.

(58) Manning, G. S. *Q. Rev. Biophys.* **1978**, *11*, 179-246.

(59) Hambley, T. W. *J. Chem. Soc.-Dalton Trans.* **2001**, 2711-2718.

(60) Kozelka, J.; Legendre, F.; Reeder, F.; Chottard, J. C. *Coord. Chem. Rev.* **1999**, *192*, 61-82.

(61) Legendre, F.; Bas, V.; Kozelka, J.; Chottard, J. C. *Chemistry-A European Journal* **2000**, *6*, 2002-2010.

(62) Davies, M. S.; Berners-Price, S. J.; Hambley, T. W. *Inorg. Chem.* **2000**, *39*, 5603-5613.

(63) Davies, M. S.; Berners-Price, S. J.; Hambley, T. W. *J. Am. Chem. Soc* **1998**, *120*, 11380-11390.

(64) Zou, Y.; Van Houten, B.; Farrell, N. *Biochemistry* **1994**, *33*, 5404-5410.

(65) Redon, S.; Bombard, S.; Elizondo-Riojas, M. A.; Chottard, J. C. *Biochemistry* **2001**, *40*, 8463-8470.

(66) Villanueva, J. M.; Jia, X.; Yohannes, P. G.; Doetsch, P. W.; Marzilli, L. G. *Inorg. Chem.* **1999**, *38*, 6069-6080.

(67) Brabec, V.; Vrana, O.; Boudny, V. *Progress In Biophysics & Molecular Biology* **1996**, *65*, PB113-PB113.

(68) Snygg, A. S.; Brindell, M.; Stochel, G.; Elmroth, S. K. C. *Dalton Trans.* **2005**, 1221-1227.

(69) Monjardet-Bas, V.; Elizondo-Riojas, M. A.; Chottard, J. C.; Kozelka, J. *Angew. Chem., Int. Ed.* **2002**, *41*, 2998-3001.

(70) Baik, M. H.; Friesner, R. A.; Lippard, S. J. *J. Am. Chem. Soc.* **2003**, *125*, 14082-14092.

(71) Mantri, Y.; Lippard, S. J.; Baik, M. H. *J. Am. Chem. Soc.* **2007**, *129*, 5023-5030.

(72) Yang, E.; van Nimwegen, E.; Zavolan, M.; Rajewsky, N.; Schroeder, M.; Magnasco, M.; Darnell, J. E. *Genome Res.* **2003**, *13*, 1863-1872.

(73) Schoch, G.; Topp, H.; Held, A.; Hellerschoch, G.; Ballauff, A.; Manz, F. *Eur. J. Clin. Nutr.* **1990**, *44*, 647-658.

(74) Nakano, K.; Nakao, T.; Schram, K.H.; Hammargren, W.M.; McClure, T.D.; Katz, M.; Petersen, E. *Clin. Chim. Acta* **1993**, *218*, 169-183.

(75) Marway, J. S.; Anderson, G.J.; Miell, J.P.; Ross, R.; Grimble, G.K.; Bonner, A.B.; Gibbons, W.A.; Peters, T.J.; Preedy, V.R. Clin. Chim. Acta 1996, 252, 123-135.

(76) Sander, G.; Topp, H.; Hellerschoch, G.; Wieland, J.; Schoch, G. *Clin. Sci.* **1986**, *71*, 367-374.

Chapter III

(1) Dyson, P. J.; Sava, G. *Dalton Trans.* **2006**, 1929-1933.

(2) Akoboshi, M.; Kawai, K.; Maki, H.; Akuta, K.; Ujeno, Y.; Miyahara, T. *Jpn. J. Cancer Res.* **1992**, *83*, 522-526.

(3) Boulikas, T.; Vougiouka, M. *Oncol. Rep.* **2003**, *10*, 1663-1682.

(4) Jamieson, E. R.; Lippard, S. J. *Chem. Rev.,* **1999**, *99*, 2467-2498.

(5) Schmittgen, T. D.; Ju, J.-F.; Danenberg, K. D.; Danenberg, P. V. *Int. J. Oncol.* **2003**, *23*, 785-789.

(6) Rosenberg, J. M.; Sato, P. H. *Mol. Pharmacol.* **1993**, *43*, 491-497.

(7) Heminger, K. A.; Hartson, S. D.; Rogers, J.; Matts, R. L. *Arch. Biochem. Biophys.* **1997**, *344*, 200-207.

(8) Mattick, J. S. *Nat. Rev. Genet.* **2004**, *5*, 316-323.

(9) Kong, Q. M.; Lin, C. L. G. *Cell. Mol. Life Sci.* **2010**, *67*, 1817-1829.

(10) Olmo, N.; Turnay, J.; González de Buitrago, G.; López de Silanes, I.; Gavilanes, J.G.; Lizarbe, M. A. *Eur. J. Biochem.* **2001**, *268*, 2113-23.

(11) Jetzt, A. E., Cheng, J. S., Tumer, N. E., and Cohick, W. S. *Int. J. Biochem. Cell B.* **2009**, *41*, 2503-2510.

(12) Mroczek, S.; Kufel, J. *Nucleic Acids Res.* **2008**, *36*, 2874-2888.

(13) Mei, Y.; Yong, J.; Liu, H.; Shi, Y.; Meinkoth, J.; Dreyfuss, G.; Yang, X. *Mol. Cell* **2010**, *37*, 668-678.

(14) Menacho-Marquez, M.; Murguia, J. R. *Clin. Trans. Oncol.* **2007**, *9*, 221-228.

(15) McCarthy, J. E. G. *Microbiol. Mol. Biol. R.* **1998**, *62*, 1492–1553.

(16) Phizicky, E.M.; Hopper, A. K. *Genes Dev.* **2010**, *24*, 1832-1860.

(17) Barr M.M. *Physiol. Genomics* **2003**, *13*, 15-24.

(18) Ishida, S.; Herskowitz, I. *Yeast as a Tool in Cancer Reasearch*; Springer: Dordrecht, The Netherlands, 2007; pp 393-408.

(19) Sinani, D.; Adle, D. J.; Kim, H.; Lee, J. *J. Biol. Chem.* **2007**, *282*, 26775-26785.

(20) Liao, C.; Hu, B.; Arno, M.; Panaretou, B. *Mol. Pharmacol.* **2007**, *71*, 416-425.

(21) Fuertes, M. A.; Castilla, J.; Alonso, C.; Perez, J. M *Curr. Med.Chem*.**2003**, *10*, 257-266.

(22) Carmona-Gutierrez, D.; Eisenberg, T.; Buttner, S.; Meisinger, C.; Kroemer, G.; Madeo, F. *Cell Death Differ.* **2010**, *17*, 763-773.

(23) Jung, Y.; Lippard, S. J. *Chem. Rev.* **2007**, *107*, 1387-1407.

(24) Hoffmann, R. L. *Toxicol. Environ. Chem.* **1988**, *17*, 139-151.

(25) Beretta, G. L.; Gatti, L.; Tinelli, S.; Corna, E.; Colangelo, D.; Zunino, F.; Perego P. *Biochem. Pharmacol.* **2004**, *68*, 283-291.

(26) Song, I. S.; Savaraj, N.; Siddik, Z. H.; Liu, P. M.; Wei, Y. J.; Wu, C. J.; Kuo, M. T. *Mol Cancer Ther* **2004**, *3*, 1543-1549.

(27) Zisowsky, J.; Koegel, S.; Leyers, S.; Devarakonda, K.; Kassack, M. U.; Osmak, M.; Jaehde, U. *Biochem Pharmacol* **2007**, *73*, 293-307.

(28) Almeida, B.; Silva, A.; Mesquita, A.; Sarripalo-Marques, B.; Rodrigues, F.; Ludovico, P. *Biochim. Biophys. Acta* **2008**, *1783*, 1436-1448.

(29) Frohlich, K.-U.; Fussi, H.; Ruckenstuhl, C. *Semin. Cancer Biol.* **2007**, *17*, 112-121.

(30) Blank, M.; Shiloh, Y. *Cell Cycle* **2007**, *6*, 686-695.

(31) Sorenson, C. M.; Eastman, A. *Cancer Res.* **1988**, *48*, 4484.

(32) Grossmann, K. F.; Brown, J. C.; Moses, R. E. *Mutat. Res.* **1999**, *434*, 29-39.

(33) Tyson, C. B.; Lord, P. G.; Wheals, A. E. *J. Bacteriol.* **1979**, *138*, 92-98

(34) Eisenberg, T.; Carmona-Gutierrez, D.; Buttner, S.; Tavernarakis, N.; Madeo, F. *Apoptosis*, **2010**, *15*, 257-268.

(35) Madeo, F.; Frohlich, E.; Ligr, M.; Grey, M.; Sigrist, S. J.; Wolf, D. H.; Frohlich, K. U. *J. Cell Biol.* **1999**, *145*, 757-767.

(36) Li, X. P.; Baricevic, M.; Saidasan, H.; Tumer, N. E. *Infect. Immun.* **2007**, *75*, 417-428.

(37) Liang, Q.; Zhou, B. *Mol. Biol. Cell* **2007**, *18*, 4741-4749.

(38) Dudgeon, D. D.; Zhang, N.; Ositelu, O.O.; Kim, H.; Cunningham, K.W. *Eukaryot. Cell.* **2008** , *7,* 2037-2051.

(39) Burger, H.; Capello, A.; Schenk, P. W.; Stoter, G.; Brouwer, J.; Nooter, K. *Biochem. Bioph. Res. Co.* **2000**, *269,* 767–774.

(40) Schenk, P. W.; Brok, M.; Boersma, A. W. M.; Brandsma, J. A.; Den Dulk, H.; Burger, H.; Stoter, G.; Brouwer, J.; Nooter, K. *Mol. Pharmacol.* **2003**, *64*, 259-268.

(41) Moran, U.; Phillips, R.; Milo, R. *Cell* **2010**, *141*, 1262.

(42) Tamaki, H.; Yun, C.-W.; Mizutani, T.; Tsuzuki, T.; Takagi, Y.; Shinozaki, M.; Kodama, Y.; Shirahige, K.; Kumagai, H. *Genes to Cells* **2005**, *10*, 193-206.

(43) Bergamo, A.; Messori, L.; Piccoli, F.; Cocchietto, M.; Sava, G. *Inv. New Drugs* **2003**, *21*, 401–411.

(44) Eide, D. J.; Clark, S.; Nair, T. M.; Gehl, M.; Gribskov, M.; Guerinot, M. L.; Harper, J. F. *Genome Biology* **2005,** *6*, R77.

(45) Bancroft, D. P.; Lepre, C. A.; Lippard, S. J. *JACS* **1990**, *112*, 6860-6870.

(46) Cannone, J. J.; Subramanian, S.; Schnare, M. N.; Collett, J. R.; D'Souza, L. M.; Du, Y.; Feng, B.; Lin, N.; Madabusi, L.V.; MÜller, K. M.; Pande, N.; Shang, Z.; Yu, N.; Gutell, R. R. (2002). The Comparative RNA Web (CRW) Site: An Online Database of Comparative Sequence and Structure Information for Ribosomal, Intron, and Other RNAs. BioMed Central Bioinformatics, 3 :15.

(47) Ju, Q.; Warner, J. R. *Yeast* **1994**, *10*, 151-157.

(48) Warner, J. R. *Trends Biochem. Sci.* **1999**, *24*, 437-440.

(49) Chapman, E. G.; Hostetter, A. H.; Osborn, M. F.; Miller, A. L.; DeRose, V. J. *Metal Ions in Life Sciences: Structural and Catalytic Roles of Metal Ions in RNA*; Royal Society of Chemistry: Cambridge, UK, 2011; in press.

(50) Hilleren, P.; Parker, R. *Annu. Rev. Genet.* **1999**, *33*, 229-260.

(51) Chapman, E. G.; DeRose, V. J. *J. Am. Chem. Soc.* **2010**, *132*, 1946-1952.

(52) Hagerlof, M.; Papsai, P.; Chow, C. S.; Elmroth, S. K. C. *J. Biol. Inorg. Chem.* **2006**, *11*, 974-990.

(53) Rijal, K.; Chow, C. S. *Chem. Comm.* **2009**, 107-109.

(54) Motorin, Y.; Muller, S.; Behm-Ansmant, I.; Brantant, C. *Method. Enzymol.* **2007**, *425*, 21-53.

(55) Rose, M. D.; Winston, F.; Hieter, P. *Methods in Yeast Genetics: a Laboratory Course Manual*; Cold Spring Harbor Laboratory Press: NewYork, NY, 1990; pp 140-142.

(56) Madeo, F.; Frohlich, E.; Frohlich, K.-U. *J. Cell Biol.* **1997**, *139*, 729-734.

(57) Sherman, F. *Method. Enzymol.* **2002**, *350*, 3-41.

(58) Goffeau, A.; Barrell, B. G.; Bussey, H.; Davis, R. W.; Dujon, B.; Feldmann, H.; Galibert, F.; Hoheisel, J. D.; Jacq, C.; Johnston, M.;, Louis, E. J.; Mewes, H. W.; Murakami, Y.; Philippsen, P.; Tettelin, H.; Oliver, S. G. *Science* **1996**, *274*, 546-567.

Chapter IV

(1) Hannon, M. J. *Pure Appl. Chem.* **2007**, *79*, 2243-2261.

(2) Dyson, P. J.; Sava, G. *Dalton Trans.* **2006**, 1929-1933.

(3) Rademaker-Lakhai, J. M.; van den Bongard, D.; Pluim, D.; Beijnen, J. H.; Schellens, J. H. M. *Clin. Cancer Res.* **2004**, *10*, 3717-3727.

(4) Levina, A.; Mitra, A.; and Lay, P. A. *Metallomics* **2009**, *1*, 458-470.

(5) Kostova, I. *Curr. Med. Chem.* **2006**, *13*, 1085-1107.

(6) Bergamo, A.; Gagliardi, R.; Scarcia, V.; Furlani, A.; Alessio, E.; Mestroni, G.; Sava, G. *J. Pharmacol. Exp. Ther.* **1999**, *289*, 559-564.

(7) Sava, G.; Capozzi, I.; Bergamo, A.; Gagliardi, R.; Cocchietto, M.; Masiero, L.; Onisto, M.; Alessio, E.; Mestroni, G.; Garbisa, S. *Int. J. Cancer* **1996**, *68*, 60-66.

(8) Sava, G.; Bergamo, A.; Zorzet, S.; Gava, B.; Casarsa, C.; Cocchietto, M.; Fulani, A.; Scarcia, V.; Serli, B.; Iengo, E.; Alessio, E.; Mestroni, G. *Eur. J. Cancer* **2002**, *38,* 427-435.

(9) Ravera, M.; Baracco, S.; Cassino, C.; Zanellos, P.; Osella, D. *Dalton Trans*. **2004**, 2347-2351.

(10) Gullino, P.M. *Adv. Exp. Biol. Med.* **1976**, *75*, 521–536.

(11) Richard, D. E.; Berra, E.; Pouyssegur, J. *Biochem. Biophys. Res. Commun.* **1999**, *266,* 718–722.

(12) Gerweck, L. E.; Vijayappa, S.; Kozin, S. *Mol. Cancer Ther.* **2006**, *5*, 1275–1279.

(13) Brabec, V.; Novakova, O. *Drug Resist. Update.* **2006**, *9*, 111-122.

(14) Pizarro, A. M.; Sadler, P. J. *Biochimie* **2009**, *91*, 1198-1211.

(15) Pluim, D.; van Waardenburg, R. C. A. M.; Beijnen, J. H.; Schellens, J. H. M. *Cancer. Chemother. Pharmacol.* **2004**, *54*, 71-78.

(16) Galori, E.; Vettori, C.; Alesso, E.; Vilchez, F. G.; Vilaplana, R.; Orioli, P.; Casini, A.; Messori, L. *Arch. Biochem. Biophys.* **2000**, *376*, 156-162.

(17) Messori, L.; Casini, A.; Vullo, D.; Haroutiunian, S. G.; Dalian, E. B.; Orioli, P. *Inorg. Chim. Acta* **2000**, *303*, 283-286.

(18) Jung, Y.; Lippard, S. J. *Chem. Rev.* **2007**, *107*, 1387-1407.

(19) Bacac, M.; Hotze, A. C. G.; van der Schilden, K.; Haasnoot, J. G.; Pacor, S.; Alessio, E.; Sava, G.; Reedijk, J. *J. Inorg. Biochem.* **2004**, *98*, 402-412.

(20) Schluga, P.; Hartinger, C. G.; Egger, A.; Reisner, E.; Galanski, M.; Jakupec, M. A.; Keppler, B. K. *Dalton Trans.* **2006**, 1796-1802.

(21) Groessl, M.; Tsybin, Y. O.; Hartinger, C. G.; Keppler, B. K.; Dyson, P. J. *J. Biol. Inorg. Chem.* **2010**, *15*, 677-688.

(22) Malina, J.; Novakova, O.; Keppler, B. K.; Alessio, E.; Brabec, V. *J. Biol. Inorg. Chem.* **2001**, *6*, 435-445.

(23) Mattick, J. S. *Nat. Rev. Genet.* **2004**, *5*, 316-323.

(24) Kong, Q. M.; Lin, C. L. G. *Cell. Mol. Life Sci.* **2010**, *67*, 1817-1829.

(25) Olmo, N.; Turnay, J.; González de Buitrago, G.; López de Silanes, I.; Gavilanes, J.G.; Lizarbe, M. A *Eur. J. Biochem.* **2001**, *268*, 2113-23.

(26) Jetzt, A. E.; Cheng, J. S.; Tumer, N. E.; Cohick, W. S. *Int. J. Biochem. Cell B.* **2009**, *41*, 2503-2510.

(27) Mroczek, S.; Kufel, J. *Nucleic Acids Res.* **2008**, *36*, 2874-2888.

(28) Mei, Y.; Yong, J.; Liu, H.; Shi, Y.; Meinkoth, J.; Dreyfuss, G.; Yang, X. *Mol. Cell* **2010**, *37*, 668-678.

(29) Akaboshi, M.; Kawai, K.; Maki, H.; Akuta, K.; Ujeno, Y.; Miyahara, T. *Jpn. J. Cancer Res.* **1992**, *83*, 522-526.

(30) Schmittgen, T. D.; Ju, J.-F.; Danenberg, K. D.; Danenberg, P. V. *Int. J. Oncol*. **2003**, *23*, 785-789.

(31) Heminger, K. A.; Hartson, S. D.; Rogers, J.; Matts, R. L. *Arch. Biochem. Biophys*. **1997**, *344*, 200-207.

(32) Menacho-Marquez, M.; Murguia, J. R. *Clin. Trans. Oncol.* **2007**, *9*, 221-228.

(33) McCarthy, J. E. G. *Microbiol. Mol. Biol. R.* **1998**, *62*, 1492–1553.

(34) Phizicky, E.M.; Hopper, A. K. *Genes Dev.* **2010**, *24*, 1832-1860.

(35) Barr M.M. *Physiol. Genomics* **2003**, *13*, 15-24.

(36) Alessio, E.; Balducci, G.; Calligaris, M.; Costa, G.; Attia, W. M.; Mestroni, G. *Inorg Chem*. **1991**, *30*, 609-618.

(37) Witkowsky, L. Senior Thesis, Willamette University, 2006.

(38) Tyson, C. B.; Lord, P. G.; Wheals, A. E. *J. Bacteriol.* **1979**, *138*, 92-98.

(39) Chapman, E. G.; DeRose, V. J. *J. Am. Chem. Soc.* **2010**, *132*, 1946-1952.

(40) Ragas, J. A.; Simmons, T. A.; Limbach, P. A. *Analyst* **2000**, *125*, 575–581.

(41) National Institute of Standards and Technology. Physical Measurement Laboratory: Basic Atomic Spectroscopic Data. http://physics.nist.gov/PhysRefData/Handbook/Tables/rutheniumtable1.htm (accessed Jan 5, 2011).

(42) Ang, W. H.; Daldini, E.; Scolaro, C.; Scopelliti, R. Juillerat-Jeannerat, L.; Dyson, P. J. *Inorg. Chem.* **2006**, *45*, 9006-9013.

(43) Bergamo, A.; Messori, L.; Piccoli, F.; Cocchietto, M.; Sava, G. *Inv. New Drugs* **2003**, *21*, 401–411.

(44) Warner, J. R. *Trends Biochem. Sci.* **1999**, *24*, 437-440.

(45) Horn, H. F.; Vousden, K. H. *Oncogene 26*, **2007**,1306-1316.

(46) Hinnebusch, A. G. *Genes Dev.* **2009**, *23*, 891-895.

(47) Brindell, M.; Stawoska, I.; Supel, J.; Skoczowski, A.; Stochel, G.; van Eldik, R. *J. Biol. Inorg. Chem.* **2008**, *13*, 909-918.

(48) Brindell, M.; Piotrowska, D.; Shoukry, A. A.; Stochel, G.; van Eldik, R. *J. Biol. Inorg. Chem*. **2007**, *12*, 809–818.

(49) Calligaris, M.; Carugo, O. *Coord. Chem. Rev.* **1996**, *153*, 83–154.

Chapter V

(1) Jung, Y.; Lippard, S. J. *Chem. Rev.* **2007**, *107*, 1387-1407.

(2) Brabec, V.; Novakova, O. *Drug Res. Update.* **2006**, *9*, 111-122.

(3) Malina, J.; Novakova, O.; Keppler, B. K.; Alessio, E.; Brabec, V. *J. Biol. Inorg. Chem.* **2001**, *6*, 435-445.

(4) Pluim, D.; van Waardenburg, R. C. A. M.; Beijnen, J. H.; Schellens, J. H. M. *Cancer. Chemother. Pharmacol.* **2004**, *54*, 71-78.

(5) Mei, Y. D.; Yong, J.; Liu, H. T.; Shi, Y. G.; Meinkoth, J.; Dreyfuss, G.; Yang, X. L. *Mol. Cell* **2010**, *37*, 668-678.